THYROID
Volume 00, Number 00, 2022

DOI: 10.1089/thy.2022.0404

Different Hypothalamic Mechanisms Control Decreased Circulating Thyroid Hormone Levels in Infection and Fasting-Induced Non-Thyroidal Illness Syndrome in Male Thyroid Hormone Action Indicator Mice

Richárd Sinkó,[1,2] Petra Mohácsik,[1] Dóra Kővári,[3] Veronika Penksza,[3] Gábor Wittmann,[3] Lilla Mácsai,[1] Tatiana L. Fonseca,[4] Antonio C. Bianco,[4] Csaba Fekete,[3] and Balázs Gereben[1]

Background: Non-Thyroidal Illness Syndrome (NTIS) caused by infection or fasting is hallmarked by reduced circulating thyroid hormone (TH) levels. To better understand the role of local TH-action in the development of NTIS, we assessed tissue-specific changes of TH signaling in Thyroid Hormone Action Indicator (THAI) mice.
Methods: NTIS was induced in young adult THAI mice by bacterial lipopolysaccharide (LPS)-administration or by 24 or 48 hours' fasting. Tissue-specific TH-action was assessed by the detection of changes of the *Luciferase* reporter of THAI mice with quantitative polymerase chain reaction along with tissue-specific examination of regulators of TH metabolism and signaling. Age dependence of revealed alterations of hypothalamic TH-action was also studied in 1-year-old male THAI mice.
Results: LPS-treatment increased TH-action in the hypothalamic arcuate nucleus-median eminence (ARC-ME) region preceded by an increase of type 2 deiodinase (D2) expression in the same region and followed by the suppression of *proTrh* expression in the hypothalamic paraventricular nucleus (PVN). In contrast, LPS decreased both TH-action and D2 activity in the pituitary at both ages. *Tshβ* expression and serum free thyroxine (fT4) and free triiodothyronine (fT3) levels decreased in LPS-treated young adults. *Tshβ* expression and serum fT4 levels were not significantly affected by LPS treatment in aged animals. In contrast to LPS treatment, TH-action remained unchanged in the ARC-ME of 24 and 48 hours fasted animals accompanied with a modest decrease of *proTrh* expression in the PVN in the 24-hour group. *Tshβ* expression and fT3 level were decreased in both fasted groups, but the fT4 decreased only in the 48 hours fasted animals.
Conclusions: Although the hypothalamo-pituitary-thyroid (HPT) axis is inhibited both in LPS and fasting-induced NTIS, LPS achieves this by centrally inducing local hyperthyroidism in the ARC-ME region, while fasting acts without affecting hypothalamic TH signaling. Lack of downregulation of *Tshβ* and fT4 in LPS-treated aged THAI mice suggests age-dependent alterations in the responsiveness of the HPT axis. The LPS-induced tissue-specific hypo-, eu-, and hyperthyroidism in different tissues of the same animal indicate that under certain conditions TH levels alone could be a poor marker of tissue TH signaling. In conclusion, decreased circulating TH levels in these two forms of NTIS are associated with different patterns of hypothalamic TH signaling.

Keywords: aging, fasting, hypothalamo-pituitary-thyroid axis, Non-Thyroidal Illness Syndrome, Thyroid Hormone Action Indicator Mouse, tissue-specific thyroid hormone action

[1]Laboratory of Molecular Cell Metabolism, Institute of Experimental Medicine, Budapest, Hungary.
[2]János Szentágothai PhD School of Neurosciences, Semmelweis University, Budapest, Hungary.
[3]Laboratory of Integrative Neuroendocrinology, Institute of Experimental Medicine, Budapest, Hungary.
[4]Section of Adult and Pediatric Endocrinology, University of Chicago, Chicago, Illinois, USA.

Introduction

The Non-Thyroidal Illness Syndrome (NTIS) is caused by fasting or serious disease conditions such as infection and hallmarked by central inhibition of the hypothalamo-pituitary-thyroid (HPT) axis.[1–3] Similar to humans, fasting and bacterial lipopolysaccharide (LPS) administration, a model of infection, also causes NTIS in rodents.[4–7]

Despite decreased circulating thyroid hormone (TH) levels, we have suggested that LPS-induced increase of the activity of the TH activating type 2 deiodinase (D2) enzyme in tanycytes of the mediobasal hypothalamus (MBH) may cause local hyperthyroidism in the MBH and therefore may be a key mediator of the effect of LPS on HPT axis suppression.[4] This hypothesis was, however, debated by Mebis et al based on the absence of increased triiodothyronine (T3) content in the whole hypothalamus of a rabbit NTIS model.[8] As the available methods were not sufficiently sensitive to determine the T3 content of the very small MBH, our hypothesis could not be directly proven.

Diano et al observed a twofold increase of D2 activity also in the MBH of fasted rats and suggested that increased TH activation in the MBH could contribute to fasting-induced inhibition of the HPT axis.[9]

To overcome the challenge of the direct assessment of tissue-specific TH-action, we generated the Thyroid Hormone Action Indicator (THAI) mouse model that allows tissue-specific detection of TH-action and gauges TH signaling within a physiological context.[10] To better understand the development of NTIS, we studied in THAI mice whether local TH-action is changed in the MBH and could contribute to the development of LPS- and fasting-induced NTIS along with measuring tissue-specific TH-action and parameters of the HPT axis. The impact of aging was also studied on the revealed alterations of hypothalamic TH signaling.

Materials and Methods

Methods are detailed in Supplemental Data.

Animals

We used 3-month-old (young adult) and 1-year-old (aged) male THAI line #23 FVB/Ant mice that allows tissue-specific assessment of TH-action.[10] In this transgenic mouse model, the expression of the luciferase reporter is driven by a minimal viral promoter that was made TH sensitive by the insertion of three copies of the TH response element of the human *dio1* gene.[10] Animals were housed under standard environmental conditions (light between 06:00 and 18:00 hours, temperature 22 ± 1°C, mouse chow, and water *ad libitum*). All experimental protocols were reviewed and approved by the Animal Welfare Committee at the Institute of Experimental Medicine, Hungary (PEI/001/1550-10/2014 - PE/EA/1490-7/2017).

LPS treatment, fasting, and microdissection of brain areas

Mice were treated *i.p.* with LPS (150 μg/animal; *Escherichia coli* 0127:B8; Sigma) or saline as control and decapitated 6, 8, and 10 hours after injection (animal number is given in the legends). Treatment time was optimized based on preliminary experiments between 4 and 24 hours; 6–10 hours was found to be appropriate to observe the well-known hallmarks of acute NTIS. Animals were fasted for 24 or 48 hours followed by tissue collection and microdissection.[11]

Taqman real-time PCR

Reverse transcription-quantitative polymerase chain reaction was performed on Viia 7 Real-time PCR instrument (Applied Biosystems). Accession numbers of used Taqman probes are listed in Supplementary Table S1. The sequence of the *dCpG Luciferase* probe has been previously published.[10]

ProTrh messenger RNA in situ hybridization

Hybridization was performed using a 741 base (corresponding to the 106–846 nucleotides of the mouse *proTrh* messenger RNA [mRNA]; BC053493) single-stranded [^{35}S]UTP labeled cRNA probe for mouse *proTrh* as previously described.[12]

Deiodination assay

D2 activity of whole pituitary samples was assayed in the presence of ^{125}I-thyroxine (T4) and released iodine was counted, as previously described.[13]

Determination of circulating hormone levels

Serum free T4 (fT4), free T3 (fT3), and serum thyrotropin (TSH) were determined as provided in Supplementary Data.

Simple Western blot (WES)

Thyrotropin-releasing hormone-degrading ectoenzyme (TRH-DE) content of microdissected arcuate nucleus-median eminence (ARC-ME) samples was measured with WES Simple Western capillary electrophoresis system.

Data analysis

Student's two-sample two-sided *t*-test was used to analyze two groups; one-way analysis of variance followed by Tukey and Dunnett *post hoc* test was used to compare more than two groups.

Results

TH signaling undergoes marked changes in NTIS in regulatory regions of the HPT axis

In the PVN of young adult THAI mice, the expression of *proTrh* mRNA was significantly decreased between 6 and 8 hours (Fig. 1A). The LPS-treatment also reduced the *Tshβ* mRNA level in the pituitary (Fig. 1B), and serum TSH level was also decreased at 10 hours (Supplementary Fig. S1). In the serum, circulating fT4 and fT3 levels were markedly decreased (Fig. 1C, D) as expected.[4,5]

Earlier, we showed that LPS-treatment results in a marked increase of tanycytic D2 activity that is independent from decreased peripheral TH levels.[4,14] Based on this, we hypothesized that the increased TH activating capacity of tanycytes induces local hyperthyroidism in the MBH despite the lower serum fT4 levels, and it inhibits the hypophysiotropic TRH neurons by enhancing negative TH feedback.[4,14]

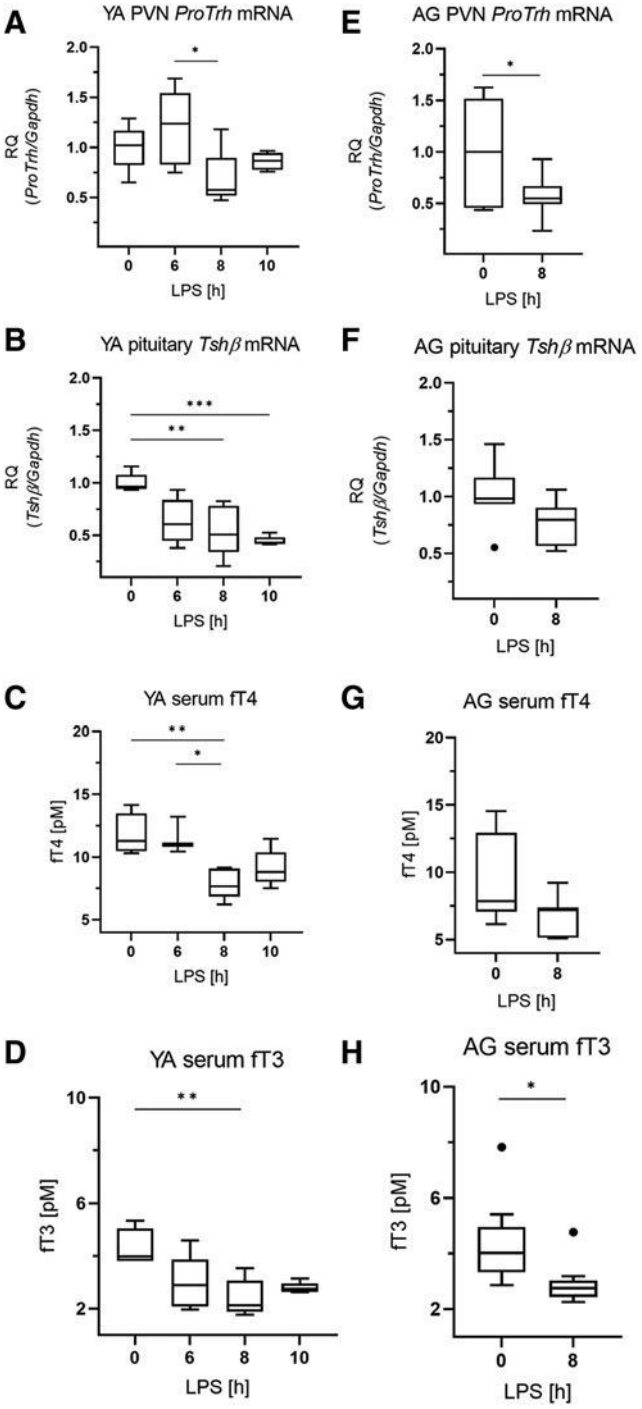

FIG. 1. Age-dependent responsiveness of the HPT axis in LPS-induced NTIS. Male THAI mice were treated with 150 μg/animal LPS *i.p.* (**A**–**D**) YA (2–3 months old), (**A**) PVN *proTrh* mRNA levels levels, (**B**) pituitary *Tshβ* mRNA levels, (**C**) serum fT4 levels, (**D**) serum fT3 levels, (**E**–**H**) AG (1 year old), (**E**) PVN *proTrh* mRNA levels, (**F**) pituitary *Tshβ* mRNA levels, (**G**) serum fT4 levels, (**H**) serum fT3 levels $n(\mathrm{YA}) = 5$/group. $n(\mathrm{AG}) = 6$–9/group; figure shows Tukey Box Plots, $\alpha = 0.05$; $^{*}p < 0.05$, $^{**}p < 0.01$, $^{***}p < 0.001$. AG, aged adults; fT3, free triiodothyronine; fT4, free thyroxine; HPT, hypothalamo-pituitary-thyroid; LPS, lipopolysaccharide; mRNA, messenger RNA; NTIS, Non-Thyroidal Illness Syndrome; PVN, paraventricular nucleus; RQ, relative quantity; THAI, Thyroid Hormone Action Indicator; YA, young adults.

To determine how LPS-treatment impacts local TH economy in the MBH, we tested the effect of LPS-treatment on TH-action in the ARC-ME region using the THAI mouse model.

The LPS-treatment resulted in a time-dependent elevation of *Luciferase* expression (marker of TH-action) in the ARC-ME region that became statistically significant 8 hours after LPS injection (Fig. 2A). The observed increase of local TH signaling was preceded by a marked increase of D2 expression in the ARC-ME region (6 hours after LPS-treatment) (Fig. 2B).

In contrast to the hypothalamus, LPS-treatment decreased *Luciferase* expression in the pituitary, indicating a reduction of TH signaling in this tissue (Fig. 3A). This was accompanied with decreased D2-mediated TH activation and decreased D3-mediated TH inactivation (Fig. 3B, C, respectively). Expression of TH transporters *Oatp1c1 (Slco1c)* and *Mct8 (Slc16a2)* remained unchanged in the pituitary (Fig. 3D, E).

Responsiveness of the HPT axis is age-dependent in NTIS

Since TH economy is subjected to age-mediated changes,[15] we also performed studies in aged adult (1 year old) THAI animals to study whether the revealed changes of TH

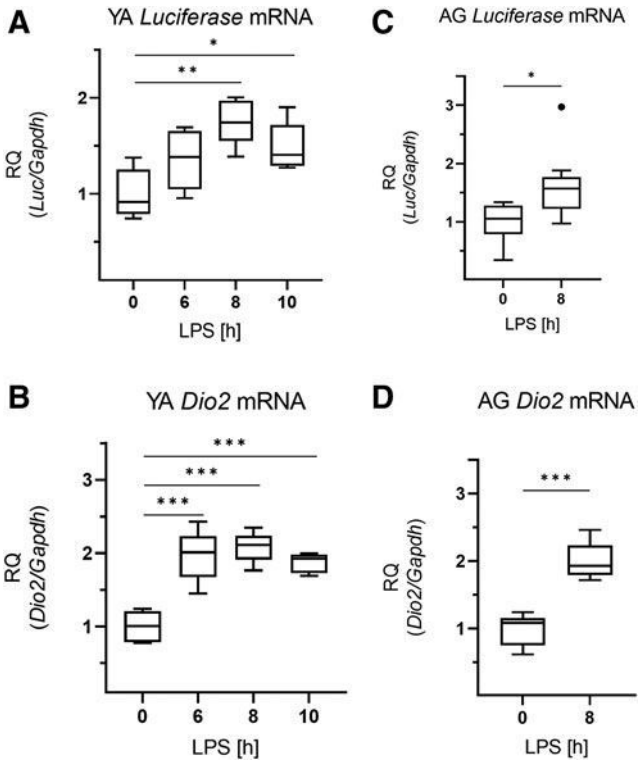

FIG. 2. Thyroid hormone action in the hypothalamus in LPS-induced NTIS. Male THAI mice were treated with 150 μg/animal LPS *i.p.*; *Luciferase* expression represents local TH-action. (**A**, **B**) YA (2–3 months old), (**A**) ARC-ME *Luciferase* mRNA levels, (**B**) ARC-ME *Dio2* mRNA levels, (**C**, **D**) AG (1 year old), (**C**) ARC-ME *Luciferase* mRNA levels, (**D**) ARC-ME *Dio2* mRNA levels. $n(\mathrm{YA}) = 5$/group; $n(\mathrm{AG}) = 8$–9/group; figure shows Tukey Box Plots, $\alpha = 0.05$; $^{*}p < 0.05$, $^{**}p < 0.01$, $^{***}p < 0.001$. ARC-ME, arcuate nucleus-median eminence; TH, thyroid hormone.

signaling in NTIS are age-dependent. In 1-year-old mice, a similar decrease of *proTrh* mRNA level was observed in the PVN after LPS-treatment compared with young adults (Fig. 1E), indicating that the hypothalamic response of the HPT axis was age-independent.

However, in contrast to young adults, neither the expression of *Tshβ* in the pituitary nor the circulating fT4 levels was significantly decreased in aged animals (Fig. 1F, G). Serum TSH of aged animals was significantly lower in the controls compared with young adults (1.02 vs. 0.37, $p = 0.001$), and TSH levels of the LPS-treated aged group were below the limit of detection. Therefore, the magnitude of the impact of LPS on serum TSH could not be compared in an age-dependent manner.

fT3 levels were significantly decreased by LPS-treatment in both age groups (Fig. 1D, H). Similar to young adults, the LPS-induced increases of *Luciferase* and *Dio2* expressions were also observed in the ARC-ME region of aged animals (Fig. 2C, D). In the pituitary of aged animals, the findings on *Luciferase*, D2 activity, *Dio3*, and *Oatp1c1* (Fig. 3F–I) were similar to young adults, except that *Mct8* expression was slightly increased in the aged group (Fig. 3J).

To understand the mechanisms underlying the observed age-related difference in *Tshβ* regulation, we studied factors with potential to alter central components of the HPT axis. *ProTrh* mRNA expression in the PVN of young adults and aged animals was compared by *in situ* hybridization, and no significant difference could be found ($p = 0.099$) (Fig. 4A, B). The major regulator of TRH peptide degradation, the *Trh-de* was also studied. The *Trh-de* mRNA was significantly decreased 8 hours after the LPS injection in the ARC-ME samples of both age groups, and this drop in *Trh-de* expression was significantly higher in the aged animals (0.48 vs. 0.60, $p = 0.021$) (Fig. 5A, D).

However, this change was not reflected in the amount of TRH-DE protein in the ARC-ME region in neither age group, assessed by Capillary Microwestern (Fig. 5B, E; Supplementary Fig. S2). The expression of pituitary *Trh-r1*, the canonical receptor of TRH signaling in the pituitary, was markedly decreased after LPS-treatment, but no age-related differences were observed (Fig. 5C, F).

Coexistence of eu- and hypothyroidism in peripheral tissues after LPS-treatment

Hepatic *Luciferase* expression was not influenced by LPS-treatment in young adults, although hepatic *Dio1* expression was markedly decreased by the treatment (Fig. 6A, B). In contrast, *Luciferase* expression of LPS treated mice was

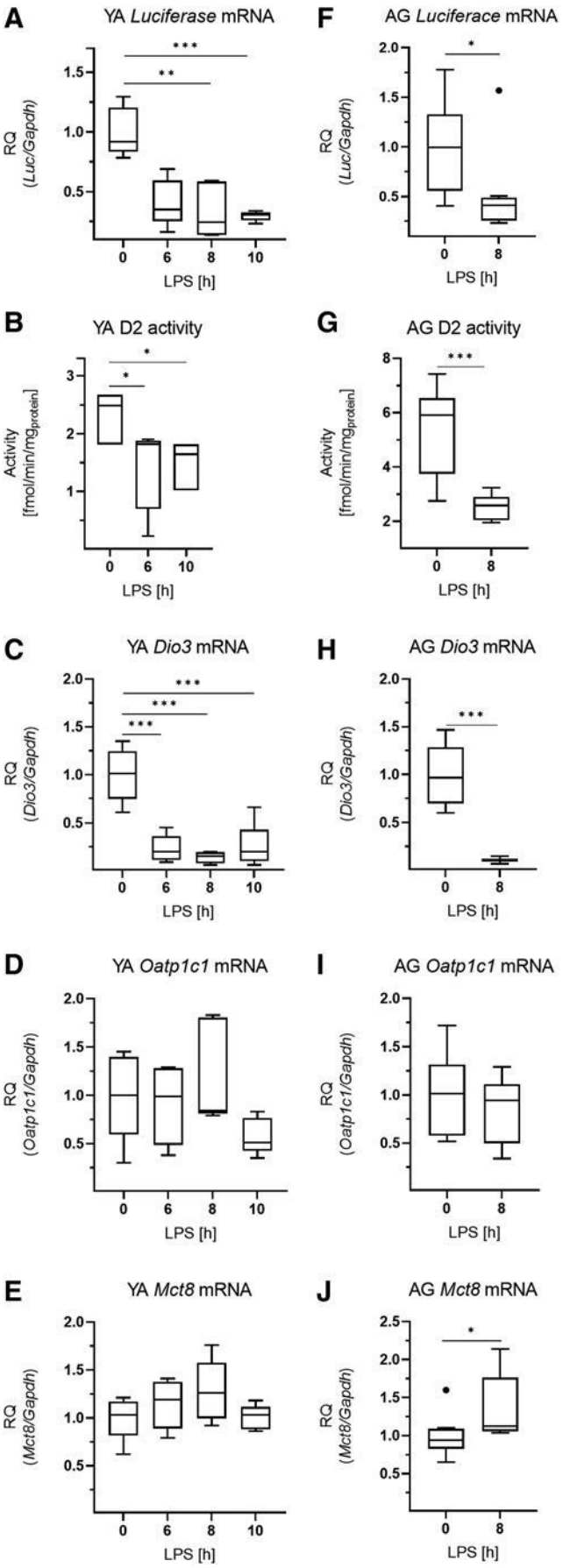

FIG. 3. Thyroid hormone action in the pituitary in LPS-induced NTIS. Male THAI mice were treated with 150 μg/animal LPS *i.p.*; *Luciferase* expression represents local TH-action. (**A**–**E**) YA (2–3 months old), (**A**) *Luciferase* mRNA levels, (**B**) D2 activity, (**C**) *Dio3* mRNA levels, (**D**) *Oatp1c1* mRNA levels, (**E**) *Mct8* mRNA levels (**F**–**J**) AG (1 year old), (**F**) *Luciferase* mRNA levels, (**G**) D2 activity, (**H**) *Dio3* mRNA levels, (**I**) *Oatp1c1* mRNA levels, (**J**) *Mct8* mRNA levels. n(YA) = 5/group; n(AG) = 7–9/group; figure shows Tukey Box Plots, $\alpha = 0.05$; $^{*}p < 0.05$, $^{**}p < 0.01$, $^{***}p < 0.001$. D2, type 2 deiodinase.

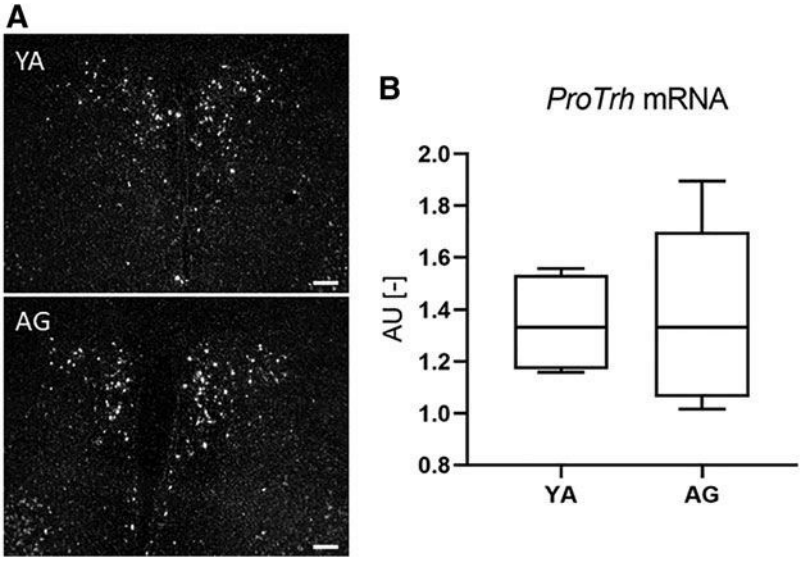

FIG. 4. *proTrh* expression in the PVN of YA and aged THAI mice. (**A**) Representative dark-field micrographs of *proTrh in situ* hybridization at the mid-level PVN of YA (3 months old, upper panel) and AG (1 year old, lower panel) THAI mice. (**B**) Quantification of the *proTrh* mRNA hybridization signal. $n(\mathrm{YA}) = 4$/group; $n(\mathrm{AG}) = 5$/group; figure shows Tukey Box Plots, $\alpha = 0.05$; Scale bar: 100 μm.

significantly decreased in the small intestine, representing reduced TH signaling 10 hours after the treatment (Fig. 6C). Similar changes were observed in aged animals (Fig. 6D–F).

Response of the HPT axis during fasting is accompanied by unaltered hypothalamic TH signaling

ProTrh expression was decreased by $\sim$15% in the PVN after 24 hours' fasting by *in situ* hybridization, while this decrease was already absent after 48 hours (Fig. 7A–D). *Tshβ* expression in the pituitary was decreased by both 24 and 48 hours' fasting (Fig. 8A, D). Serum fT3 but not fT4 was decreased after 24 hours (Fig. 8B, C), while both fT4 and fT3 were decreased after 48 hours' fasting (Fig. 8E, F). Fasting was accompanied by unchanged *Luciferase* expression in the ARC-ME region after both 24 and 48 hours' fasting, indicating unaltered hypothalamic TH signaling (Fig. 9A, C) while *Luciferase* expression was decreased in the pituitary (Fig. 9B, D). No changes of TH signaling were revealed that could be responsible for the response of the HPT axis during fasting, thus age-dependent studies under this condition were omitted.

Discussion

The NTIS frequently occurs in hospitalized patients and is hallmarked by central inhibition of TRH secretion and by reduced serum TSH and TH levels, yet its pathogenesis is still only partially understood.[1,16,17] In rodents, infection-induced NTIS can be mimicked by LPS-treatment. Earlier studies demonstrated that LPS-treatment also influences local TH metabolism in certain organs, suggesting both central and peripheral modulation of the TH-action.[4,5,18]

Data from our and other laboratories indicated that localized hypothalamic increase of D2 activity in tanycytes could play a role in the development of NTIS in rats and mice.[4,5] While circulating TH levels has an $\sim$50% decrease 12 hours after LPS-administration, the D2 activity in the tanycytes increases fourfold.[4] Thus, we suggested that the net effect of these changes could be local hyperthyroidism in the MBH that can modulate the feedback regulation of hypophysiotropic TRH neurons and, therefore, could contribute to the inhibition of the HPT axis by LPS-treatment.[4] This hypothesis was also supported by the absence of LPS-induced inhibition of the HPT axis in D2 knockout mice.[6] However, the concept was questioned by data reporting that T3 concentration in the homogenate of complete hypothalamic blocks was not influenced by LPS-treatment.[8]

Therefore, we took advantage of THAI mouse, a transgenic mouse model allowing the tissue-specific assessment of endogenous changes in local TH-action.[10] THAI mice were treated with LPS and TH signaling was measured in the ARC-ME region where D2 expressing tanycytes and the axon terminals of the hypophysiotropic TRH neurons are located.[19,20]

Our data revealed increased TH-action in the ARC-ME region despite falling circulating TH levels. The increase of *Luciferase* expression in this hypothalamic region is preceded by the increase of D2 expression in tanycytes, further supporting that the LPS-induced increase of D2 activity in these cells can induce local hyperthyroidism in the neuropil surrounding the tanycytes. The ARC-ME region is critical in the feedback regulation of the hypophysiotropic TRH neurons.

The axon terminals of these cells terminate around the fenestrated capillaries of the external zone of the ME.[21] As the ME is located outside of the blood–brain barrier, circulating T3 can freely enter into the extracellular space of the ME. The T3 content of this region, however, also depends on the T3 released from tanycytes after conversion of the prohormone T4 to the active T3. In the external zone of the ME, the end feet processes of tanycytes and the axon terminals of the hypophysiotropic TRH neurons are in close contact and MCT8 is also present on the surface of TRH axons.[21]

This anatomical relationship suggests that the T3 content of the ME is monitored by the hypophysiotropic TRH neurons and it plays a critical role in the negative feedback regulation of the TRH synthesis. The demonstrated local hyperthyroidism in the hypothalamic ARC-ME was followed by the decrease of *proTrh* expression in the PVN. This indicates that local increase of TH-action in the MBH plays a major role in impaired HPT activity.

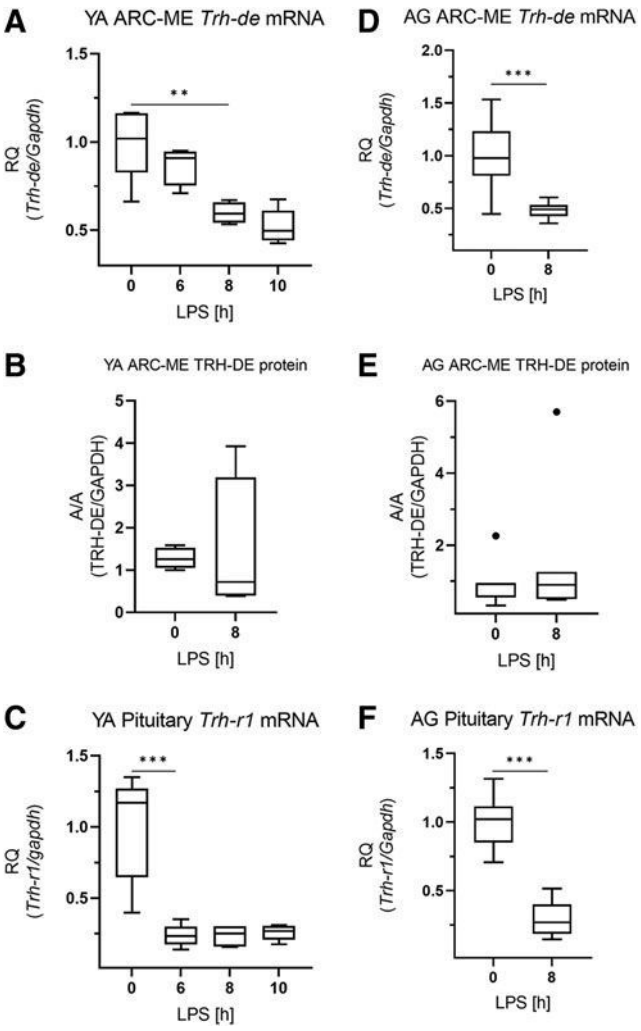

FIG. 5. Regulators of TRH action in the HPT axis in LPS-induced NTIS. Male THAI mice were treated with 150 μg/animal LPS *i.p.* (**A**–**C**) YA (2–3 months old), (**A**) ARC-ME *Trh-de* mRNA levels, (**B**) ARC-ME TRH-DE protein levels, (**C**) pituitary *Trh-r1* mRNA levels, (**D**–**F**) AG (1 year old), (**D**) ARC-ME *Trh-de* mRNA levels, (**E**) ARC-ME TRH-DE protein levels, (**F**) pituitary *Trh-r1* mRNA levels. n(YA) = 5/group; n(AG) = 7–9/group; figure shows Tukey Box Plots, $\alpha = 0.05$; $^{**}p < 0.01$, $^{***}p < 0.001$. TRH, thyrotropin-releasing hormone; TRH-DE, thyrotropin-releasing hormone-degrading ectoenzyme.

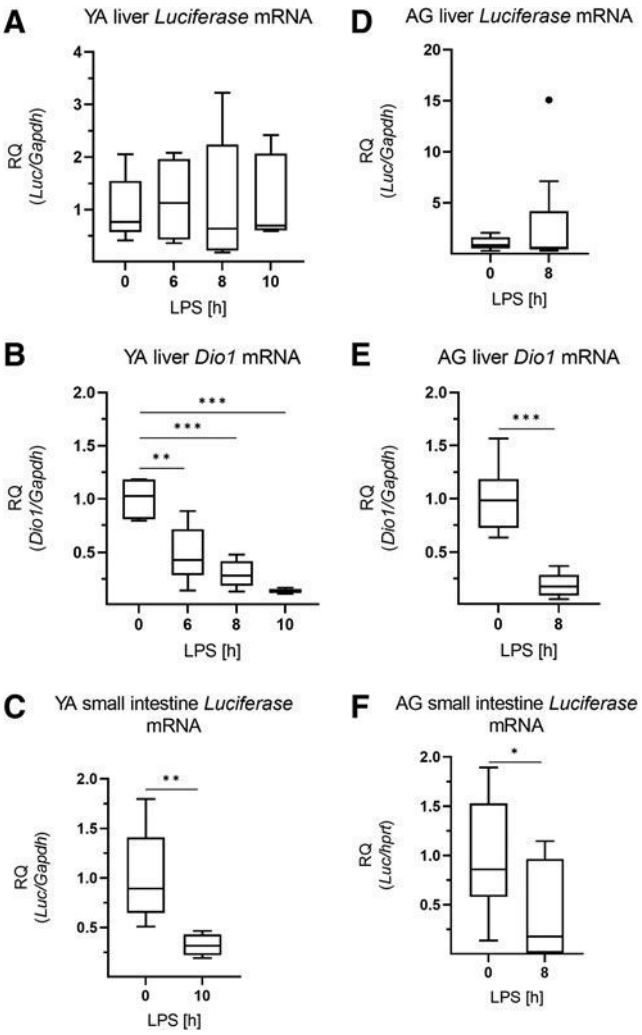

FIG. 6. Local thyroid hormone action of peripheral tissues in LPS-induced NTIS. Male THAI mice were treated with 150 μg/animal LPS *i.p.*; *Luciferase* expression represents local TH-action. (**A**–**C**) YA (2–3 months old), (**A**) hepatic *Luciferase* mRNA levels, (**B**) hepatic *Dio1* mRNA levels, (**C**) small intestine *Luciferase* mRNA levels, (**D**–**F**) AG (1 year old), (**D**) hepatic *luciferase* mRNA levels, (**E**) hepatic *Dio1* mRNA levels, (**F**) small intestine *Luciferase* mRNA levels. n(YA) = 5/group; n(AG) = 7–9/group; figure shows Tukey Box Plots, $\alpha = 0.05$; $^{*}p < 0.05$, $^{**}p < 0.01$, $^{***}p < 0.001$.

This is also supported by fact that the TRH expression is decreased in the PVN at the same time when the *Luciferase* expression is increased in the ARC-ME region. Therefore, the LPS-induced local hyperthyroidism is likely sufficient to inhibit the hypophysiotropic TRH neurons, despite the fact that the increased D2 activity of tanycytes is not sufficient to increase the TH-action in the entire hypothalamus after LPS-treatment.

Intriguingly, TH-action is regulated differently in peripheral tissues. In contrast to the ARC-ME, pituitary TH-action was decreased by LPS that was a net result of lower circulating TH levels and the simultaneous decrease of D2 activity in this tissue. Since D2 activity is negatively regulated by TH availability,[22] it is likely that the LPS itself or the LPS-induced cytokines could be responsible for decreased D2 activity of the pituitary.

The direct action of these substances is supported by the presence of cytokine and toll-like receptors in the pituitary.[23,24] Surprisingly, D2 activity and *Dio3* expressions changed parallel in the pituitary. As *Dio3* expression is regulated positively by TH,[22] it is likely that the decreased *Dio3* expression represents a compensatory mechanism that tries to preserve pituitary TH-action to suppression of *Tsh*.

As a hallmark of NTIS, pituitary *Tshβ* expression was decreased as found earlier in LPS-injected rats and mice[4,5] accompanied with decreased serum TSH. The revealed

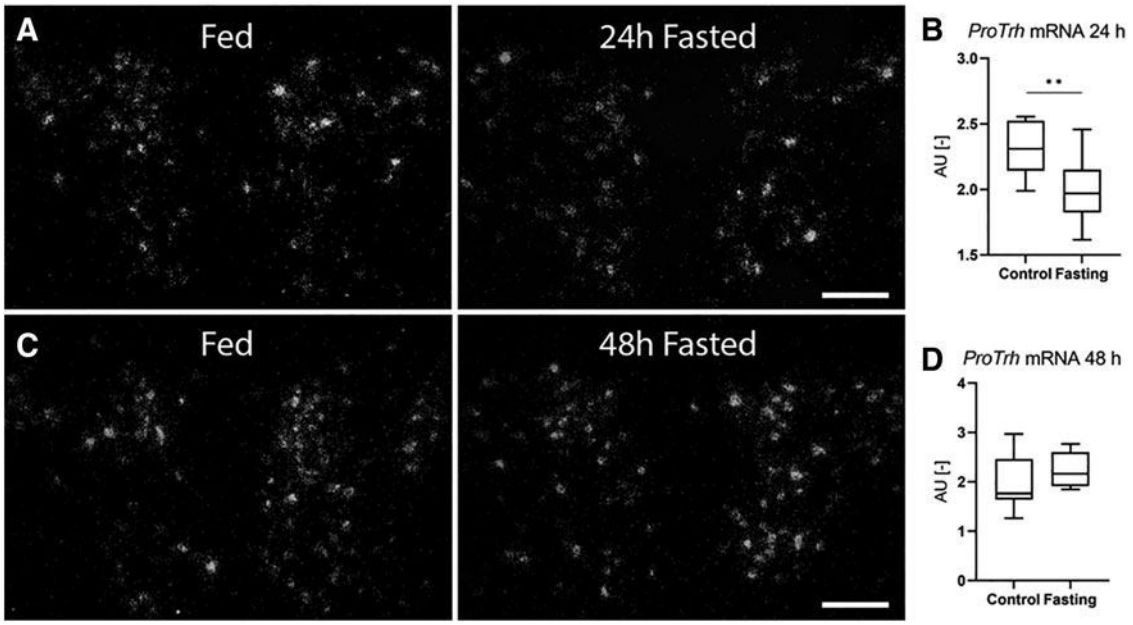

FIG. 7. *proTrh* expression in the PVN of fasting THAI mice. (**A**, **B**) 24 hours fasting, (**C**, **D**) 48 hours' fasting. (**A**, **C**) Representative dark-field micrographs of *proTrh in situ* hybridization at the mid-level PVN of fasting YA. (**B**) Quantification of the *proTrh* mRNA hybridization signal of (**A**), (**D**) Quantification of the *proTrh* mRNA hybridization signal of (**C**). n(24 hours) = 10–11/group; n(48 hours) = 7–8/group; figure shows Tukey Box Plots, $\alpha = 0.05$; $^{**}p < 0.01$. Scale bar: 100 μm.

decrease in pituitary TH signaling is interesting, since *Tshβ* is negatively regulated by TH.[20] This finding reveals that the decreased *Tshβ* expression in LPS-induced NTIS is not the consequence of local pituitary TH-action, but it is likely that the result of the decreased TRH expression and release overrides the stimulatory effect of local pituitary hypothyroidism on *Tshβ* expression.

Accumulating data support the hypothesis of a life-stage specific optimum of tissue TH signaling. Decreased TH levels have been associated with longer lifespan in animal models.[15,25–27] In addition, human clinical studies revealed a negative correlation between longevity and circulating TH levels.[28] We studied how tissue-specific TH-action is modulated by age during the challenge of LPS-induced NTIS.

Our findings on *Tshβ* and circulating fT4 of 1-year-old THAI mice demonstrated an age-evoked impaired responsiveness of the HPT axis that hindered to develop the significantly decreased *Tshβ* and circulating fT4 of young adults, characteristic hallmarks of NTIS. This age-dependent difference was not reflected in fT3 levels, which is not surprising since peripheral TH metabolism plays an important role in the regulation of the circulating fT3 levels.[22] Although *proTrh* expression in the PVN decreased similarly in aged and in young adults, this change could not be translated in aged animals neither to decreased *Tshβ* expression nor to the fall of circulating fT4 levels.

We speculated whether this is caused by an elevated basal *proTrh* mRNA expression in the PVN of aged animals; thus, a similar level of LPS-induced reduction in *proTrh* expression could result in higher *Tshβ* levels in aged animals. Since *situ* hybridization did not reveal an age-dependent difference in *proTrh* expression in the PVN, we rejected this idea. Age-dependent differences in local pituitary TH-action were absent, therefore we looked for age-dependent changes of modulators of TRH levels.

TRH-DE (or pyroglutamil peptidase II) is an exocellular deactivator of the TRH peptide and is highly expressed by the tanycytes[29] but LPS-treatment did not change TRH-DE protein level in the MBH. In addition to the lower *proTrh* mRNA levels in the PVN, the decreased expression of pituitary *Trh-r1* also points toward a suppressed TRH signal on thyrotrophic cells in the pituitary after LPS-treatment. As the decrease of *Trh-r1* expression was not age-dependent, it is likely that the age-dependent regulation of TSH expression is not due to age-dependent regulation of TRH release, but rather an intrinsic feature of the thyrotropes.

The set-point of the HPT axis that determines the aimed range of circulating TH levels is pre-set around birth and remains unchanged during the entire lifespan.[20] Since a different optimum of TH homeostasis is suggested for specific life periods, the fixed set-point represents a potential bottleneck in deregulation of TH homeostasis that could lead to tissue-dysfunctions during aging. Our data demonstrate that under specific conditions, responsiveness of the HPT axis undergoes age-dependent changes despite the fixed set-point.

In addition, NTIS also generated an age-independent but a tissue-specific pattern of TH-action in peripheral organs. Our finding on unchanged hepatic TH-action up to 10 hours after LPS injection differs from data showing a $\sim$20% decreased hepatic T3 content in LPS-treated female mice at this time point.[18] It is unclear why this decrease was not reflected in hepatic TH-action. Since our studies were performed in males, sex- or strain-specific effects cannot be excluded, but modulation of TH transport or the TH receptor complex could be also the reason for this effect.

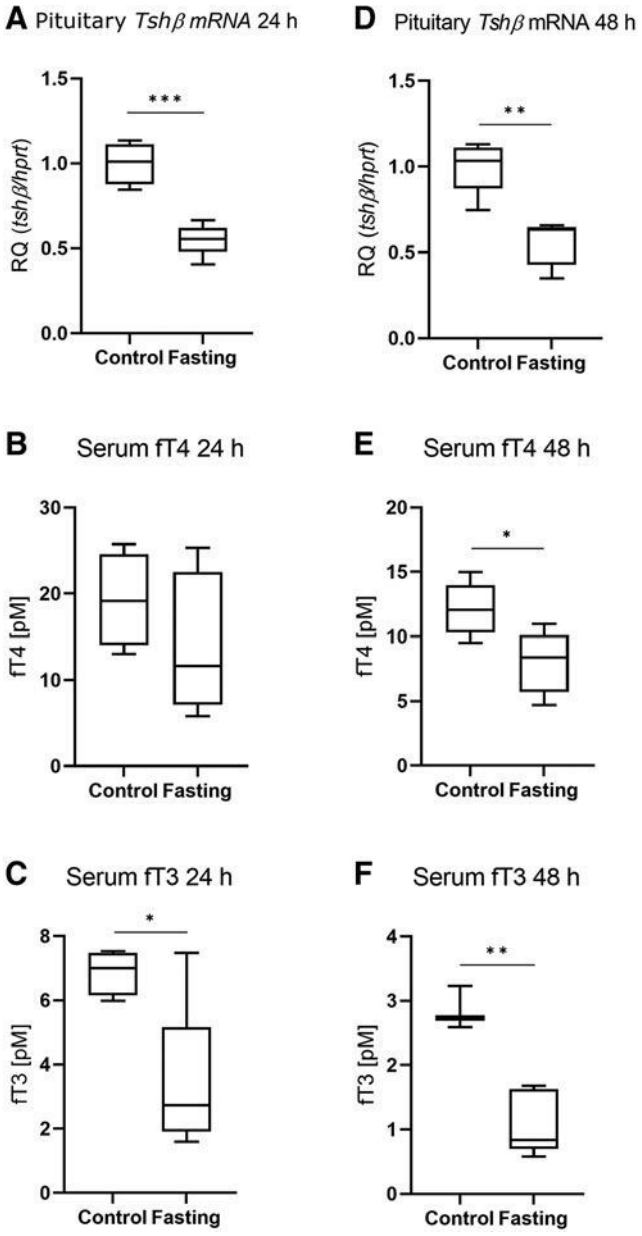

FIG. 8. Responsiveness of the HPT axis in fasting animals. Male THAI mice were fasted for 24 and 48 hours. (**A**–**C**) 24 hours' fasting, (**D**–**F**) 48 hours' fasting, (**A**) pituitary *Tshβ* mRNA levels, (**B**) serum fT4 levels, (**C**) serum fT3 levels, (**D**) pituitary *Tshβ* mRNA levels, (**E**) serum fT4 levels, (**F**) serum fT3 levels. $n(24 \text{ hours}) = 4–5/\text{group}$; $n(48 \text{ hours}) = 3–5/\text{group}$; figure shows Tukey Box Plots, $\alpha = 0.05$; $^{*}p < 0.05$, $^{**}p < 0.01$, $^{***}p < 0.001$.

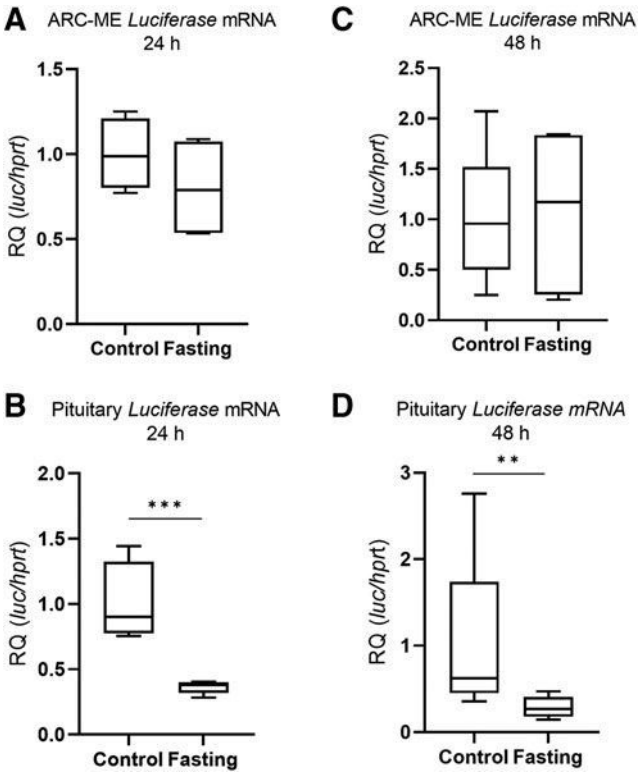

FIG. 9. Thyroid Hormone action in the HPT axis in fasting animals. Male THAI mice were fasted for 24 and 48 hours, *Luciferase* expression represents local TH-action. (**A**, **B**) 24 hours' fasting, (**C**, **D**) 48 hours' fasting, (**A**) ARC-ME *Luciferase* mRNA levels, (**B**) pituitary *Luciferase* mRNA levels, (**C**) ARC-ME *Luciferase* mRNA levels, (**D**) pituitary *Luciferase* mRNA levels; $n(24 \text{ hours}) = 4–5/\text{group}$; $n(48 \text{ hours}) = 5/\text{group}$; figure shows Tukey Box Plots, $\alpha = 0.05$; $^{**}p < 0.01$, $^{***}p < 0.001$.

In addition, our finding on unaltered hepatic TH-action also underlines that the decrease of *Dio1*, a known TH-regulated marker gene in the liver, is not the result of decreased TH signaling, but likely a direct effect of cytokines that were shown to interfere with *Dio1* expression.[30] This further substantiates that endogenous TH-responsive genes face serious limitations when used to monitor changes of tissue-specific TH-action.

In contrast to LPS-induced NTIS, fasting was not associated with altered hypothalamic TH signaling although *proTrh* expression was decreased in the PVN after 24 hours' fasting accompanied with decreased circulating TH levels and pituitary *Tshβ* expression. In rats, *proTrh* expression is robustly decreased in the PVN,[7] while available data on mice are limited and controversial.[31–34] Our studies based on repeated experiments on 24 and 48 hours' fasted mice pointed out that the decrease of *proTrh* expression in the PVN of mice is moderate compared with that of rats.

We also ran pilot studies with similar results on fasting C57Bl/6 mice that indicated that modest response of *proTrh* expression in the PVN of fasting mice is not specific for the used FBV/Ant background. Our findings demonstrate that in contrast to LPS-induced NTIS, the hypothalamic regulation of *proTrh* expression in fasted mice is not associated with a signature of elevated TH signaling in the MBH. Decreased pituitary TH-action was found in both LPS and fasting-induced NTIS.

Although this could indicate that TSHβ is not regulated dominantly by local TH-action in the pituitary in either condition, it should be also considered that thyrotrophs represent only a subpopulation of the pituitary and our measurement is the net result of the full anterior pituitary, thus the thyrotroph-specific conditions are unknown.

Our data also demonstrate that THAI mice can reveal local tissue-specific changes of TH-action independently from

circulating TH levels. These findings strongly call for the development of approaches to allow assessment of tissue TH-action in patients.

Acknowledgments

The authors thank Andrea Juhász for her excellent technical support.

Authors' Contributions

R.S.: Methodology (lead), writing—review and editing. P.M., D.K., V.P., G.W., L.M., and T.L.F.: Methodology. A.C.B.: Methodology, writing—original draft (supporting). C.F. and B.G.: Methodology, conceptualization, writing—review and editing.

Author Disclosure Statement

A.C.B. is a consultant for AbbVie, Synthonics, Sention, and Thyron. R.S., P.M., D.K., V.P., G.W., L.M., T.L.F., C.F., and B.G. have nothing to disclose.

Funding Information

This work was supported by the National Research, Development and Innovation Office (NKFIH) of Hungary Grants K125247 (to B.G.), K138487 (to C.F.), the Hungarian National Brain Research Program 2017-1.2.1-NKP-2017-00002 (to C.F. and B.G.), and NIH 2R01DK058538-14A1 (to A.C.B. and B.G.). R.S., P.M., D.K., V.P., G.W., L.M., and T.L.F. have nothing to report.

Supplementary Material

Supplementary Data
Supplementary Figure S1
Supplementary Figure S2
Supplementary Table S1

References

1. Boelen A, Kwakkel J, Fliers E. Beyond low plasma T3: Local thyroid hormone metabolism during inflammation and infection. Endocr Rev 2011;32(5):670–693; doi: 10.1210/er.2011-0007
2. De Groot LJ. Dangerous dogmas in medicine: The nonthyroidal illness syndrome. J Clin Endocrinol Metab 1999; 84(1):151–164; doi: 10.1210/jcem.84.1.5364
3. Van den Berghe G. Non-thyroidal illness in the ICU: A syndrome with different faces. Thyroid 2014;24(10):1456–1465; doi: 10.1089/thy.2014.0201
4. Fekete C, Gereben B, Doleschall M, et al. Lipopolysaccharide induces type 2 iodothyronine deiodinase in the mediobasal hypothalamus: Implications for the nonthyroidal illness syndrome. Endocrinology 2004;145(4):1649–1655.
5. Boelen A, Kwakkel J, Thijssen-Timmer DC, et al. Simultaneous changes in central and peripheral components of the hypothalamus-pituitary-thyroid axis in lipopolysaccharide-induced acute illness in mice. J Endocrinol 2004;182(2):315–323.
6. Freitas BC, Gereben B, Castillo M, et al. Paracrine signaling by glial cell-derived triiodothyronine activates neuronal gene expression in the rodent brain and human cells. J Clin Invest 2010;120(6):2206–2217; doi: 10.1172/JCI41977
7. Legradi G, Emerson CH, Ahima RS, et al. Leptin prevents fasting-induced suppression of prothyrotropin-releasing hormone messenger ribonucleic acid in neurons of the hypothalamic paraventricular nucleus. Endocrinology 1997; 138(6):2569–2576.
8. Mebis L, Debaveye Y, Ellger B, et al. Changes in the central component of the hypothalamus-pituitary-thyroid axis in a rabbit model of prolonged critical illness. Crit Care 2009;13(5):R147; doi: 10.1186/cc8043
9. Diano S, Naftolin F, Goglia F, et al. Fasting-induced increase in type II iodothyronine deiodinase activity and messenger ribonucleic acid levels is not reversed by thyroxine in the rat hypothalamus. Endocrinology 1998;139(6):2879–2884.
10. Mohacsik P, Erdelyi F, Baranyi M, et al. A transgenic mouse model for detection of tissue-specific thyroid hormone action. Endocrinology 2018;159(2):1159–1171; doi: 10.1210/en.2017-00582
11. Palkovits M. Microdissection of individual brain nuclei and areas. In: Neuromethods. (Boulton AA, Baker GB. eds.) Humana Press: Totowa, NJ, USA; 1986; pp. 1–17.
12. Fekete C, Kelly J, Mihaly E, et al. Neuropeptide Y has a central inhibitory action on the hypothalamic-pituitary-thyroid axis. Endocrinology 2001;142(6):2606–2613; doi: 10.1210/endo.142.6.8207
13. Bianco AC, Anderson G, Forrest D, et al. American thyroid association guide to investigating thyroid hormone economy and action in rodent and cell models. Thyroid 2014; 24(1):88–168; doi: 10.1089/thy.2013.0109
14. Fekete C, Sarkar S, Christoffolete MA, et al. Bacterial lipopolysaccharide (LPS)-induced type 2 iodothyronine deiodinase (D2) activation in the mediobasal hypothalamus (MBH) is independent of the LPS-induced fall in serum thyroid hormone levels. Brain Res 2005;1056(1):97–99.
15. Bowers J, Terrien J, Clerget-Froidevaux MS, et al. Thyroid hormone signaling and homeostasis during aging. Endocr Rev 2013;34(4):556–589; doi: 10.1210/er.2012-1056
16. Warner MH, Beckett GJ. Mechanisms behind the nonthyroidal illness syndrome: An update. J Endocrinol 2010; 205(1):1–13; doi: 10.1677/JOE-09-0412
17. Mebis L, Van den Berghe G. Thyroid axis function and dysfunction in critical illness. Best Pract Res Clin Endocrinol Metab 2011;25(5):745–757; doi: 10.1016/j.beem.2011.03.002
18. Boelen A, van der Spek AH, Bloise F, et al. Tissue thyroid hormone metabolism is differentially regulated during illness in mice. J Endocrinol 2017;233(1):25–36; doi: 10.1530/JOE-16-0483
19. Gereben B, McAninch EA, Ribeiro MO, et al. Scope and limitations of iodothyronine deiodinases in hypothyroidism. Nat Rev Endocrinol 2015;11(11):642–652; doi: 10.1038/nrendo.2015.155
20. Fekete C, Lechan RM. Central regulation of hypothalamic-pituitary-thyroid axis under physiological and pathophysiological conditions. Endocr Rev 2014;35(2):159–194; doi: 10.1210/er.2013-1087
21. Kallo I, Mohacsik P, Vida B, et al. A novel pathway regulates thyroid hormone availability in rat and human hypothalamic neurosecretory neurons. PLoS One 2012;7(6): e37860; doi: 10.1371/journal.pone.0037860
22. Gereben B, Zeold A, Dentice M, et al. Activation and inactivation of thyroid hormone by deiodinases: Local action with general consequences. Cell Mol Life Sci 2008;65(4): 570–590; doi: 10.1007/s00018-007-7396-0
23. Breuel KF, Kougias P, Rice PJ, et al. Anterior pituitary cells express pattern recognition receptors for fungal glucans:

Implications for neuroendocrine immune involvement in response to fungal infections. Neuroimmunomodulation 2004; 11(1):1–9; doi: 10.1159/000072963
24. Haedo MR, Gerez J, Fuertes M, et al. Regulation of pituitary function by cytokines. Horm Res 2009;72(5):266–274; doi: 10.1159/000245928
25. Brown-Borg HM. Hormonal regulation of longevity in mammals. Ageing Res Rev 2007;6(1):28–45; doi: 10.1016/j.arr.2007.02.005
26. Buffenstein R, Pinto M. Endocrine function in naturally long-living small mammals. Mol Cell Endocrinol 2009; 299(1):101–111; doi: 10.1016/j.mce.2008.04.021
27. Dell'agnello C, Leo S, Agostino A, et al. Increased longevity and refractoriness to Ca(2+)-dependent neurodegeneration in Surf1 knockout mice. Hum Mol Genet 2007; 16(4):431–444; doi: 10.1093/hmg/ddl477
28. Jansen SW, Akintola AA, Roelfsema F, et al. Human longevity is characterised by high thyroid stimulating hormone secretion without altered energy metabolism. Sci Rep 2015;5:11525; doi: 10.1038/srep11525
29. Sanchez E, Vargas MA, Singru PS, et al. Tanycyte pyroglutamyl peptidase II contributes to regulation of the hypothalamic-pituitary-thyroid axis through glial-axonal associations in the median eminence. Endocrinology 2009; 150(5):2283–2291; doi: 10.1210/en.2008-1643
30. Yu J, Koenig RJ. Regulation of hepatocyte thyroxine 5'-deiodinase by T3 and nuclear receptor coactivators as a model of the sick euthyroid syndrome. J Biol Chem 2000; 275(49):38296–38301.
31. Abel ED, Ahima RS, Boers ME, et al. Critical role for thyroid hormone receptor beta2 in the regulation of paraventricular thyrotropin-releasing hormone neurons. J Clin Invest 2001;107(8):1017–1023; doi: 10.1172/JCI10858
32. Vella KR, Ramadoss P, Lam FS, et al. NPY and MC4R signaling regulate thyroid hormone levels during fasting through both central and peripheral pathways. Cell Metab 2011;14(6):780–790; doi: 10.1016/j.cmet.2011.10.009
33. Minakhina S, De Oliveira V, Kim SY, et al. Thyroid hormone receptor phosphorylation regulates acute fasting-induced suppression of the hypothalamic-pituitary-thyroid axis. Proc Natl Acad Sci U S A 2021;118(39):e2107943118; doi: 10.1073/pnas.2107943118
34. Campos AMP, Wasinski F, Klein MO, et al. Fasting reduces the number of TRH immunoreactive neurons in the hypothalamic paraventricular nucleus of male rats, but not in mice. Neurosci Lett 2021;752:135832; doi: 10.1016/j.neulet.2021.135832

Address correspondence to:
Csaba Fekete, MD, PhD
Laboratory of Integrative Neuroendocrinology
Institute of Experimental Medicine
43 Szigony str.
Budapest 1083
Hungary

E-mail: fekete.csaba@koki.hu

Balázs Gereben, DVM, PhD
Laboratory of Molecular Cell Metabolism
Institute of Experimental Medicine
43 Szigony str.
Budapest 1083
Hungary

E-mail: gereben.balazs@koki.hu

Supplemental Data

Materials and Methods

Tissue collection and microdissection

After decapitation, trunk blood was collected in Eppendorf tubes, stored on ice and the serum was separated by centrifugation 1 hour later. The sera were stored at -80°C until further processing. Pituitary, liver and small intestine were removed and immediately frozen in powered dry ice. Brains were removed from the skull, snap frozen in -40°C isopentane. Coronal, 1 mm thick slice containing the paraventricular nucleus (PVN) and 2 mm thick slice containing the arcuate nucleus-median eminence (ARC-ME) region were cut with blades in precooled brain matrix (Electron Microscopy Sciences). ARC-ME and PVN hypothalamic areas were microdissected with punch needle from frozen sections placed on pre-cooled glass slides using the Palkovits Punch technique under a Stemi 508 stereomicroscope (Zeiss). The samples were collected in precooled Eppendorf tubes and stored at –80°C.

Taqman Real-time quantitative PCR

According to manufacturer's instructions total RNA was isolated from peripheral tissue samples with RNeasy Mini Kit (Qiagen), while RNeasy Lipid Tissue Mini kit (Qiagen) was used for RNA isolation from punched brain areas. Qiagen RNase-free DNase set (ref: 79254) was used to eliminate genomic DNA contamination. Total RNA (1µg) was reverse transcribed with High-Capacity cDNA Reverse Transcription Kit (Thermo Fisher Scientific). cDNA concentration was determined with Qubit ssDNA assay kit. 10 ng cDNA was used in each Taqman reaction. Reactions were assayed on Viia 7 Real-time PCR instrument (Applied Biosystems), mRNA expression of target genes was detected with Taqman Gene expression probe sets using Taqman Fast Universal PCR Mastermix (Thermo Fisher Scientific). *Gapdh*

expression proved to be stable in all used challenge conditions (no significant difference between groups and low variance in groups) and was used as housekeeping.

5.55 ng of cDNA was used to preamplify the gene of interest and the housekeeping gene in small intestine samples in aged animals using Taqman Preamp Master Mix (Applied Biosystems). Reaction product was diluted 1:5 and subjected to Taqman PCR with equal volumes of diluted preamplification product in each reaction. *Hprt1* expression was proved to be stable in all used challenge conditions (no significant difference between groups and low variance in groups) and was used as housekeeping for preamplified samples. Accession numbers of used Taqman probes are listed in Supplemental Table 1. The sequence of the *dCpG Luciferase* probe has been previously published (12).

ProTrh mRNA in situ hybridization

Under anaesthesia, blood was collected from the caudal vena cava and then, the animals were decapitated. The brains were removed from the skull and frozen in chilled isopentane (24h fasting experiment) or on powdered dry ice (48h fasting experiment) Serial 12 μm thick coronal sections through the rostro-caudal extent of the PVN were cut on a cryostat (Leica CM3050 S, Leica Microsystems) and adhered to Superfrost Plus glass slides (Fisher Scientific Co.) to obtain five sets of slides, each set containing every fifth section through the PVN. The tissue sections were stored at -80°C until prepared for *in situ* hybridization histochemistry.

Every fifth section of the PVN was hybridized with a 741 base (corresponding to the 106-846 nucleotides of the mouse *proTrh* mRNA; BC053493) single stranded [^{35}S]UTP labeled cRNA probe for mouse *proTrh* following methods as previously described (15). In vitro transcription was performed using SP6 polymerase (Roche) and [^{35}S] α-UTP (Perkin Elmer). The hybridization was performed under coverslips in a buffer containing 50% formamide, a 2-fold concentration of standard sodium citrate (2XSSC), 10% dextran sulfate, 0.5% sodium

dodecyl sulfate, 250 µg/ml denatured salmon sperm DNA, and $3x10^5$ cpm of radiolabeled probe for 16h at 56°C. Slides were dipped into Kodak NTB autoradiography emulsion (Eastman Kodak, Rochester, N.Y.) diluted 1:1 in distilled water, and the autoradiograms developed after 4 (24h fasting) or 5 (48h fasting) days of exposure at 4°C. The slides were immersed in 0.005% cresyl violet acetate (Sigma-Aldrich) for 2 minutes to obtain fluorescent counterstaining of cell nuclei, dehydrated in ascending ethanol series and xylenes, and coverslipped with DPX mountant (Sigma-Aldrich). *In situ* hybridization autoradiograms were visualized under darkfield illumination using a Zeiss Axioimager M1 microscope equipped with MRc5 digital camera (Zeiss) and analyzed with Image J software (NIH). The background density points were removed by thresholding the image. The area covered by *proTrh* hybridization signal in the PVN was measured in four sections containing the mid-level of the PVN identified by the fluorescent counterstaining.

Determination of circulating TH and TSH levels

Serum free T4 (fT4) and free T3 (fT3) levels were measured with AccuLite CLIA Microwells kit (Monobind Inc., Lake Forest, CA USA) according to the manufacturer's instructions. Serum TSH was determined using a MILLIPLEXTM Rat thyroid panel (Millipore Corporation) and read on a Magpix (Millipore Sigma).

Deiodination assay of pituitary samples

In order to determine D2 activity, whole pituitary samples were homogenized with sonication in PE buffer (0.1M potassium phosphate, 1 mM EDTA, pH 6.9) containing 0.25M sucrose and 10 mM DTT. Protein content was determined with Bradford's method. Lysates containing 100 µg protein were assayed in the presence of freshly purified 100.000 cpm ^{125}I-T4, 1nM T4, 100

nM T3, 1mM PTU and 20 mM DTT for 180 min at 37 °C in duplicate followed by separation of released iodine and counting in a gamma counter.

Simple Western Blot (WES)

Microdissected ARC-ME samples were homogenized by sonication in 50 µl lysis buffer (50 mM HEPES, 5 mM $MgCl_2$, 1 mM EDTA, 0.1 M NaCl) containing 0.05 V/V% Triton, 1 mM DTT and 1 tablet/10.5 ml Roche complete protease inhibitor cocktail. Total protein content was determined with Qubit Protein Assay kit (Life Technologies). WES Simple Western capillary electrophoresis system (Protein Simple) was used to determine TRH-DE levels using the 12-230 kDa Separation module (ref: SM-W004). Samples were prepared according to manufacturer's instructions, using 1X sample buffer and 10 min heat denaturation on 70 °C. Samples were loaded onto WES in a concentration of 1,6 mg/ml. TRH-DE (ref: AF2985) and GAPDH (ref: AF5718) antibodies were obtained from R&D Systems, optimal dilutions were determined as 1:100 for GAPDH and 1:50 for TRH-DE. WES anti-goat detection module (DM-006) was used for multiplex detection. Optimal run settings for WES were determined as 32 min separation time, 60 min primary antibody incubation time, other settings were default of instrument. TRH-DE peak areas were normalized with GAPDH peak areas.

Data Analysis

Microsoft Excel and STATISTICA v13 was used to analyse data. Prism version 8.3 was used to prepare the graphs. Figures show Tukey Box-Plot; box represents the two middle quartiles, lower whisker represents lower quartile, upper whisker represents upper quartile, line represents median, dots represent outlier data. Figure legend "n" shows mice used in groups. Null hypothesis significance tests were conducted with 95 % level of confidence; Student's two sample two-sided t-test was used to analyse two groups; one-way analysis of variance

(ANOVA) followed by Tukey and Dunnett post-hoc test was used to compare more than two groups. Models were deemed adequate based on residual plots and residual normal plots. Used methods are detailed under each figure.

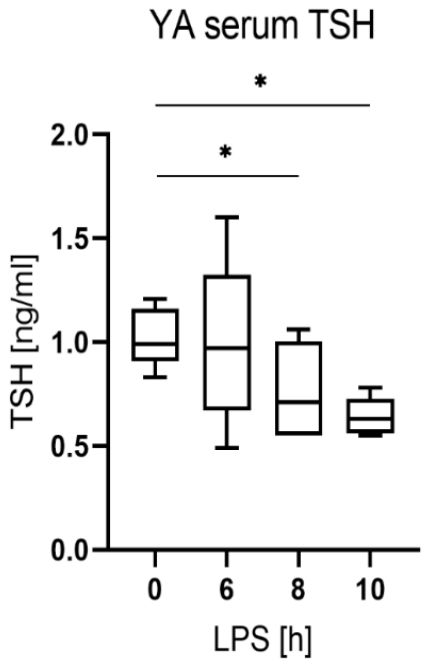

Supplemental Figure 1. Serum TSH in NTIS

Male young adult (YA) THAI mice were treated with 150 µg/animal LPS *i.p.*

n= 5/group; figure shows Tukey Box Plots, $\alpha = 0.05$; *: $p<0.05$

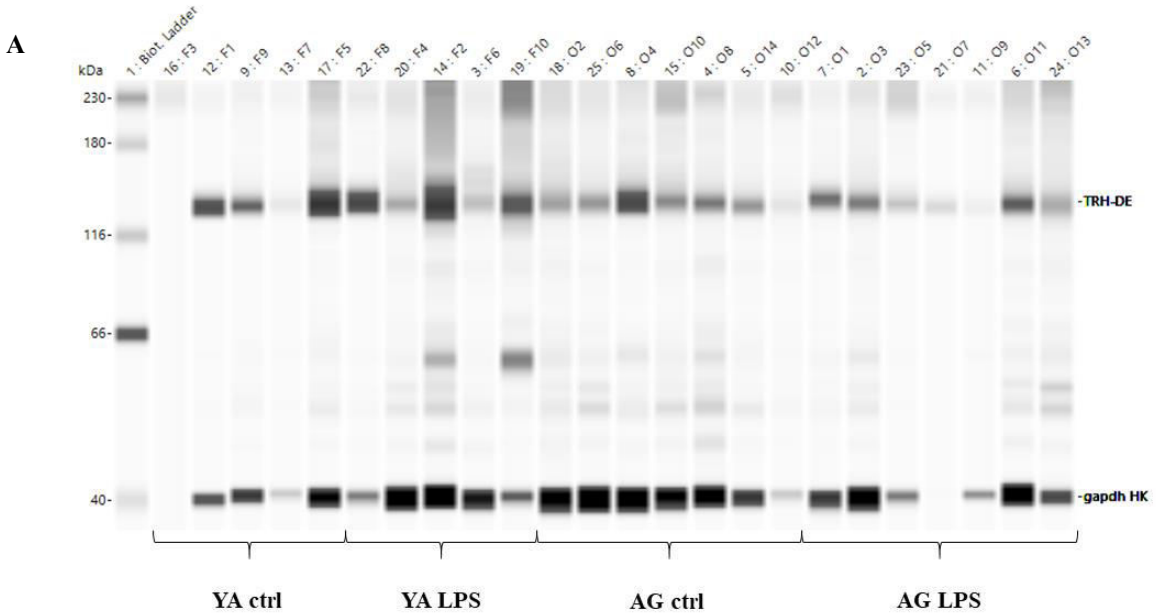

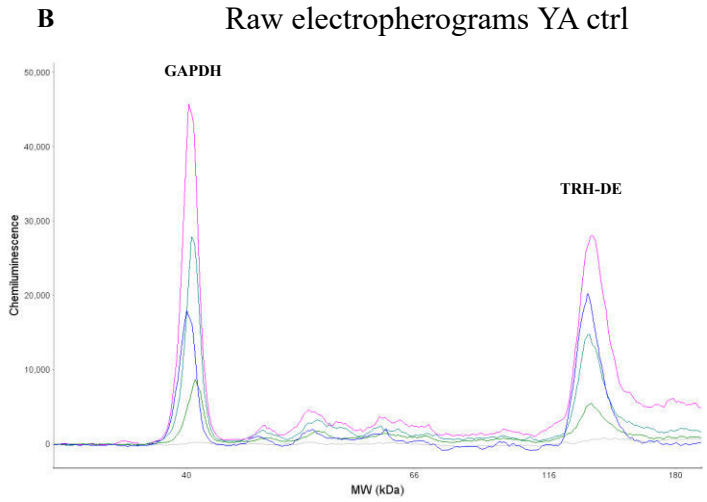

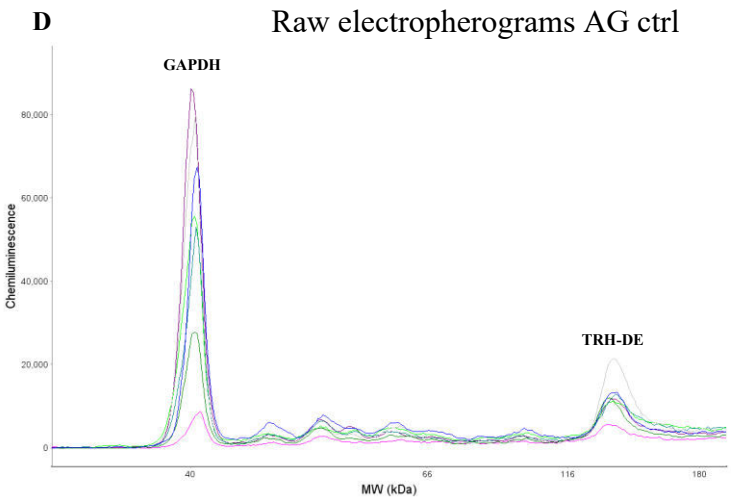

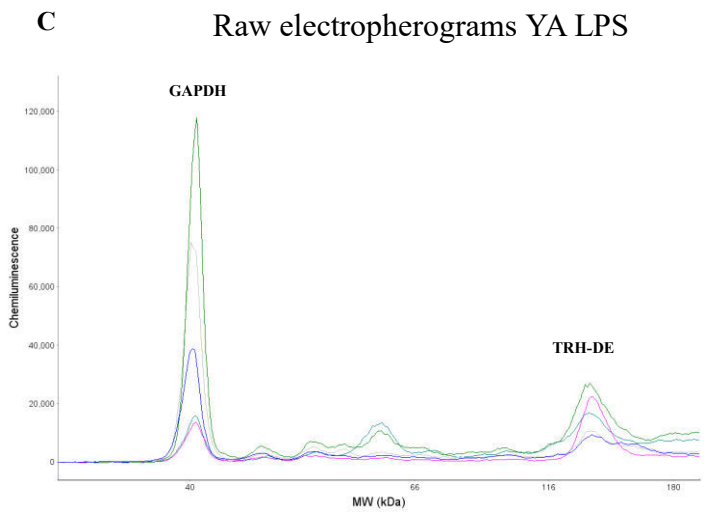

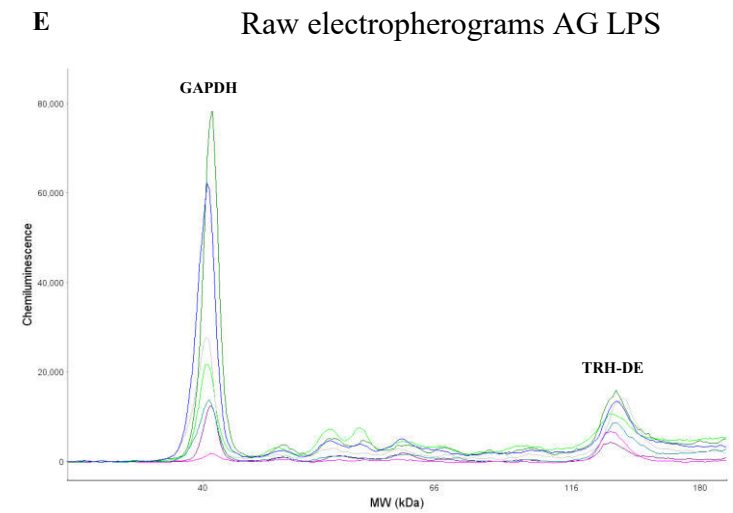

Supplemental Figure 2. Raw electropherograms and digital gel image of TRH-DE WES simple western capillary electrophoresis

Male THAI mice were treated with 150 µg/animal LPS *i.p.* n= 5-7/group

A: digitally generated gel image of all electropherograms; B-E: raw electropherograms of WES; B-C: young adults (YA); B: 0 h LPS treatment; C: 8 h LPS treatment; D-E: aged adults (AG); D: 0 h LPS treatment; E: 8 h LPS treatment

Supplemental Table 1: Taqman probes and gene names

Gene symbol	Gene name	Assay ID
Dio1	deiodinase, iodothyronine, type I	Mm00839358_m1
Dio2	deiodinase, iodothyronine, type II	Mm00515664_m1
Dio3	deiodinase, iodothyronine type III	Mm00548953_s1
Gapdh	glyceraldehyde-3-phosphate dehydrogenase	Mm99999915_g1
Hprt1	hypoxanthine guanine phosphoribosyl transferase	Mm01545399_m1
Luc	THAI mouse dCpG luciferase	custom probe, see ref. [12]
Mct8	monocarboxylate transporter 8	Mm01232724_m1
Oatp1c1	solute carrier organic anion transporter family member 1c1	Mm00451845_m1
proTrh	Thyrotropin-releasing hormone	Mm01963590_s1
Trh-de	TRH degrading ectoenzyme	Mm00455443_m1
Trh-r1	TRH receptor 1	Mm00443262_m1
Tshβ	Thyroid-stimulating hormone	Mm03990915_g1

International Journal of
Molecular Sciences

MDPI

Article

Tetrabromobisphenol A and Diclazuril Evoke Tissue-Specific Changes of Thyroid Hormone Signaling in Male Thyroid Hormone Action Indicator Mice

Richárd Sinkó [1,2], Kristóf Rada [1], Anna Kollár [3], Petra Mohácsik [1], Miklós Tenk [3], Csaba Fekete [4] and Balázs Gereben [1,*]

[1] Laboratory of Molecular Cell Metabolism, Institute of Experimental Medicine, H-1083 Budapest, Hungary
[2] János Szentágothai PhD School of Neurosciences, Semmelweis University, H-1085 Budapest, Hungary
[3] Department of Microbiology and Infectious Diseases, University of Veterinary Medicine, H-1143 Budapest, Hungary
[4] Laboratory of Integrative Neuroendocrinology, Institute of Experimental Medicine, H-1083 Budapest, Hungary
* Correspondence: gereben.balazs@koki.hu

Abstract: Thyroid hormone (TH) signaling is a prerequisite of normal tissue function. Environmental pollutants with the potential to disrupt endocrine functions represent an emerging threat to human health and agricultural production. We used our Thyroid Hormone Action Indicator (THAI) mouse model to study the effects of tetrabromobisphenol A (TBBPA; 150 mg/bwkg/day orally for 6 days) and diclazuril (10.0 mg/bwkg/day orally for 5 days), a known and a potential hormone disruptor, respectively, on local TH economy. Tissue-specific changes of TH action were assessed in 90-day-old THAI mice by measuring the expression of a TH-responsive luciferase reporter in tissue samples and by in vivo imaging (14-day-long treatment accompanied with imaging on day 7, 14 and 21 from the first day of treatment) in live THAI mice. This was followed by promoter assays to elucidate the mechanism of the observed effects. TBBPA and diclazuril impacted TH action differently and tissue-specifically. TBBPA disrupted TH signaling in the bone and small intestine and impaired the global TH economy by decreasing the circulating free T4 levels. In the promoter assays, TBBPA showed a direct stimulatory effect on the *hdio3* promoter, indicating a potential mechanism for silencing TH action. In contrast, diclazuril acted as a stimulator of TH action in the liver, skeletal muscle and brown adipose tissue without affecting the Hypothalamo-Pituitary-Thyroid axis. Our data demonstrate distinct and tissue-specific effects of TBBPA and diclazuril on local TH action and prove that the THAI mouse is a novel mammalian model to identify TH disruptors and their tissue-specific effects.

Keywords: TBBPA; diclazuril; endocrine disruption; tissue-specific thyroid hormone action; thyroid hormone action indicator mouse

Citation: Sinkó, R.; Rada, K.; Kollár, A.; Mohácsik, P.; Tenk, M.; Fekete, C.; Gereben, B. Tetrabromobisphenol A and Diclazuril Evoke Tissue-Specific Changes of Thyroid Hormone Signaling in Male Thyroid Hormone Action Indicator Mice. *Int. J. Mol. Sci.* **2022**, *23*, 14782. https://doi.org/10.3390/ijms232314782

Academic Editor: Heike Heuer

Received: 26 October 2022
Accepted: 23 November 2022
Published: 26 November 2022

1. Introduction

Thyroid hormone (TH) signaling is a well-known, fundamental regulator of cellular functions. Physiological levels of TH action represent a prerequisite of normal tissue function during development and adulthood [1]. Tissue TH action is regulated by a complex machinery that allows the generation and maintenance of tissue-specific signatures of TH action that can be independent of the relatively stable circulating serum TH levels [2–6].

Environmental pollutants with endocrine disruptor activity represent a growing concern, since these molecules reach the food chain via water and agricultural production and consequently can seriously impact human and animal health [7–9]. Despite intense efforts and progress made in the screening of potential endocrine disruptor activities, our knowledge is still limited concerning the impact of these molecules on tissue-specific TH action. This is also associated with the limitations of the available experimental models [10–12]. While in recent years the number of novel test systems has appeared to be growing, a

common aspect of most in vivo models is the use of endogenous genes as markers of TH action. These genes are simultaneously regulated by numerous signaling systems, with potential interference between direct and indirect effects of the tested disruptor on TH economy [13,14]. Therefore, the assessment of endocrine disruptor activity in mammalian tissues remains a major challenge.

We generated the THAI transgenic mouse model, which has been proven suitable to selectively assess tissue-specific TH action in an unbiased manner using a TH-responsive luciferase reporter system while all members of the local TH signaling machinery remain intact [15–17]. We used this model to assess the endocrine disruptor activity of two compounds, tetrabromobisphenol A (TBBPA) and diclazuril.

Tetrabromobisphenol A (TBBPA) is the most common flame retardant used for the production of printed electronic circuit boards, various plastic products and textiles [18,19]. It is discharged into the environment during manufacturing, use and disposal of electrical equipment, which results in the contamination of air, water, soil, sediments and sewage sludge [20,21]. TBBPA was found to be a TH disrupting agent by studying *Rana* and *Xenopus* metamorphosis [10,22].

Alarmingly, TBBPA was also detected in aquatic food samples at concentrations as high as 207.3 ng/g lipid weight, further increasing human exposure [23]. Consequently, TBBPA was also found in human tissues, milk and serum, and its concentrations reached 37 ng/g in breast milk and 649 ng/g in umbilical cord serum [8,24,25]. In addition, TBBPA showed neurotoxic, nephrotoxic and hepatotoxic effects and also impacted reproductive health in various animal models [10,26,27]. In human studies, it has been shown to affect the endocrine and immune systems especially during development and pregnancy [12,28,29]. The acute toxicity indicated by the LD50 was determined to be between 5 and 10 g/bwkg after a single oral dose in mice, rats and rabbits [30].

Diclazuril is widely used as an antiprotozoal agent and acts by targeting the chlorophyll a-D1 complex. It is used to prevent and treat coccidiosis in multiple species and is also applied against equine protozoal myeloencephalitis, and to a lesser extent, toxoplasmosis and neosporosis [31,32]. Its oral or subcutaneous dosages up to 5000 mg/bwkg caused no mortality in mice and rats [33].

Coccidiosis poses an especially significant health risk in poultry, with significant economic consequences. As chickens are often treated with medicated food containing diclazuril, human exposure is a realistic scenario. Thus, the effect of diclazuril on the human TH economy needs to be further investigated [34]. Diclazuril is considered to be safe against toxoplasmosis during pregnancy in a mouse model [35]. However, continuous exposure leads to stable plasma levels, which raises human concerns and calls for further studies. Furthermore, its potential to disrupt hormonal signaling is poorly documented, but its ability to bind androgen receptors was shown, along with data of its potential to antagonize TH receptors in a high-throughput cell-based reporter gene assay [36,37].

Our data obtained in the THAI mouse demonstrate that TBBPA and diclazuril exert a tissue-specific impact on mammalian TH action detectable in living animals and in isolated tissue samples. The obtained data demonstrated the tissue-specific effects of TBBPA and diclazuril on local and global TH economy. They also proved that the THAI mouse provides a selective in vivo tissue-specific mammalian model to screen the potential of compounds to disrupt TH signaling.

2. Results

2.1. Tissue-Specific Effects of TBBPA and Diclazuril on Peripheral TH Action

To assess the effect of TBBPA and diclazuril on TH action in different peripheral tissues, we used our THAI mouse as an animal model [15]. TH action was assessed in tissue samples by measuring the mRNA level of the TH-responsive luciferase reporter system in dissected tissues with Taqman qPCR. We administered 150 mg/bwkg/day of TBBPA for 6 days and 10.0 mg/bwkg/day of diclazuril for 5 days by oral gavage.

After the TBBPA treatment, TH action remained unchanged in the heart, interscapular brown adipose tissue (BAT), skeletal muscle, skin, small intestines and liver (Figure 1A–F). In contrast, TH action in the bone was strongly decreased (Figure 1G).

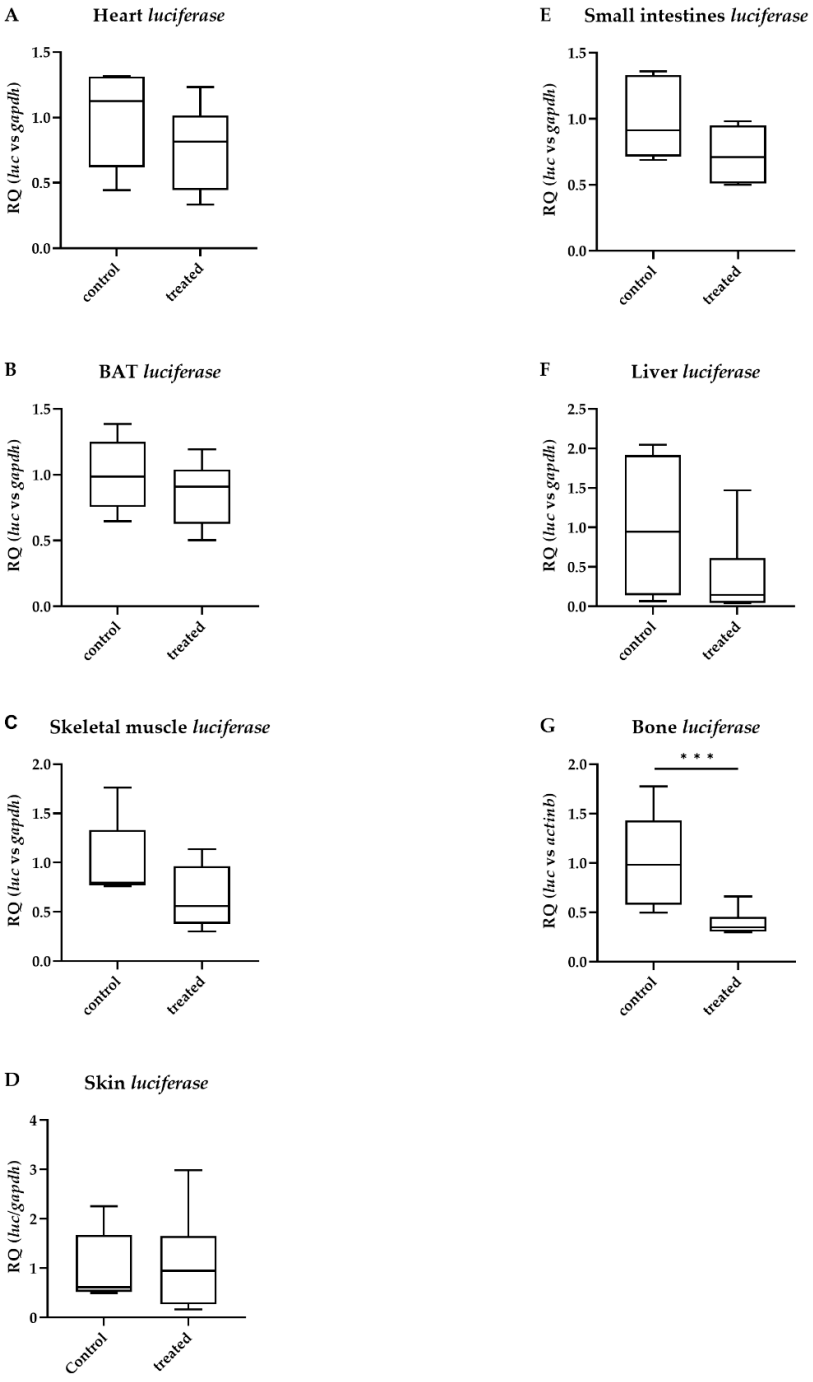

Figure 1. Peripheral thyroid hormone action after tetrabromobisphenol A (TBBPA) treatment. Thyroid hormone action quantified with *luciferase* mRNA levels in male THAI mice after six days of oral administration of 150 mg/bwkg/day of TBBPA in corn oil containing 2% Et-OH; (**A**) heart; (**B**) brown adipose tissue; (**C**) skeletal muscle; (**D**) skin; (**E**) small intestine; (**F**) liver; (**G**) bone. n = 4–6 mice/group; figure shows Tukey Box Plots, $\alpha = 0.05$; ***: $p < 0.001$.

Similarly to TBBPA, diclazuril left TH action unchanged in the heart, BAT, skin and small intestine (Figure 2A,B,D,E). However, diclazuril increased TH action in the skeletal muscle and liver (Figure 2C,F) and did not change TH action in the bone (Figure 2G).

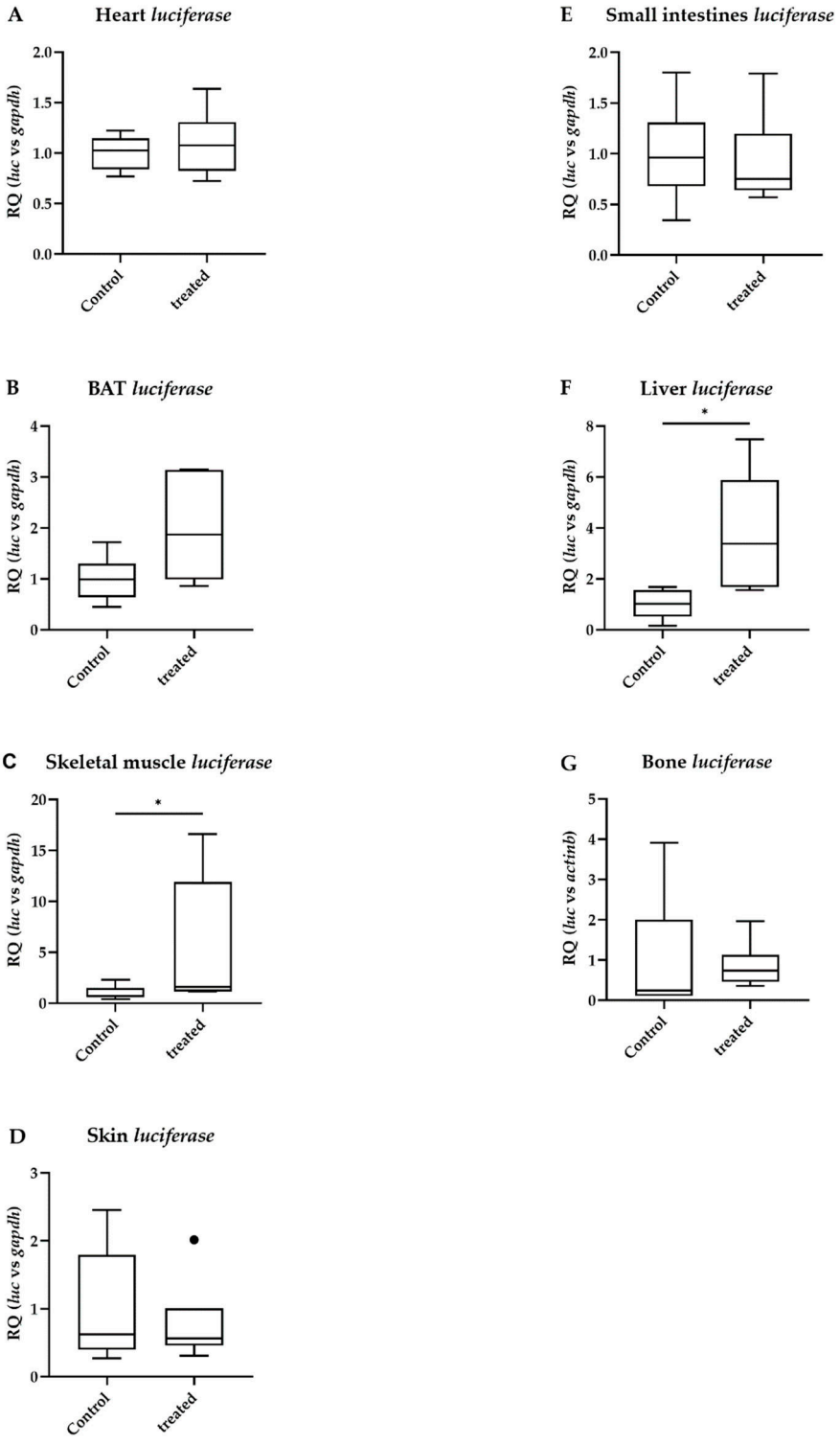

Figure 2. Peripheral thyroid hormone action after diclazuril treatment. Thyroid hormone action quantified with *luciferase* mRNA levels in male THAI mice after five days of oral administration of 10 mg/bwkg/day of diclazuril in saline suspension; (**A**) heart; (**B**) brown adipose tissue; (**C**) skeletal muscle; (**D**): skin; (**E**) small intestine; (**F**) liver; (**G**) bone. n = 5–6/group; figure shows Tukey Box Plots, $\alpha = 0.05$; *: $p < 0.05$.

2.2. Distinct Impacts of TBBPA and Diclazuril on Local TH Action in Live THAI Mice

After assessing the impact of the two compounds in various peripheral tissues, we were interested in whether a less invasive, in vivo method allowing a longer follow-up

of the same animal would be adequate to assess trending changes that did not reach significance in tissue homogenates (Figures 1 and 2). Therefore, we subjected the THAI mice to in vivo imaging according to our established protocol that allows the assessment of TH signaling in the small intestine and BAT of the THAI mouse [15]. We measured TH action in these tissues with a longer treatment time than in the previous experiments, using similar doses of the compounds. A 14-day-long treatment was accompanied with imaging on day 7, 14 and 21 from the first day of treatment. The animals were subjected to bioluminescent in vivo imaging before the first treatment, after 1 and 2 weeks of daily treatment and finally after one week from treatment withdrawal. Each animal served as a self-control for its own measurements.

In the small intestine, TH action was decreased after 2 weeks of TBBPA treatment and then recovered after the recovery week (Figure 3A). In contrast, diclazuril induced a significantly elevated TH action in BAT that also recovered after 1 week (Figure 3B). The observed changes confirmed the trend obtained in mRNA expression in tissue homogenates (Figures 1E and 2B).

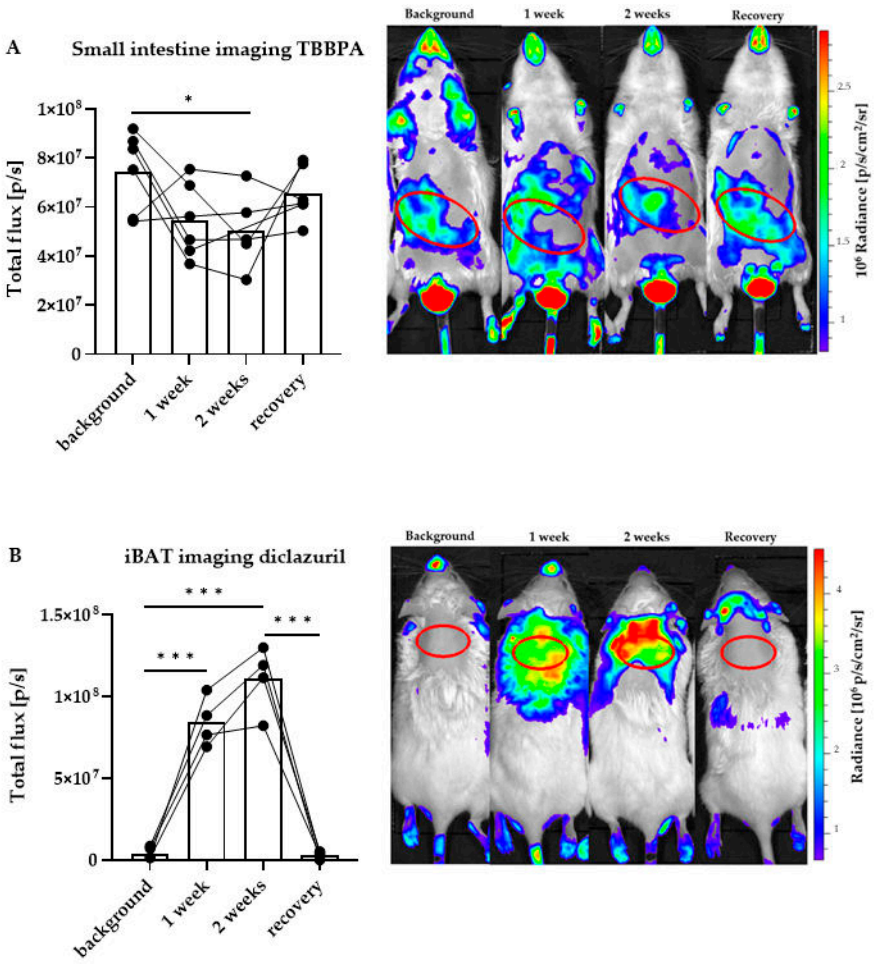

Figure 3. Quantitation of local thyroid hormone action after disruptor treatment with in vivo imaging. Representative images and quantification in male THAI mice treated orally for two weeks with 150 mg/bwkg/day of TBBPA in corn oil containing 2% Et-OH, or 10 mg/bwkg/day of diclazuril as a saline suspension, followed by one week of recovery; (**A**) ventral in vivo imaging of TBBPA treatment; (**B**) dorsal in vivo imaging of diclazuril treatment. n = 4–6 mice/group; figure shows Tukey Box Plots, $\alpha = 0.05$; *: $p < 0.05$, ***: $p < 0.001$.

2.3. TBBPA Impacts the Hypothalamo–Pituitary–Thyroid (HPT) Axis, While Diclazuril Does Not

To assess whether the observed changes were the consequence of a local impact on TH action or were associated with an altered function of the HPT axis, we measured parameters that hallmark the activity of the HPT axis in animals treated with TBBPA or diclazuril.

After TBBPA treatment, *trh* expression in microdissected hypothalamic paraventricular nucleus (PVN) samples did not change significantly, despite a trend toward an increase (63% increase, $p = 0.064$). This was accompanied by unaltered *tshb* mRNA levels in the pituitary (Figure 4A,B); in parallel, TH action remained unchanged in the microdissected hypothalamic arcuate nucleus median eminence (ARC-ME) region and in the pituitary (Figure 4C,D). Similar results were obtained with diclazuril (Figure 4E–H), except for the lack of a trend toward an increase in *trh* expression in the PVN.

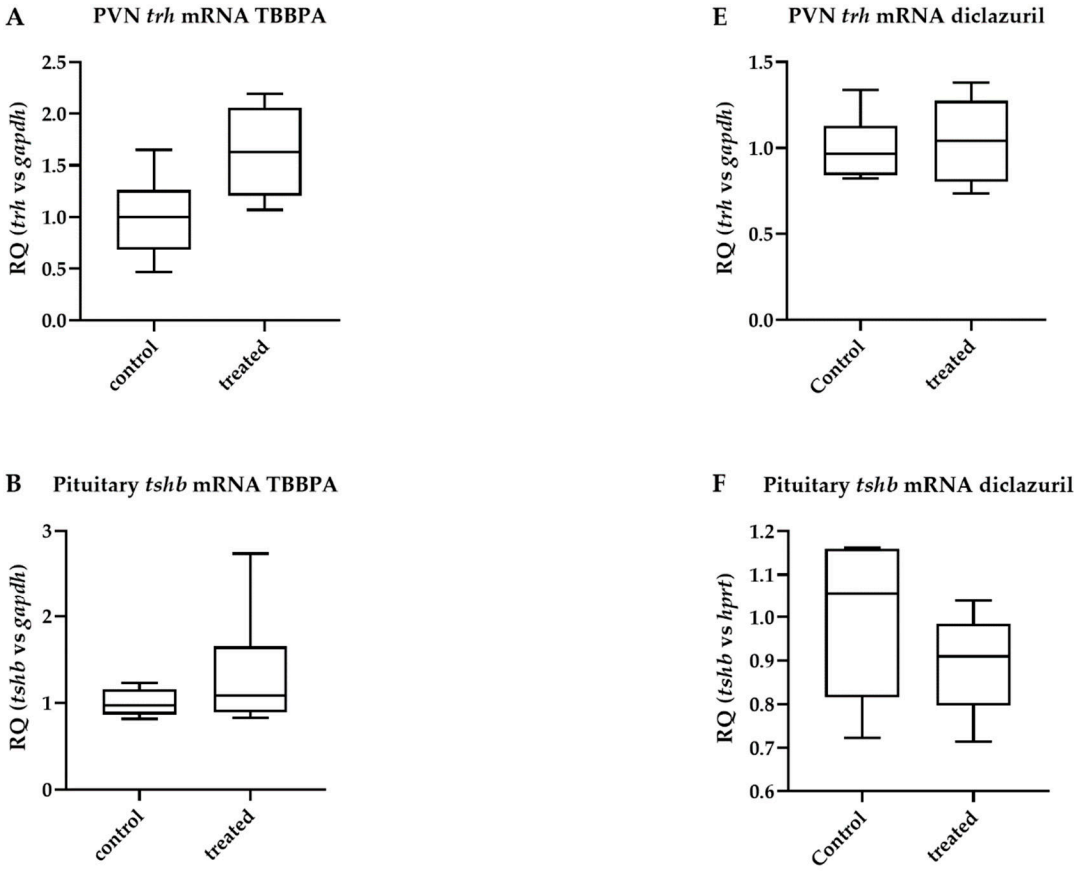

Figure 4. *Cont.*

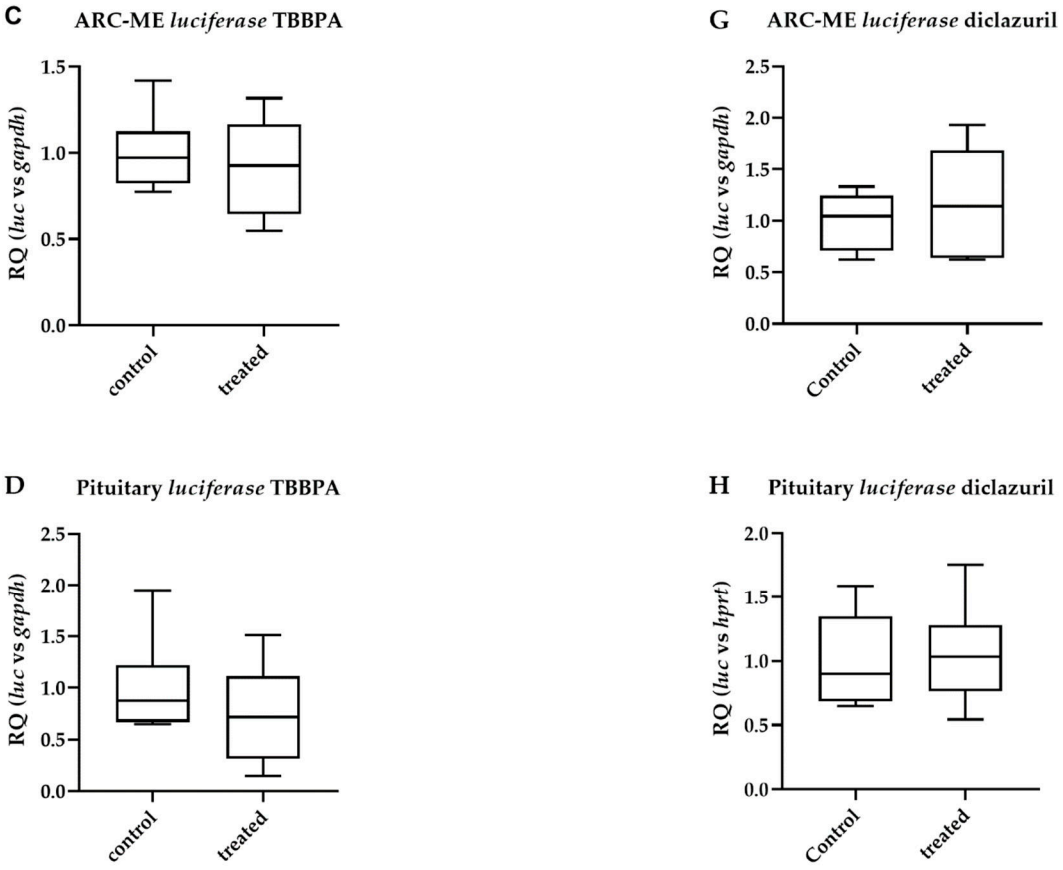

Figure 4. Hypothalamic and pituitary effects of disruptor treatment. Male THAI mice treated orally for 6 days with 150 mg/bwkg/day of TBBPA in corn oil containing 2% Et-OH or for 5 days with 10 mg/bwkg/day of diclazuril as a saline suspension; thyroid hormone action quantified with *luciferase* mRNA levels; (**A**–**D**) TBBPA; (**E**–**H**) diclazuril; (**A**) PVN *trh* mRNA after TBBPA; (**B**) pituitary *tshb* mRNA after TBBPA; (**C**) ARC-ME *luciferase* mRNA after TBBPA; (**D**) pituitary *luciferase* mRNA after TBBPA; (**E**) PVN *trh* mRNA after diclazuril; (**F**) pituitary *tshb* mRNA after diclazuril; (**G**) ARC-ME *luciferase* mRNA after diclazuril; (**H**) pituitary *luciferase* mRNA after diclazuril. n = 4–6 mice/group; figure shows Tukey Box Plots, $\alpha = 0.05$.

However, despite the unchanged central parameters, massively decreased circulating free T4 (fT4) levels were detected after TBBPA treatment, while free T3 (fT3) remained unchanged (Figure 5A,B). Both fT4 and fT3 remained unchanged after diclazuril treatment (Figure 5C,D).

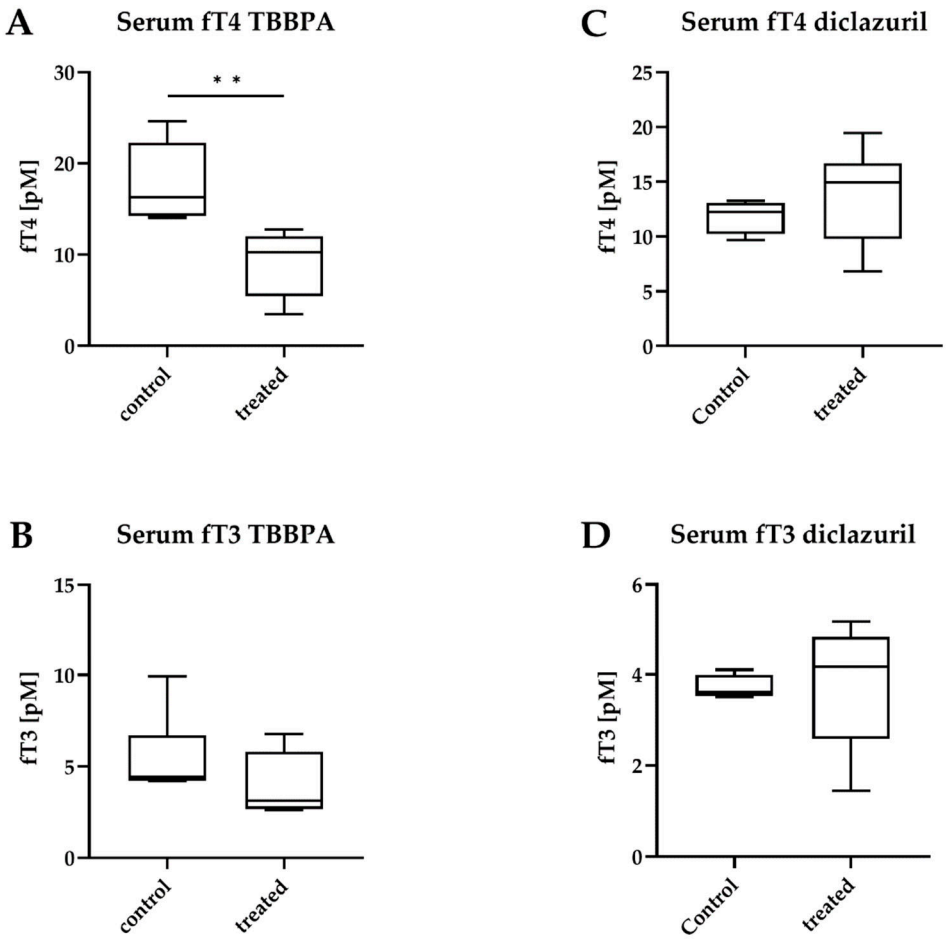

Figure 5. Circulating hormone levels after disruptor treatment. Male THAI mice treated orally for 6 days with 150 mg/bwkg/day of TBBPA in corn oil containing 2% Et-OH or for 5 days with 10 mg/bwkg/day of diclazuril as a saline suspension; (**A**,**B**) TBBPA; (**C**,**D**) diclazuril; (**A**) serum free T4 (fT4) after TBBPA; (**B**) serum free T3 (fT3) after TBBPA; (**C**) serum fT4 after diclazuril; (**D**) serum fT3 after diclazuril. n = 4–6 mice/group; figure shows Tukey Box Plots, $\alpha = 0.05$; **: $p < 0.01$.

2.4. Diclazuril Does Not Impact the Cerebral Cortex; the Effect of TBBPA on dio3 Expression Is Counterbalanced by Local Mechanisms

Having studied the impact of TBBPA or diclazuril on the HPT axis, we also investigated how the cerebral cortex, a region protected by the blood–brain barrier, was affected by these compounds. Both treatments resulted in unchanged cortical TH action (Figure 6A,C).

Since the cortex is known to be programmed to maintain T3 homeostasis [2], we tried to characterize local regulators of TH action in the cortex under the present treatment. Monocarboxylate transporter 8 (MCT8) is one of the major TH transporters with a critical function in the brain. Neither TBBPA nor diclazuril had an effect on the mRNA levels of *mct8*, suggesting unaltered TH transport (Figure 6B,D).

Neuronal TH action is heavily regulated by type 3 deiodinase (D3), the main TH-degrading enzyme [38]. To further characterize the cortical effects of TBBPA or diclazuril, we also studied how *dio3* was impacted. TBBPA exerted a tissue-specific effect on *dio3* expression; it was decreased in the cortex, increased in the hippocampus and remained unchanged in the pituitary and liver (Figure 7A).

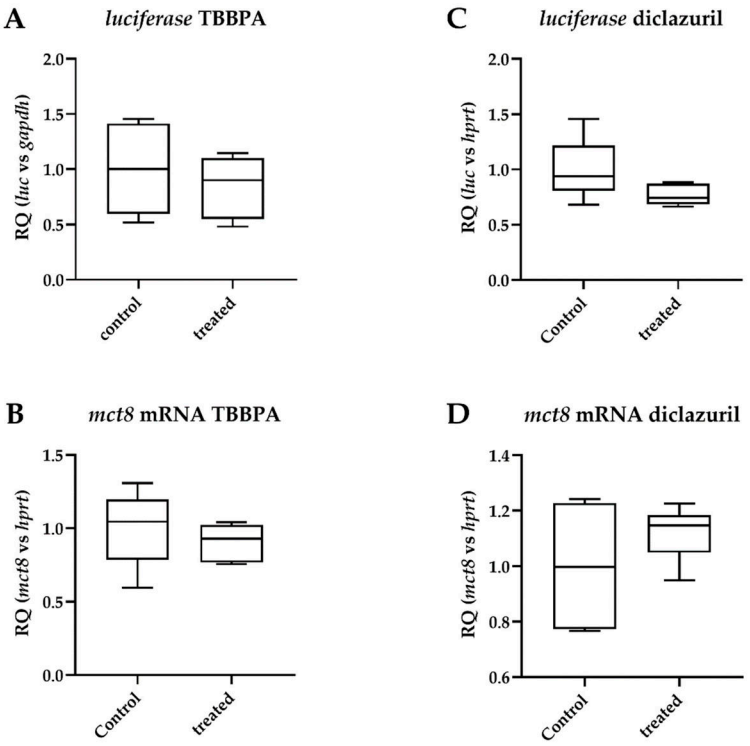

Figure 6. Changes in parameters of thyroid hormone action in the cerebral cortex after disruptor treatment. Male THAI mice treated orally for 6 days with 150 mg/bwkg/day of TBBPA in corn oil containing 2% Et-OH or for 5 days with 10 mg/bwkg/day of diclazuril as a saline suspension; thyroid hormone action quantified with *luciferase* mRNA levels; (**A**,**B**) TBBPA; (**C**,**D**) diclazuril; (**A**) *luciferase* mRNA after TBBPA; (**B**) *mct8* mRNA after TBBPA; (**C**) preamplified *luciferase* mRNA after diclazuril; (**D**) *mct8* mRNA after diclazuril. n = 5–6 mice/group; figure shows Tukey Box Plots, $\alpha = 0.05$.

A

Treatment	Tissue	Fold change			p value
		mean	SD	regulation	
TBBPA	hippocampus	3.84	2.68	↑	0.0304
	pituitary	1.39	0.54	↔	0.2616
	cortex	0.49	0.16	↓	0.0258
	liver	0.31	0.20	↔	0.1076
Diclazuril	cortex	1.25	0.31	↔	0.1557

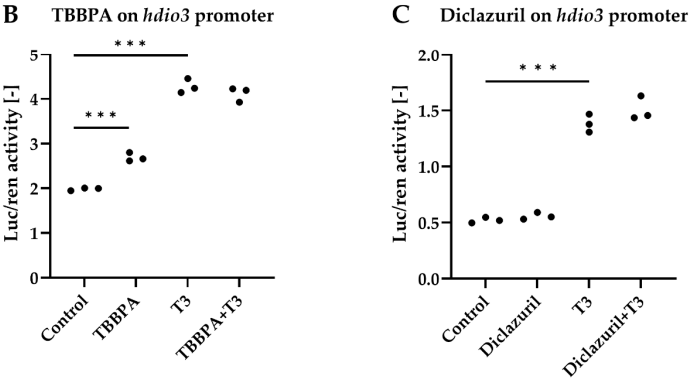

Figure 7. Regulation of *dio3* expression by TBBPA and diclazuril. (**A**) of *dio3* mRNA changes in different tissues of male THAI mice treated orally for 6 days with 150 mg/bwkg/day of TBBPA in corn oil containing 2% Et-OH or for 5 days with 10 mg/bwkg/day of diclazuril as a saline suspension; (**B**,**C**) transfected HEK293T cultures treated with 50 nM T3 and/or 1 μM TBBPA or diclazuril measured with Dual-Luciferase Reporter Assay. n = 4–6 mice/group for A, $\alpha = 0.05$; ***: $p < 0.001$.

To understand whether these were indirect, compensatory changes or direct effects of TBBPA on the *dio3* promoter, we performed promoter assays in HEK293T cell cultures transfected with a luciferase reporter linked to a *dio3* promoter, which enabled the bioluminescent quantitation of promoter activity. TBBPA increased *dio3-luciferase* expression in hormone-free medium and did not have an additive effect in the presence of 50 nM T3, that, as expected, also induced reporter expression in the presence of TRβ (Figure 7B). In contrast, diclazuril did not regulate *dio3* promoter activity either in the cerebral cortex or in the in vitro promoter assay (Figure 7A,C). Interestingly, TBBPA is likely able to impact the local TH action in various tissues by directly interacting with the *dio3* promoter, but this effect seems to be insufficient to alter cortical TH action, as shown by the unaltered *luciferase* mRNA level.

3. Discussion

Environmental pollution is growing due to industrialization and intense arable and livestock farming. Many of the polluting compounds have been used widely for a long time, which has led to their accumulation in the environment [9]. As a consequence, chemical compounds reach the human population, and there is growing evidence suggesting that this interaction is associated with the development of human diseases [39–41]. Therefore, it has become critically important to uncover the potential hazards these molecules could exert on the population.

Endogenous, non-peptide hormones that control sexual functions, growth, cellular metabolism and differentiation often contain aromatic rings as a molecular backbone. Unsurprisingly, many cyclic and aromatic chemicals can interact with these molecules, thus interfering with various hormonal actions. Hormones of the thyroid gland represent no exceptions due to their aromatic amino acids that are critical for tissue function.

Impairments of TH action result in tissue disfunction, with documented consequences on human health [1,6]. TH economy is regulated by two major regulatory systems. Circulating TH levels are maintained centrally by the HPT axis, yet the target tissues have a striking autonomy to develop their own TH action by a cell-type specific local, intracellular regulatory system that involves TH activation and inactivation by deiodination, TH uptake by specific transporters and the TH receptor complex [4,5]. Due to this complex regulation, compounds like endocrine disruptors can affect TH economy also without affecting the circulating TH levels [42]. Therefore, it is of increasing interest to study the impact of endocrine disruptors on TH economy in a tissue-specific context.

In order to assess TH action in specific tissues of mice in the most unbiased way possible, we generated the THAI transgenic mouse model that expresses a specifically TH-responsive luciferase reporter system [15]. This model provides a proven approach to quantify the local TH action in microdissected brain regions, peripheral tissue samples and live mice by in vivo imaging [15–17]. Importantly, the assessment of TH signaling in this model is free from the confounding effects of non-TH-dependent pathways that are also able to impact the expression of endogenous TH-responsive genes, e.g., *enpp2*, a well-known endogenous TH marker gene that is also regulated by estrogen [43]. However, the reporter system of the THAI mouse overcomes these problems and provides a highly selective approach to assess TH action. While the THAI mouse provides a model to assess the disruptor potency of specific compounds in an intact mammalian tissue context, species-specific differences should be also kept in mind when extrapolating data. The picture could be further complicated by the species-specific metabolism of specific compounds, giving rise to bioactive metabolites. However, the THAI mouse can be subjected to in vivo imaging that allows to perform self-controlled experiments. This provides the advantage of studying the kinetics of the impact of disruptor exposure even during an extended time period that could much better model the real-life exposure of humans and animals. In addition, it also contributes to facilitating the reduction of the number of used experimental animals.

TBBPA and diclazuril treatments were performed according to literature data [27,44]. In comparison to the used dose, TBBPA concentration is significantly lower in human

tissues (see Introduction), but it is obvious that only a fraction of the orally given dose will be deposited in tissues; furthermore, our exposure time was considerably shorter compared to real-life exposure.

TBBPA, a commonly used flame retardant, is known to impact TH economy. It was shown in an in vitro reporter assay in cultured neural cells that TBBPA can directly interfere with the response to T3 of TH-regulated genes [45]. It was also shown that TBBPA treatment decreased the circulating T4 levels in rats, which was accompanied with unchanged T3 and TSH levels [46].

We observed the same phenomenon in THAI mice. fT4 was decreased along with a strong trend toward an increase of TRH expression in the PVN that did not reach statistical significance. Based on this, it can be speculated that TBBPA acts at the level of the thyroid gland, e.g., by interfering with the hormone synthesis; the observed decrease in TH signaling in the bone and small intestine could be a direct consequence of decreased T4 levels. This hypothesis is supported by data showing that TH signaling in these tissues are markedly sensitive to the circulating TH levels compared to what observed in other tissues [15].

Tissue-specific TH action is a net result of TH availability and in certain tissues partially relies on the local deactivation of TH by the T3-degrading D3 enzyme. In *hdio3* promoter assays, we found that TBBPA stimulated the *dio3* promoter. This discovery suggests that altering the D3-encoding *dio3* gene activity can be another checkpoint where TBBPA potentially interferes with local TH action. This would represent a novel example of how endocrine disruptors act via altering hormone metabolism/inactivation, one of the categories listed by the recent Consensus Statement on the characteristics of endocrine-disrupting chemicals [47]. Generally, increased net *dio3* activity in the periphery could contribute to the observed lowered fT4 along with a relatively intact HPT axis. However, the tissue-specific changes of *dio3* expression point towards a more complex phenomenon, which makes it difficult to formulate generalized conclusions about the peripheral TH metabolism.

Importantly, the statistically not significant change in *trh* expression in the PVN does not exclude the possibility of the large observed difference being a functional response of the HPT axis. This seems to be controversial, since another study using hypothalamic in vivo transfection of a *trh-luc* construct into the mouse hypothalamus found either an increase or a decrease in *trh* transcription depending on the TBBPA treatment regime [27]. However, it is difficult to compare these findings with our data, since we measured endogenous *trh* expression in microdissected PVN samples in contrast to the mentioned study in which the transcriptional activity of a ~500-bp *trh* 5′FR-luc was assessed in the whole hypothalamus [27]. It can be speculated that the impact of TBBPA on the HPT axis is a net effect of various minor effects resulting in the partial downregulation of the global TH economy.

The veterinary drug diclazuril is used as a coccidiostatic agent [31,32]. Our data also provided evidence that in addition to TBBPA, diclazuril acts as a modulator of tissue-specific TH signaling. In contrast to TBBPA, all effects of diclazuril we observed in the THAI mice were stimulatory of TH action. Interestingly, these changes were accompanied with unchanged circulating TH levels and unchanged HPT axis parameters and a lack of a direct effect on the *dio3* promoter.

Considering that muscle, liver and fat have been reported to accumulate diclazuril [48], it is not surprising that the largest effects observed in the THAI mouse were found in these tissues. A longer exposure also allowed us to visualize the effect on BAT with in vivo imaging. Based on this, it is likely that the prolonged exposure increased the stimulatory capabilities of the drug on local TH action. However, after the recovery week, the observed effect disappeared, indicating a fast clearance in vivo. While these remarks suggest that diclazuril is rather an endocrine modulator than a disruptor, our data hint towards diclazuril being able to substantially modify the local TH action under continuous exposure.

In the case that the observed stimulatory effect of diclazuril occurred in treated poultry, this could result in elevated tissue energy expenditure and metabolism by increasing TH-dependent gene expression in the muscle and liver. While it has been thought that BAT-dependent thermogenesis is absent in the chicken, this has been recently questioned by demonstrating the emergence of beige-like fat as a physiological adaptation to cold [49]. This induction of BAT TH signaling by diclazuril could contribute to non-shivering thermogenesis and energy loss also in the chicken, but further studies are required to directly prove this hypothesis. Additionally, an effect of diclazuril on the growth performance and feed conversion of the chicken was studied, although the topic has not been widely investigated yet, and the results are controversial [50].

Medication may have a direct influence on growth performance, which might originate either from the direct modulation of tissue-specific TH signaling by a drug or from its inhibitory effect on subclinical or clinical coccidiosis, which of course per se negatively influences growth performance and body weight gain. In order to reveal a direct modulatory effect, studies on further target species are needed in the absence of coccidial infection. Would such effect truly exist, its connection to altered TH action would be plausible.

In summary, our data provide evidence of a tissue specific disruption of TH signaling by TBBPA in the mouse, while also revealing the stimulatory effect of diclazuril on TH signaling without affecting the HPT axis. The current experiments also prove that THAI mouse can be used as an in vivo model to assess the potential of specific compounds to disrupt TH economy. In the BAT and small intestine, THAI mouse also provides a tool to perform self-controlled longitudinal studies on live mice to assess modulation of TH signaling.

4. Materials and Methods

4.1. Animals

The experiments were performed on ~90-day-old male THAI#4 mice; in vivo imaging experiments were performed on white furred THAI mice. Animals had food and water ad libitum and were housed under standard conditions. The experimental protocol was reviewed and approved by the Animal Welfare Committee at the Institute of Experimental Medicine (PE/EA/106-2/2021).

4.2. Animal Treatment and Sample Collection

TBBPA (Sigma) was delivered by oral gavage in corn oil containing 2% Et-OH as a saline suspension, in a dose of 150 mg/bwkg/day as described [27]. The treatment lasted 6 days, and control animals received the vehicle. Diclazuril (Sigma-Aldrich, St. Louis, MO, USA) was delivered by oral gavage in a dose of 10.0 mg/bwkg/day as a saline suspension as described [44]. Diclazuril treatment lasted 5 days, and control animals received the vehicle. Following the last treatment, the animals were sacrificed by decapitation, and trunk blood was collected. Peripheral tissues and brain regions were harvested and flash-frozen in dry ice. The PVN and ARC-ME regions were microdissected with the Palkovits punch technique; bone was collected from the distal part of the tibia and skeletal muscle was collected from musculus gastrocnemius. Treatment for in vivo imaging was continued for 14 days, followed by a 7-day-long withdrawal.

4.3. In Vivo Imaging

In vivo imaging was performed on anesthetized animals according to our established protocol, as previously described [15]. In short, THAI mice were anesthetized with ketamine–xylazine (50 and 10 µg/bwkg, respectively) i.p. Hair covering the abdominal or scapular regions was removed by a commercial depilatory cream, and D-luciferin (sodium salt, Gold Biotechnology, St. Louis, MO, USA) was introduced i.p. (150 µg/bwg). Images were taken after 15 min of incubation with 3 min acquisition time. Measurements were taken after 7, 14 and 21 days after the first day of treatment.

4.4. Serum Hormone Measurements

FT4 and fT3 levels were measured with the AccuLite CLIA Microwells kit (cat. no. 1275-300B and 1375-300B, respectively, Monobind Inc., Lake Forest, CA, USA) according to the manufacturer's instructions in a Luminoskan Ascent (Thermo Fisher Scientific, Waltham, MA, USA) machine. However, TBBPA being a structural analogue, we were curious about whether it directly distorted the results. Spiked samples were used to elucidate this; control and treated animal sera were spiked with TBBPA in excess and resulted in the same concentrations as the unspiked samples. We concluded that the CLIA method was fit for our analytical purpose.

4.5. Taqman qPCR

Total RNA from tissues was isolated with the NucleoSpin RNA kit (Macherey-Nagel, Düren, Germany) according to the manufacturer's instructions, with the following modifications. Non-brain samples were first homogenized with 1 mL Trizol reagent, extracted with 200 µL of chloroform and separated by centrifugation (15 min, 12,000× *g* on 4 °C). The supernatant was processed using the kit, as instructed. Then, 1 µg of total RNA was transcribed with the High-Capacity Reverse Transcription kit (Applied Biosystems, Waltham, MA, USA), as instructed. The product cDNA content was measured with the Qubit ssDNA assay (Invitrogen, Waltham, MA, USA), using 10 ng of cDNA in all Taqman reactions (Viia7, Applied Biosystems). The Taqman gene expressions assays are detailed in Table 1 (Thermo Fisher Scientific, Waltham, MA, USA). qPCR on microdissected brain regions of the THAI mouse was performed as described [17]. If a gene of interest was measured above 34 cycles, preamplification was performed with 5.55 ng of cDNA/reaction (Applied Biosystems). The preamplified DNA was not normalized for DNA content but only with respect to preamplified *hprt*. The details of qPCR are shown in the figure legends when relevant.

Table 1. Taqman gene expression assays.

Gene Symbol	Gene Name	Assay ID
actinb	β actin	Mm02619580_g1
dCpG luciferase	dCpG luciferase reporter (custom made)	AIY9ZTZ
dio3	deiodinase, iodothyronine type III	Mm00548953_s1
gapdh	glyceraldehyde-3-phosphate dehydrogenase	Mm99999915_g1
hprt1	hypoxanthine guanine phosphoribosyl transferase	Mm01545399_m1
slc16a2	MCT8, monocarboxylate transporter 8	Mm01232724_m1
trh	Thyrotropin releasing hormone	Mm01963590_s1
tshb	thyroid stimulating hormone, beta subunit	Mm03990915_g1

4.6. Cell Transfection and Luciferase Assay

The *hdio3* promoter–reporter construct contains 4327 bp of the 5′-flanking region plus 224 bp of the 5′-untranslated region of the human *dio3* gene. It was a gift of Prof. M. Dentice (University of Naples Federico II Italy) and was prepared as earlier described [51]. HEK293T cells were plated on 24-well plates in normal medium (89% DMEM, 10% FBS, 1% penicillin–streptomycin). Before transfection, the medium was changed to a hormone-free medium containing charcoaled FBS. The cells were transfected with the *dio3-luciferase* reporter, *Renilla luciferase* reporter and TRβ with X-tremeGene HP DNA transfection reagent (cat. no. 06366236001, Roche Basel, Switzerland) overnight. Then, the medium was replaced with hormone-free medium containing 50 nM T3 and/or 1 µM of TBBPA/diclazuril. The cells were harvested after 24 h of treatment. Luciferase and Renilla activity were measured with the Dual-Luciferase Reporter Assay System (Promega, Madison, WI, USA) according to the manufacturer's instructions in a Luminoskan Ascent (Thermo Scientific, Waltham, MA, USA) machine as previously described [52].

4.7. Data Analysis

Data were analyzed with STATISTICA v13 software (Tibco Software, Palo Alto, CA, USA). Figures were prepared with Prism 9.3 (GraphPad Software Inc., San Diego, CA, USA). The figures show Tukey Box Plots; the box represents the two middle quartiles, the lower whisker represents the lower quartile, the upper whisker represents the upper quartile, the line represents the median, the dots represent outlier data. The number of used animals is indicated in figure legends. Null-hypothesis significance tests were conducted with a 95% level of confidence. The Student's two sample two-sided t test was used to analyze two groups; one-way analysis of variance (ANOVA) followed by Tukey post-hoc test was used to compare more than two groups; ANOVA was applied as within-subjects ANOVA for in vivo imaging data. The models were deemed adequate based on residual plots and residual normal plots.

Author Contributions: Conceptualization: B.G., C.F., M.T. and A.K.; methodology: K.R., P.M., C.F. and B.G.; validation: R.S., C.F. and B.G.; formal analysis: R.S.; investigation: K.R., A.K., P.M. and R.S.; writing—original draft preparation: R.S., K.R. and B.G.; writing—review and editing: B.G. and C.F.; visualization: R.S.; supervision: B.G. and C.F.; project administration: B.G.; funding acquisition: B.G. and C.F. All authors have read and agreed to the published version of the manuscript.

Funding: This work was supported by grants to Project no. RRF-2.3.1-21-2022-00011, titled National Laboratory of Translational Neuroscience implemented with the support provided by the Recovery and Resilience Facility of the European Union within the framework of Programme Széchenyi Plan Plus and the National Research, Development and Innovation Office (NKFIH) of Hungary (K125247).

Institutional Review Board Statement: The experimental protocol was reviewed and approved by the Animal Welfare Committee at the Institute of Experimental Medicine, Hungary (PE/EA/106-2/2021).

Informed Consent Statement: Not applicable.

Data Availability Statement: Data are available on request.

Acknowledgments: We thank Andrea Juhász for her excellent technical support.

Conflicts of Interest: The authors declare no conflict of interest.

References

1. Larsen, P.R.; Davies, T.F.; Hay, I.D. The Thyroid Gland. In *Williams Textbook of Endocrinology*, 9th ed.; Wilson, J.D., Foster, D.W., Kronenberg, H.M., Larsen, P.R., Eds.; W.B. Saunders Co.: Philadelphia, PA, USA, 1998; pp. 389–515.
2. Gereben, B.; Zavacki, A.M.; Ribich, S.; Kim, B.W.; Huang, S.A.; Simonides, W.S.; Zeold, A.; Bianco, A.C. Cellular and molecular basis of deiodinase-regulated thyroid hormone signaling. *Endocr. Rev.* **2008**, *29*, 898–938. [CrossRef] [PubMed]
3. Boelen, A.; Kwakkel, J.; Fliers, E. Beyond low plasma T3: Local thyroid hormone metabolism during inflammation and infection. *Endocr. Rev.* **2011**, *32*, 670–693. [CrossRef] [PubMed]
4. Fekete, C.; Lechan, R.M. Central regulation of hypothalamic-pituitary-thyroid axis under physiological and pathophysiological conditions. *Endocr. Rev.* **2014**, *35*, 159–194. [CrossRef] [PubMed]
5. Gereben, B.; McAninch, E.A.; Ribeiro, M.O.; Bianco, A.C. Scope and limitations of iodothyronine deiodinases in hypothyroidism. *Nat. Rev. Endocrinol.* **2015**, *11*, 642–652. [CrossRef]
6. Bianco, A.C.; Dumitrescu, A.; Gereben, B.; Ribeiro, M.O.; Fonseca, T.L.; Fernandes, G.W.; Bocco, B. Paradigms of Dynamic Control of Thyroid Hormone Signaling. *Endocr. Rev.* **2019**, *40*, 1000–1047. [CrossRef]
7. Diamanti-Kandarakis, E.; Palioura, E.; Kandarakis, S.A.; Koutsilieris, M. The impact of endocrine disruptors on endocrine targets. *Horm. Metab. Res.* **2010**, *42*, 543–552. [CrossRef] [PubMed]
8. Feiteiro, J.; Mariana, M.; Cairrao, E. Health toxicity effects of brominated flame retardants: From environmental to human exposure. *Environ. Pollut.* **2021**, *285*, 117475. [CrossRef]
9. Guarnotta, V.; Amodei, R.; Frasca, F.; Aversa, A.; Giordano, C. Impact of Chemical Endocrine Disruptors and Hormone Modulators on the Endocrine System. *Int. J. Mol. Sci.* **2022**, *23*, 5710. [CrossRef]
10. Dong, M.; Li, Y.; Zhu, M.; Li, J.; Qin, Z. Tetrabromobisphenol A Disturbs Brain Development in Both Thyroid Hormone-Dependent and -Independent Manners in Xenopus laevis. *Molecules* **2021**, *27*, 249. [CrossRef]
11. Beck, K.R.; Sommer, T.J.; Schuster, D.; Odermatt, A. Evaluation of tetrabromobisphenol A effects on human glucocorticoid and androgen receptors: A comparison of results from human- with yeast-based in vitro assays. *Toxicology* **2016**, *370*, 70–77. [CrossRef]

12. Mughal, B.B.; Fini, J.B.; Demeneix, B.A. Thyroid-disrupting chemicals and brain development: An update. *Endocr. Connect.* **2018**, *7*, R160–R186. [CrossRef] [PubMed]
13. Li, J.; Li, Y.; Zhu, M.; Song, S.; Qin, Z. A Multiwell-Based Assay for Screening Thyroid Hormone Signaling Disruptors Using thibz Expression as a Sensitive Endpoint in Xenopus laevis. *Molecules* **2022**, *27*, 798. [CrossRef]
14. Myosho, T.; Ishibashi, A.; Fujimoto, S.; Miyagawa, S.; Iguchi, T.; Kobayashi, T. Preself-Feeding Medaka Fry Provides a Suitable Screening System for in Vivo Assessment of Thyroid Hormone-Disrupting Potential. *Environ. Sci. Technol.* **2022**, *56*, 6479–6490. [CrossRef]
15. Mohacsik, P.; Erdelyi, F.; Baranyi, M.; Botz, B.; Szabo, G.; Toth, M.; Haltrich, I.; Helyes, Z.; Sperlagh, B.; Toth, Z.; et al. A Transgenic Mouse Model for Detection of Tissue-Specific Thyroid Hormone Action. *Endocrinology* **2018**, *159*, 1159–1171. [CrossRef] [PubMed]
16. Liu, S.; Shen, S.; Yan, Y.; Sun, C.; Lu, Z.; Feng, H.; Ma, Y.; Tang, Z.; Yu, J.; Wu, Y.; et al. Triiodothyronine (T3) promotes brown fat hyperplasia via thyroid hormone receptor alpha mediated adipocyte progenitor cell proliferation. *Nat. Commun.* **2022**, *13*, 3394. [CrossRef]
17. Sinkó, R.; Mohácsik, P.; Kővári, D.; Penksza, V.; Wittmann, G.; Mácsai, L.; Fonseca, T.L.; Bianco, A.C.; Fekete, C.; Gereben, B. Different hypothalamic mechanisms control decreased circulating thyroid hormone levels in infection and fasting-induced Non-Thyroidal Illness Syndrome in male Thyroid Hormone Action Indicator Mice. *Thyroid* 2022, in press. [CrossRef]
18. Tong, F.; Gu, X.; Gu, C.; Xie, J.; Xie, X.; Jiang, B.; Wang, Y.; Ertunc, T.; Schaffer, A.; Ji, R. Stimulation of Tetrabromobisphenol A Binding to Soil Humic Substances by Birnessite and the Chemical Structure of the Bound Residues. *Environ. Sci. Technol.* **2016**, *50*, 6257–6266. [CrossRef] [PubMed]
19. Sunday, O.E.; Bin, H.; Guanghua, M.; Yao, C.; Zhengjia, Z.; Xian, Q.; Xiangyang, W.; Weiwei, F. Review of the environmental occurrence, analytical techniques, degradation and toxicity of TBBPA and its derivatives. *Environ. Res.* **2022**, *206*, 112594. [CrossRef]
20. Yuan, X.; Li, T.; He, Y.; Xue, N. Degradation of TBBPA by nZVI activated persulfate in soil systems. *Chemosphere* **2021**, *284*, 131166. [CrossRef]
21. Lyche, J.L.; Rosseland, C.; Berge, G.; Polder, A. Human health risk associated with brominated flame-retardants (BFRs). *Environ. Int.* **2015**, *74*, 170–180. [CrossRef]
22. Kitamura, S.; Kato, T.; Iida, M.; Jinno, N.; Suzuki, T.; Ohta, S.; Fujimoto, N.; Hanada, H.; Kashiwagi, K.; Kashiwagi, A. Anti-thyroid hormonal activity of tetrabromobisphenol A, a flame retardant, and related compounds: Affinity to the mammalian thyroid hormone receptor, and effect on tadpole metamorphosis. *Life Sci.* **2005**, *76*, 1589–1601. [CrossRef]
23. Liu, A.F.; Qu, G.B.; Yu, M.; Liu, Y.W.; Shi, J.B.; Jiang, G.B. Tetrabromobisphenol-A/S and Nine Novel Analogs in Biological Samples from the Chinese Bohai Sea: Implications for Trophic Transfer. *Environ. Sci. Technol.* **2016**, *50*, 4203–4211. [CrossRef] [PubMed]
24. Barghi, M.; Shin, E.S.; Kim, J.C.; Choi, S.D.; Chang, Y.S. Human exposure to HBCD and TBBPA via indoor dust in Korea: Estimation of external exposure and body burden. *Sci. Total Environ.* **2017**, *593–594*, 779–786. [CrossRef]
25. Cariou, R.; Antignac, J.P.; Zalko, D.; Berrebi, A.; Cravedi, J.P.; Maume, D.; Marchand, P.; Monteau, F.; Riu, A.; Andre, F.; et al. Exposure assessment of French women and their newborns to tetrabromobisphenol-A: Occurrence measurements in maternal adipose tissue, serum, breast milk and cord serum. *Chemosphere* **2008**, *73*, 1036–1041. [CrossRef]
26. Wu, H.; Wang, J.; Xiang, Y.; Li, L.; Qie, H.; Ren, M.; Lin, A.; Qi, F. Effects of tetrabromobisphenol A (TBBPA) on the reproductive health of male rodents: A systematic review and meta-analysis. *Sci. Total Environ.* **2021**, *781*, 146745. [CrossRef]
27. Decherf, S.; Seugnet, I.; Fini, J.B.; Clerget-Froidevaux, M.S.; Demeneix, B.A. Disruption of thyroid hormone-dependent hypothalamic set-points by environmental contaminants. *Mol. Cell Endocrinol.* **2010**, *323*, 172–182. [CrossRef] [PubMed]
28. Huang, H.; Liang, J.; Tang, P.; Yu, C.; Fan, H.; Liao, Q.; Long, J.; Pan, D.; Zeng, X.; Liu, S.; et al. Associations of bisphenol exposure with thyroid hormones in pregnant women: A prospective birth cohort study in China. *Environ. Sci. Pollut. Res. Int.* **2022**, *29*, 87170–87183. [CrossRef]
29. Clayton, E.M.; Todd, M.; Dowd, J.B.; Aiello, A.E. The impact of bisphenol A and triclosan on immune parameters in the U.S. population, NHANES 2003-2006. *Environ. Health Perspect.* **2011**, *119*, 390–396. [CrossRef]
30. Darnerud, P.O. Toxic effects of brominated flame retardants in man and in wildlife. *Environ. Int.* **2003**, *29*, 841–853. [CrossRef] [PubMed]
31. Hackstein, J.H.; Mackenstedt, U.; Mehlhorn, H.; Meijerink, J.P.; Schubert, H.; Leunissen, J.A. Parasitic apicomplexans harbor a chlorophyll a-D1 complex, the potential target for therapeutic triazines. *Parasitol. Res.* **1995**, *81*, 207–216. [CrossRef]
32. Stock, M.L.; Elazab, S.T.; Hsu, W.H. Review of triazine antiprotozoal drugs used in veterinary medicine. *J. Vet. Pharmacol. Ther.* **2018**, *41*, 184–194. [CrossRef]
33. European Medicines Agency, V.M.E.U. Committee for Veterinary Medicinal Products. In *Diclazuril. Summary Report (1)*; EMEA/MRL/086/96-FINAL; European Medicines Agency: Amsterdam, The Netherlands, 1996.
34. Peek, H.W.; Landman, W.J. Coccidiosis in poultry: Anticoccidial products, vaccines and other prevention strategies. *Vet. Q.* **2011**, *31*, 143–161. [CrossRef]
35. Oz, H.S. Novel Synergistic Protective Efficacy of Atovaquone and Diclazuril on Fetal-Maternal Toxoplasmosis. *Int. J. Clin. Med.* **2014**, *5*, 921–932. [CrossRef] [PubMed]
36. Park, Y.; Park, J.; Lee, H.S. Endocrine disrupting potential of veterinary drugs by in vitro stably transfected human androgen receptor transcriptional activation assays. *Environ. Pollut.* **2021**, *286*, 117201. [CrossRef] [PubMed]

37. Paul-Friedman, K.; Martin, M.; Crofton, K.M.; Hsu, C.W.; Sakamuru, S.; Zhao, J.; Xia, M.; Huang, R.; Stavreva, D.A.; Soni, V.; et al. Limited Chemical Structural Diversity Found to Modulate Thyroid Hormone Receptor in the Tox21 Chemical Library. *Environ. Health Perspect.* **2019**, *127*, 97009. [CrossRef]
38. Bianco, A.C.; Salvatore, D.; Gereben, B.; Berry, M.J.; Larsen, P.R. Biochemistry, cellular and molecular biology and physiological roles of the iodothyronine selenodeiodinases. *Endo. Rev.* **2002**, *23*, 38–89. [CrossRef]
39. Demeneix, B.A. Evidence for Prenatal Exposure to Thyroid Disruptors and Adverse Effects on Brain Development. *Eur. Thyroid J.* **2019**, *8*, 283–292. [CrossRef]
40. Mughal, B.B.; Demeneix, B.A. Endocrine disruptors: Flame retardants and increased risk of thyroid cancer. *Nat. Rev. Endocrinol.* **2017**, *13*, 627–628. [CrossRef]
41. Caporale, N.; Leemans, M.; Birgersson, L.; Germain, P.L.; Cheroni, C.; Borbely, G.; Engdahl, E.; Lindh, C.; Bressan, R.B.; Cavallo, F.; et al. From cohorts to molecules: Adverse impacts of endocrine disrupting mixtures. *Science* **2022**, *375*, eabe8244. [CrossRef]
42. Zoeller, R.T. Endocrine disrupting chemicals and thyroid hormone action. *Adv. Pharmacol.* **2021**, *92*, 401–417. [CrossRef] [PubMed]
43. Sarvari, M.; Kallo, I.; Hrabovszky, E.; Solymosi, N.; Rodolosse, A.; Liposits, Z. Long-Term Estrogen Receptor Beta Agonist Treatment Modifies the Hippocampal Transcriptome in Middle-Aged Ovariectomized Rats. *Front. Cell Neurosci.* **2016**, *10*, 149. [CrossRef]
44. Lindsay, D.S.; Blagburn, B.L. Activity of diclazuril against Toxoplasma gondii in cultured cells and mice. *Am. J. Vet. Res.* **1994**, *55*, 530–533. [PubMed]
45. Guyot, R.; Chatonnet, F.; Gillet, B.; Hughes, S.; Flamant, F. Toxicogenomic analysis of the ability of brominated flame retardants TBBPA and BDE-209 to disrupt thyroid hormone signaling in neural cells. *Toxicology* **2014**, *325*, 125–132. [CrossRef]
46. Cope, R.B.; Kacew, S.; Dourson, M. A reproductive, developmental and neurobehavioral study following oral exposure of tetrabromobisphenol A on Sprague-Dawley rats. *Toxicology* **2015**, *329*, 49–59. [CrossRef]
47. La Merrill, M.A.; Vandenberg, L.N.; Smith, M.T.; Goodson, W.; Browne, P.; Patisaul, H.B.; Guyton, K.Z.; Kortenkamp, A.; Cogliano, V.J.; Woodruff, T.J.; et al. Consensus on the key characteristics of endocrine-disrupting chemicals as a basis for hazard identification. *Nat. Rev. Endocrinol.* **2020**, *16*, 45–57. [CrossRef]
48. Zhang, M.; Qiu, J.; Li, X.; Zhang, W.; Fan, J.; Zhou, H.; He, L. Determination of residual enantiomers of diclazuril in chicken edible tissues by high performance liquid chromatography. *J. Chromatogr. B Analyt. Technol. Biomed. Life Sci.* **2019**, *1118–1119*, 203–209. [CrossRef] [PubMed]
49. Sotome, R.; Hirasawa, A.; Kikusato, M.; Amo, T.; Furukawa, K.; Kuriyagawa, A.; Watanabe, K.; Collin, A.; Shirakawa, H.; Hirakawa, R.; et al. In vivo emergence of beige-like fat in chickens as physiological adaptation to cold environments. *Amino Acids* **2021**, *53*, 381–393. [CrossRef]
50. Asadi Iraee, H.; Asadi Iraee, M.; Youssefi, M.R.; Abouhosseini Tabari, M. Growth performance parameters in chicken experimental coccidiosis treated with Diclazuril and Clopidol: The need for assessing new anticoccidial resources. *Iran. J. Vet. Med.* **2015**, *9*, 189–194.
51. Dentice, M.; Luongo, C.; Huang, S.; Ambrosio, R.; Elefante, A.; Mirebeau-Prunier, D.; Zavacki, A.M.; Fenzi, G.; Grachtchouk, M.; Hutchin, M.; et al. Sonic hedgehog-induced type 3 deiodinase blocks thyroid hormone action enhancing proliferation of normal and malignant keratinocytes. *Proc. Natl. Acad. Sci. USA* **2007**, *104*, 14466–14471. [CrossRef] [PubMed]
52. Egri, P.; Fekete, C.; Denes, A.; Reglodi, D.; Hashimoto, H.; Fulop, B.D.; Gereben, B. Pituitary Adenylate Cyclase-Activating Polypeptide (PACAP) Regulates the Hypothalamo-Pituitary-Thyroid (HPT) Axis via Type 2 Deiodinase in Male Mice. *Endocrinology* **2016**, *157*, 2356–2366. [CrossRef]

A Transgenic Mouse Model for Detection of Tissue-Specific Thyroid Hormone Action

Petra Mohácsik,[1,2] Ferenc Erdélyi,[3] Mária Baranyi,[4] Bálint Botz,[5] Gábor Szabó,[3] Mónika Tóth,[1] Irén Haltrich,[6] Zsuzsanna Helyes,[5,7] Beáta Sperlágh,[4] Zsuzsa Tóth,[6] Richárd Sinkó,[1,2] Ronald M. Lechan,[8,9] Antonio C. Bianco,[10] Csaba Fekete,[1,8] and Balázs Gereben[1]

[1]Department of Endocrine Neurobiology, Institute of Experimental Medicine, Hungarian Academy of Sciences, Budapest, Hungary H-1083; [2]János Szentágothai PhD School of Neurosciences, Semmelweis University, Budapest, Hungary H-1085; [3]Medical Gene Technology Unit, Institute of Experimental Medicine, Hungarian Academy of Sciences, Budapest, Hungary H-1083; [4]Laboratory of Molecular Pharmacology, Institute of Experimental Medicine, Hungarian Academy of Sciences, Budapest, Hungary H-1083; [5]Department of Pharmacology and Pharmacotherapy, University of Pécs Medical School, Centre for Neuroscience; and Molecular Pharmacology Research Team, János Szentágothai Research Centre, Pécs, Hungary H-7624; [6]Second Department of Pediatrics, Faculty of Medicine, Semmelweis University, Budapest, Hungary H-1094; [7]Hungarian Academy of Sciences–University of Pécs, Hungarian Brain Research Program, Chronic Pain Research Group, University of Pécs Medical School, Pécs, Hungary H-7624; [8]Division of Endocrinology, Diabetes and Metabolism, Department of Medicine, Tupper Research Institute, Tufts Medical Center, Boston, Massachusetts 02111; [9]Department of Neuroscience, Tufts University School of Medicine, Boston, Massachusetts 02111; and [10]Division of Endocrinology and Metabolism, Rush University Medical Center, Chicago, Illinois 60612

Thyroid hormone (TH) is present in the systemic circulation and thus should affect all cells similarly in the body. However, tissues have a complex machinery that allows tissue-specific optimization of local TH action that calls for the assessment of TH action in a tissue-specific manner. Here, we report the creation of a TH action indicator (THAI) mouse model to study tissue-specific TH action. The model uses a firefly luciferase reporter readout in the context of an intact transcriptional apparatus and all elements of TH metabolism and transport and signaling. The THAI mouse allows the assessment of the changes of TH signaling in tissue samples or in live animals using bioluminescence, both in hypothyroidism and hyperthyroidism. Beyond pharmacologically manipulated TH levels, the THAI mouse is sufficiently sensitive to detect deiodinase-mediated changes of TH action in the interscapular brown adipose tissue (BAT) that preserves thermal homeostasis during cold stress. The model revealed that in contrast to the cold-induced changes of TH action in the BAT, the TH action in this tissue, at room temperature, is independent of noradrenergic signaling. Our data demonstrate that the THAI mouse can also be used to test TH receptor isoform-specific TH action. Thus, THAI mouse constitutes a unique model to study tissue-specific TH action within a physiological/pathophysiological context and test the performance of thyromimetics. In conclusion, THAI mouse provides an *in vivo* model to assess a high degree of tissue specificity of TH signaling, allowing alteration of tissue function in health and disease, independently of changes in circulating levels of TH. (***Endocrinology*** **159: 1159–1171, 2018)**

Thyroid hormones (THs) orchestrate a wide variety of biological processes, including development, growth, and metabolism *via* transcriptional control of hundreds of TH-dependent genes. Specific regulatory elements within these genes [TH response element (TRE)] attract two isoforms of the TH receptor (TRα and TRβ) and their

ISSN Online 1945-7170

Received 23 June 2017. Accepted 8 December 2017.
First Published Online 14 December 2017

Abbreviations: ANOVA, analysis of variance; BAT, brown adipose tissue; bw, body weight; cDNA, complementary DNA; D2, type 2 deiodinase; DR-4, direct repeat 4; FISH, fluorescence *in situ* hybridization; GAPDH, glyceraldehyde 3-phosphate dehydrogenase; HEK, human embryonic kidney; iBAT, interscapular brown adipose tissue; IP, intraperitoneal(ly); LXR, liver X receptor; mRNA, messenger RNA; NE, norepinephrine; PCR, polymerase chain reaction; RLU, relative light unit; RXR, retinoid X receptor; SEM, standard error of the mean; TH, thyroid hormone; THAI, thyroid hormone action indicator; THAIC, thyroid hormone action indicator construct; TR, thyroid hormone receptor; TRE, thyroid hormone response element.

coregulators, thus allowing for transcriptional control (1–5). An unoccupied TR remains bound to the gene and is associated with corepressors–silencing genes that are positively regulated by TH. Upon TH binding, corepressors associated with the TRs are replaced by coactivators, relieving repression and promoting gene transactivation. Therefore, TH availability within the nuclear environment defines a switch between TH-dependent gene repression and activation.

Two THs exist: the prohormone T4 that can be converted to the TR-binding molecule T3 *via* deiodination. Relatively steady circulating levels of TH are maintained by the hypothalamus-pituitary-thyroid axis that is tightly regulated by the negative-feedback effects of TH. However, the existence of multiple mechanisms that customize TH availability at the cellular level provides tissue specificity to TH action. These mechanisms include TH transmembrane transporters, enzymes that can activate or inactivate TH within the target cells, *i.e.*, the deiodinases, and differential expression of TR subtypes (6–8). The coordinated actions of TH-activating or -inactivating deiodinases (6) allow for quick modification of T3 levels within the target cells, rapidly affecting the expression of TH-responsive genes without antecedent changes in circulating T3 levels.

A corollary is that measurement of plasma TH levels under physiological and pathological conditions does not uniformly reflect TH actions in all tissues. This is suggested by conditions, such as the syndrome of resistance to TH (mutant TRα or TRβ) (2, 9), the X-linked mental retardation Allan-Herndon-Dudley syndrome caused by impaired transmembrane TH transport (mutant monocarboxylate transporter 8) (10, 11), and the commonly observed nonthyroidal illness syndrome, where circulating TH levels are uncoupled from local TH action in specific tissues (7, 12). In addition, there is evidence that TH signaling is specifically downregulated in the liver of obese subjects and in mice placed on a high-fat diet (13). Tissue specificity of TH action could also explain why some hypothyroid patients remain symptomatic despite exhibiting normal plasma thyroid-stimulating hormone levels (14, 15).

The discovery of cellular mechanisms that allow for tissue specificity of TH action inspired the development of TR isoform- and tissue-specific TH analogs (16, 17). For example, TRβ-selective TH analogs act predominantly in the liver and can be useful in treatment of hypercholesterolemia and obesity. However, progress in this field has been empirical, given current inability to assess tissue-specific TH action (15) within a physiological or pathophysiological context. Here, we developed and characterized a mammalian model: the TH action indicator (THAI) mouse, to assess tissue-specific TH signaling.

Materials and Methods

The transgenic THAI construct

Three copies of a direct repeat 4 (DR-4) TRE (of the human *DIO1* 5′-flanking region) (18) were cloned upstream to the *Herpes simplex* virus thymidine kinase minimal promoter (19). This DNA segment was linked upstream of the luciferase coding region, containing a codon-optimized and methylation-resistant dCpG luciferase-ShBle fusion protein upstream of an EF1 pAn polyadenylation cassette. The use of the dCpG luciferase reporter that is resistant to T3-induced promoter-independent downregulation avoids a phenomenon that can interfere with TH-mediated changes of the classical firefly luciferase reporter protein (19). The cassette was then assembled in a pWHERE vector (InvivoGen, San Diego, CA) that flanked the insert with H19 insulators, followed by subcloning between the half-sites of the blunted *Eco*RI site of the pt2-BH transposon-cloning vector (Addgene, Cambridge, MA) containing multiple cloning sites flanked by indirect repeats. This resulted in the generation of the THAI expression vector (Fig. 1a). Next, human embryonic kidney (HEK)293T cells stably expressing the THAI construct (THAIC) and transiently expressing TRα were incubated with T3 for 24 hours. There was readily measurable baseline luciferase activity that was 3.7-fold stimulated after T3 exposure, whereas no stimulation was observed in the absence of TRα coexpression, indicating that induction was TR dependent (Fig. 1b).

Generation of the THAIC-HEK293T cell line

HEK293T cells were cultured in Dulbecco's modified Eagle medium + 10% fetal bovine serum and transfected with the targeting THAIC (Fig. 1a) along with the pcGlobinSB100 transposase-encoding vector (20) (provided by Zsuzsanna Izsvák and Lajos Mátes) to allow Sleeping Beauty transposase-assisted genomic integration. Clone selection was performed in the presence of 150 μg/mL zeocin. Clones were cultured for 24 hours in charcoal-stripped fetal bovine serum (21), followed by the induction with 100 nM T3 for 24 hours in the presence of transiently coexpressed mouse TRα. Cells were lysed in passive lysis buffer of the dual luciferase assay system (Promega, Madison, WI) before luciferase assay.

Generation of transgenic mouse lines by transposon-mediated technology

Genomic insertion of the transgenic cassette was performed with the Sleeping Beauty transposase (22). The pronucleus of fertilized FVB/Ant (FVB.129P2-Pde6b$^+$ Tyrc-ch/AntJ) (23) oocytes was injected with a mixture containing the plasmid harboring the targeting transposon cassette (Fig. 1a; 1 ng/μL) and the *in vitro*-transcribed messenger RNA (mRNA) encoding the Sleeping Beauty transposase (24) (5 ng/μL). Four females were identified as founders using TaqMan assay on tail DNA with a luciferase probe and crossed with wild-type FVB/Ant (FVB.129P2-Pde6b$^+$ Tyrc-ch/AntJ) male mice, followed with inbred coupling of F1 generation. Indirect evidence obtained with luciferase TaqMan polymerase chain reaction (PCR) on different lines and generations suggests that a single copy of the transgenic cassette was inserted into the genome of all lines. All animal experiments were conducted in compliance with the European Communities Council Directive (2010/63/EU) and approved by the Animal Care and Use Committee of the

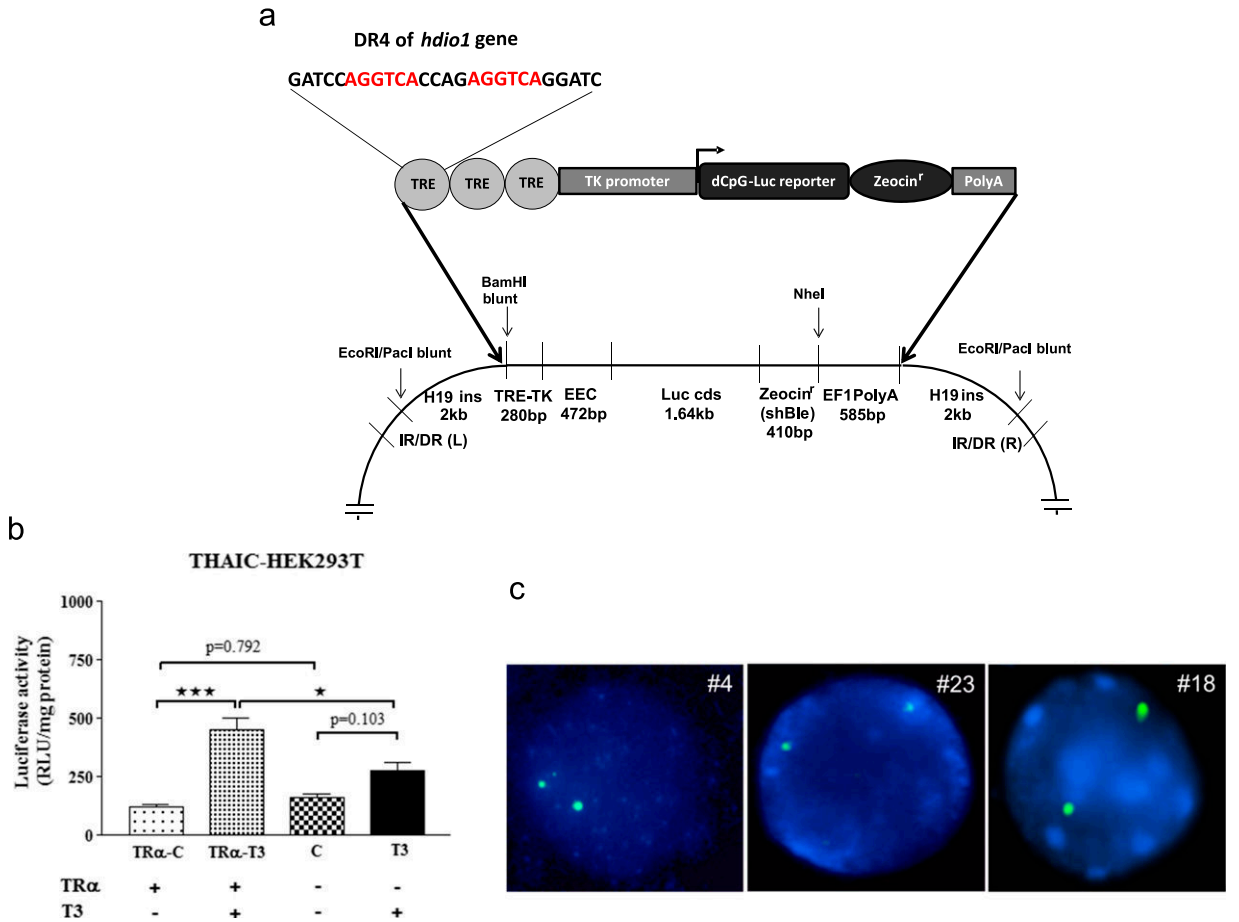

Figure 1. (a) The recombinant THAIC. (Lower) The structure of the targeting construct generated in the pt2-BH vector. The coding sequence encodes luciferase (62 kDa) fused to ShBle (14 kDa), allowing selection based on resistance to zeocin. (b) THAIC responds to T3 in a TR-dependent manner. The THAIC was stably expressed in human embryonic kidney (HEK)293T cells using Sleeping Beauty–mediated recombination followed by zeocin selection. TRα was transiently transfected, and THAIC-HEK293T cells were treated with 100 nM T3 for 24 hours. Means ± SEM; (n = 3). *$P < 0.05$, ***$P < 0.001$ by one-way analysis of variance (ANOVA), followed by Tukey *post hoc* test. (c) Fluorescence *in situ* hybridization (FISH) on homozygote THAI mouse, lines 4, 23, and 18. Hybridization with the green-colored dCpG luciferase-specific probe shows two equal-sized signals in interphase cells of homozygous animals, demonstrating the presence of two copies of the transgene in lymphocyte cultures of all three lines, indicating that a single copy was inserted into the genome of founders. C, control; EEC, expression enhancer cassette; luciferase reporter-zeocin sequences encoding a luciferase/zeocin resistance fusion protein, IR/DR (L) and (R), inverted repeat left and right; TK promoter, thymidine kinase minimal promoter.

Institute of Experimental Medicine (Hungarian Academy of Sciences, Budapest).

Characterization of transgenic lines

The F2 generation was screened for tissue luciferase activity. To characterize basal and TH-induced luciferase activity of peripheral tissues and brain regions, 60- to 70-day-old males were injected intraperitoneally (IP) with 5 μg/day/mouse of L-T4 or vehicle control for 3 days or 1 μg/g body weight (bw) of L-T3 for 1 day. Hypothyroid mice were generated by adding 0.1% sodium perchlorate and 0.5% methimazole in drinking water for 3 weeks combined with low-iodine diet (Research Diets, New Brunswick, NJ). After decapitation, tissues were removed, snap frozen on dry ice, and stored at −80°C for luciferase activity measurement. White blood cells were isolated as described (25). Bone and muscle samples originated from *Tibia* and *musculus gastrocnemius*, respectively. Three of the four lines (4, 18, and 23) were found to be TH responsive. Homozygous mice showed a twofold higher luciferase activity compared with heterozygous animals, demonstrating that activity of the reporter correlates directly with gene dosage (not shown), and were born following a Mendelian distribution. In accordance, the animals did not exhibit any identifiable phenotype.

Mouse lymphocyte cell culture and fluorescence *in situ* hybridization

Lymphocytes derived from the spleen of homozygote THAI mouse lines #4, 18, and 23 were cultured as described (26, 27). Individual spleens were homogenized to release the lymphocytes, and erythrocytes were lysed briefly (2 to 3 minutes) in sterile, distilled water, followed by the addition of physiological saline. Cell suspensions was centrifuged 5 minutes, 500 *g* at room temperature. After removing the supernatant, cells were transferred into ready-to-use LymphoChrome Karyotyping Media (Lonza Verviers, Belgium). The cells were incubated at 37°C for 24 hours, and 0.05 μg/mL Colcemid (Gibco/Thermo Fisher,) was added, 3 hours before harvest.

Chromosomal preparations were performed according to a standard Rothfels-Siminovich procedure using 0.067 M KCl, followed by fixation in methanol/acetic acid. Chromosome analysis was performed on metaphase cells G-banded with trypsin and Wright Giemsa stain. A 1045-base pair fragment of the dCpG luciferase coding sequence (nucleotides 599 to 1644) was labeled with digoxigenin using Dig-Nick translation mix (Roche, Mannheim, Germany) and precipitated with mouse COT-1 DNA (Invitrogen), according to the manufacturer's instructions. The precipitated probe was mixed with an equal volume of hybridization buffer. Fluorescence *in situ* hybridization (FISH) was performed on methanol/acetic acid-fixed cell suspensions. Slides/DNA preparation and hybridization were carried out according to standard techniques. Hybridized sections were incubated overnight at room temperature with antidigoxigenin-POD (1:100) antibody (Roche) in 1% bovine serum albumin solution. The immunoreaction signal was amplified using the tyramide signal amplification kit (Perkin Elmer Life and Analytical Sciences, Waltham, MA), according to the manufacturer's instructions. The deposited reaction product was detected with fluorescein isothiocyanate/dichlorotriazinylamino fluorescein–streptavidin antibody (Jackson ImmunoResearch, West Grove, PA). The analysis was done in at least 100 interphase nuclei and in a few metaphases, if present on the hybridization area. The interphase or metaphase cells were evaluated for each sample with an Axioskop 2 Mot Plus Microscope (Carl Zeiss GmbH, Oberkochen, Germany) and Cytovision 3.6 computer analysis system (Applied Imaging International Ltd., Newcastle, United Kingdom).

Splinkerette PCR

Splinkerette PCR was performed, as described (28). In brief, genomic DNA was digested with BstYI. A universal Splinkerette oligonucleotide was used to amplify the region between the 5′ end of the cassette and the first BstYI site. The cassette-specific oligonucleotide was specific for the multiple cloning site of the PT/2BH vector, located 3′ to the 5′ inverted terminal repeat sequence. Nested PCR was performed to reamplify the PCR product, followed by sequencing. The reporter cassette was found inserted into a region of repeat family L1 into the genome of THAI mouse line 4, as shown by Splinkerette PCR, indicating that the cassette did not alter the structure of any endogenous gene.

GC24 treatment

Seventy-day-old male THAI #4 mice were treated, as described previously, for 2 weeks to inhibit endogenous TH production. Hypothyroid mice were treated with a single, IP injection of 1.53 nM/g bw GC24 (a kind gift of Dr. Tom Scanlan; equimolar to 1 μg/g bw T3) or dimethyl sulfoxide as vehicle, 24 hours before tissue sampling. After decapitation, liver (TRβ-dominant tissue) and heart (TRα-dominant tissue) (16) were removed and snap frozen on dry ice.

GW3965 treatment

GW3965 treatment was performed IP, as described with modifications, as follows (29). Sixty-five-day-old male THAI #4 mice were subject to two IP injections of 20 μg/g bw GW3965 HCl (homogenous suspension in 10% dimethyl sulfoxide–90% saline; Adooq Bioscience, Irvine, CA) or with solvent, 3.5 and 7 hours before tissue sampling. After decapitation, the liver was removed and snap frozen on dry ice. Samples were subjected to TaqMan real-time quantitative PCR.

Luciferase assay

Tissue samples were milled to powder in liquid nitrogen and sonicated in luciferase lysis buffer (100 mM KPO_4, 4 mM EGTA, 4 mM EDTA, pH 7.8), freshly prepared with 0.7 mM phenylmethylsulfonyl fluoride and 0.1 mM dithiothreitol. Brain tissue was lysed in one step, with brief sonication in lysis buffer. After a 10-minute centrifugation at 14,000 *g* at 4°C, supernatant was removed for luciferase activity measurement. Assay on tissue samples or THAIC-HEK293T cells was performed with luciferase assay system reagent (Promega, Madison, WI) on a Luminoskan Ascent (Thermo Electron Corp. Labsystems, Vantaa, Finland) luminometer. Detected relative light unit (RLU) was normalized to protein content of the sample.

Sympathetic denervation of interscapular brown adipose tissue and cold stress

Interscapular brown adipose tissue (iBAT) was unilaterally denervated with surgical transection of its sympathetic nerves (30). Cold stress was applied 3 days after surgery. During cold stress, single housed animals were kept under standard light conditions at 4°C; water and food were available *ad libitum*. Control animals were kept at room temperature (22°C) under same conditions. After decapitation, samples from the iBAT were collected on dry ice and stored at −80°C for norepinephrine (NE) measurement, deiodination assay, and TaqMan analysis.

Analysis of NE content of iBAT samples

NE concentrations of mouse iBAT were measured using surfactant-assisted online solid-phase extraction sample preparation, followed by column-switching liquid chromatographic separation with electrochemical detection, as described (31). To prevent fat precipitation in the aqueous extraction solvent phase, the nonionic surfactant Triton X-100 was used. The native tissue was homogenized by sonication in 300 μl, 0.1 M, ice-cold perchloric acid, which contained 10 mM theophylline as an internal standard, 0.1% sodium metabisulfite as an antioxidant, and 0.01% (volume-to-volume ratio) Triton X-100 as an emulsifier. The NE content was expressed as picomoles per milligram protein.

Deiodination assay

iBAT tissue samples were homogenized with sonication in 0.1 M potassium phosphate, 1 mM EDTA, pH 6.9, buffer containing 0.25 M sucrose and 10 mM dithiothreitol. iBAT tissue lysates (100 μg protein) were assayed for 120 minutes at 37°C in duplicate to determine type 2 deiodination activity, as previously described (32).

TaqMan real-time quantitative PCR

Total RNA was isolated from iBAT tissue samples with the RNeasy Lipid Tissue Mini kit (Qiagen, Hilden, Germany), according to the manufacturer's instructions, whereas for liver samples, the Qiazol Lysis Reagent was used, followed by isolation with the Macherey-Nagel (Düren, Germany) Nucleospin RNA kit. Total RNA (1 μg) was reverse transcribed with the High-Capacity cDNA Reverse Transcription Kit (Thermo

Fisher Scientific, Waltham, MA). Complementary DNA (cDNA) concentration was determined with the Qubit single-stranded DNA assay kit. cDNA (10 ng) was used in each TaqMan reaction. mRNA expression of target genes was detected with TaqMan Gene expression probe sets using TaqMan Fast Universal PCR Mastermix (Thermo Fisher Scientific) and compared with glyceraldehyde 3-phosphate dehydrogenase (GAPDH) housekeeping gene expression. Expression of GAPDH was also analyzed under all challenge conditions used. Cold stress had no effect on GAPDH expression, either in intact or in denervated iBAT lobes. Sympathetic denervation, however, consistently downregulated GAPDH expression twofold; thus, this was taken into account when calculating results of the denervation experiments by dividing fold changes of luciferase/GAPDH and type 2 deiodinase (D2)/GAPDH rations by two. Accession numbers of used TaqMan probes are listed in Supplemental Table 1. Reactions were assayed on a Viia 7 Real-Time PCR instrument (Applied Biosystems, Waltham, MA).

iBAT measurements

All measurements, including NE concentration, D2 activity, and mRNA expression of the luciferase reporter and D2, were performed from the same iBAT samples obtained from animals undergoing cold stress and unilateral sympathetic denervation, whereas the nondenervated, intact iBAT lobe, obtained from the same animal, was used for comparison.

In vivo imaging of luciferase activity

In vivo imaging of iBAT of T3-treated and cold-stressed animals was performed 24 hours after 1 μg/g bw IP T3 injection or after 24 hours exposure to 4°C. Live imaging was obtained in ketamine–xylazine (ketamine 50 μg/g, xylazine 10 μg/g bw, IP)-anesthetized mice whose fur over the iBAT and abdominal organs had been removed with depilatory cream. All animals were moved to room temperature, 30 minutes before imaging. D-Luciferin (Gold Biotechnology, St. Louis, MO) was dissolved in PBS and IP injected (150 and 750 μg/g bw for the T3-treated and cold-stressed animals, respectively), 15 minutes before *in vivo* imaging. The animals were placed on the heated plate of the imager, 5 minutes before imaging. Emitted light was detected with an IVIS Lumina II *In vivo* Imaging System (PerkinElmer, Waltham, MA) and quantitated in all animals using a region of interest of identical size and shape. Data are reported as emitted photon/s. T3-treated or cold-stressed animals were studied using identical imaging parameters (binning and exposure time) as their corresponding controls in both dorsal and ventral positions.

Indirect calorimetry measurements

Eleven-week-old old male THAI #4 and wild-type control mice were analyzed for whole-energy expenditure, oxygen consumption, and carbon dioxide production using calorimetric cages (PhenoMaster/LabMaster, TSE Systems GmbH, Bad Homburg, Germany). Body-composition analyses were performed using an EchoMRI Whole Body Composition Analyzer (EchoMRI, Houston, TX).

TH measurements

Serum-free T4 and T3 levels were measured with AccuLite CLIA Microwells kit (Monobind, Lake Forest, CA), according to the manufacturer's instructions.

Statistics

Groups were compared with unpaired two-sample Student *t* test using a 95% level of confidence. For multiple comparison, one-way analysis of variance (ANOVA) or repeated-measures ANOVA was used, followed by Newman-Keuls or Tukey post hoc tests.

Results

The THAI mouse model integrates a highly TH-responsive reporting system that functions in the setting of endogenous levels of TH transporters, deiodinases, and TRs. We obtained three THAI mouse founders harboring a single copy of the transgenic cassette (lines 4, 23, and 18; Fig. 1c). THAI lines exhibit normal serum TH levels and bw, as well as other TH-dependent parameters, *i.e.*, lean body mass, fat mass, respiratory exchange ratio, and oxygen consumption (Supplemental Tables 2 and 3). These animals were used to study TH action using two general approaches: (1) measuring luciferase activity and mRNA in tissue sonicates or (2) measuring bioluminescence in live animals.

The THAI mouse model reports differences in TH action caused by altered TH levels or the selective actions of TH analogs

We first defined tissue-specific baseline values for the reporting system. Second, we measured the responsiveness of this system to a decrease or increase in TH levels. Within each mouse line, basal luciferase activity varied among different tissues. For example, there were up to approximately six orders-of-magnitude differences between liver and testicle, whereas in most other tissues, the variability ranged within two orders of magnitude (Tables 1 and 2). These differences are likely to reflect the overall level of transcriptional activity of the insertion site. Furthermore, when using *in vivo* bioluminescence, variable degrees of baseline activity were detected in the iBAT, anterior and posterior foot pads, tail, intestine, *saccus cecum* of the stomach, mandibular salivary gland, mouth, nose, skin, and testicles (Fig. 2a and 2b). To assess whether this reporting system detects a reduction in TH signaling, line 4 animals were rendered hypothyroid, and the reporter activity was measured. There was an ~50% to 65% decrease of luciferase activity in different brain regions (*e.g.*, the hypothalamus and cerebral cortex), the liver, and white blood cells; 75% in iBAT; 80% in the pituitary; 85% in the heart and bone; and 90% in the small intestine (Table 3). Line 4 was also studied *via in vivo* bioluminescence imaging, and an ~80% reduction in signal was observed in the intestine in live hypothyroid animals (Fig. 2a and 2b).

Next, all three mouse lines were treated with L-T4 for 3 days. Responsiveness to TH varied among mouse lines

Table 1. Responsiveness of THAI #4, 23, and 18 Mouse Lines to T4

	THAI #4 (T4)				THAI #23 (T4)				THAI #18 (T4)			
Tissue	Eu (RLU/mg Protein)	Hyper (RLU/mg Protein)	Fold (Means ± SEM)	*P* Value	Eu (RLU/mg Protein)	Hyper (RLU/mg Protein)	Fold (Means ± SEM)	*P* Value	Eu (RLU/mg Protein)	Hyper (RLU/mg Protein)	Fold (Means ± SEM)	*P* Value
Pit	0.337	0.791	2.3 ± 0.16	0.0001[a]	1.932	16.926	8.8 ± 0.62	0.0001[a]	0.066	0.54	8.2 ± 0.36	0.0001[a]
MBH	0.206	0.368	1.8 ± 0.20	0.013[a]	0.142	0.24	1.7 ± 0.29	0.103	0.372	0.602	2.2 ± 0.25	0.005[a]
HC	0.06	0.116	1.9 ± 0.03	0.0001[a]	0.035	0.047	1.5 ± 0.35	0.201	2.308	3.756	2.1 ± 0.25	0.013[a]
HT	0.377	0.488	1.3 ± 0.08	0.031[a]	0.65	0.78	1.2 ± 0.11	0.176	0.755	1.589	2.8 ± 0.35	0.004[a]
CTX	0.194	0.359	1.9 ± 0.30	0.035[a]	0.179	0.253	1.4 ± 0.13	0.017[a]	1.617	2.586	1.9 ± 1.18	0.005[a]
CER	0.938	2.162	2.3 ± 0.41	0.019[a]	0.012	0.023	1.9 ± 0.28	0.045[a]	0.045	0.063	1.8 ± 0.31	0.073
Liver	0.002	0.005	1.9 ± 0.14	0.0007[a]	0.001	0.003	2.9 ± 0.86	0.064	No detectable expression			
Heart	0.004	0.03	8.5 ± 0.31	0.0001[a]	0.001	0.001	1.0 ± 0.25	–	No detectable expression			
BAT	0.028	1.82	64.6 ± 8.1	0.0002[a]	0.005	0.038	7.2 ± 1.54	0.007[a]	No detectable expression			
Bone	0.031	0.066	2.2 ± 0.18	0.0015[a]	0.01	0.011	0.7 ± 0.11	0.057	No detectable expression			
Muscle	0.025	0.276	11.2 ± 5.7	0.0041[a]	0.004	0.003	0.7 ± 0.18	0.115	No detectable expression			
MSG	0.052	0.399	7.6 ± 2.60	0.044[a]	0.004	0.011	2.7 ± 0.77	0.072	Not determined			
Thyroid	0.115	0.176	1.5 ± 0.07	0.002[a]	0.026	0.03	0.8 ± 0.18	0.734	Not determined			
Testicle	4876	4086	0.8 ± 0.06	0.108	2909	2509	0.9 ± 0.11	0.253	Not determined			
Intestine	4.571	9.48	2.1 ± 0.30	0.012[a]	0.041	0.212	5.2 ± 1.6	0.029[a]	Not determined			
Skin	0.696	2.798	4.0 ± 0.76	0.001[a]	2.358	1.878	0.8 ± 0.17	0.544	Not determined			

Euthyroid animals were treated with L-T4 (IP 5 μg/d per animal for 3 days). Luciferase activity was assessed in tissue samples with luciferase assay and expressed as RLU per milligram protein. Luciferase activity of corresponding tissues of TH *vs* vehicle-treated animals was performed by Student *t* test (n ≥ 4).

Abbreviations: CER, cerebellum; CTX, cerebral cortex; Eu, euthyroid; HC, hippocampus; HT, hypothalamus; Hyper, hyperthyroid; MBH, mediobasal hypothalamus; MSG, mandibular salivary gland; Pit, pituitary.

[a] $P < 0.05$.

and among tissues within the same mouse line. For example, responsiveness in line 4 varied from 0.8-fold in the testes, 1.5-twofold in the brain (hypothalamus, hippocampus, cerebellum, cortex), to 64-fold in iBAT. Other highly responsive tissues were skeletal muscle, heart, mandibular salivary gland, and skin (four- to 11-fold; Table 1). Lines 23 and 18 exhibited marked response to TH in the pituitary, and line 18 showed the highest brain baseline activity (Table 1). In this setting, the mouse lines showed greater responsiveness to L-T3 compared with L-T4; *e.g.*, line 4 responded to L-T3 with a fivefold stimulation of reporter activity in the liver and 46-fold in the heart, whereas the mediobasal hypothalamus of line 23 responded to L-T3 with an ~12-fold induction of reporter activity (Table 2). In line 4 animals, a single L-T3 injection, 24 hours before imaging, induced luciferase activity in iBAT by approximately ninefold, in the small intestine by approximately threefold, and to a lesser extent, in the mandibular salivary gland; the footpads and tail showed a tendency to increase 2.2- and 2.5-fold, respectively (euthyroid *vs* hyperthyroid), which became important when hypo- and hyperthyroid animals were compared, showing eight- and 46-fold changes for footpads and tails, respectively (Fig. 2a and 2b). The iBAT was confirmed to be the source of the bioluminescence of the interscapular region (Supplemental Fig. 1a), and signal detected in the intestine was predominantly confined to the small intestine (duodenum and jejunum; Fig. 2c). Notably, despite very high basal reporter

Table 2. Responsiveness of THAI #4 and 23 Mouse Lines to T3

	THAI #4 (T3)			
Tissue	Eu (RLU/mg Protein)	Hyper (RLU/mg Protein)	Fold (Means ± SEM)	*P* Value
Liver	0.003	0.017	5.0 ± 0.6	0.009[a]
Heart	0.006	0.284	45.9 ± 5.65	0.002[a]
	#23 (T3)			
Tissue	Eu (RLU/mg Protein)	Hyper (RLU/mg Protein)	Fold (Means ± SEM)	*P* Value
MBH	0.18	2.222	12.31 ± 2.4	0.003[a]

Euthyroid animals were treated with L-T3 (IP 1 μg/g bw for 1 day). Luciferase activity was assessed in tissue samples with luciferase assay and expressed as RLU per milligram protein. Luciferase activity of corresponding tissues of TH *vs* vehicle-treated animals was performed by Student *t* test (n ≥ 4).

Abbreviation: MBH, mediobasal hypothalamus.

[a] $P < 0.05$.

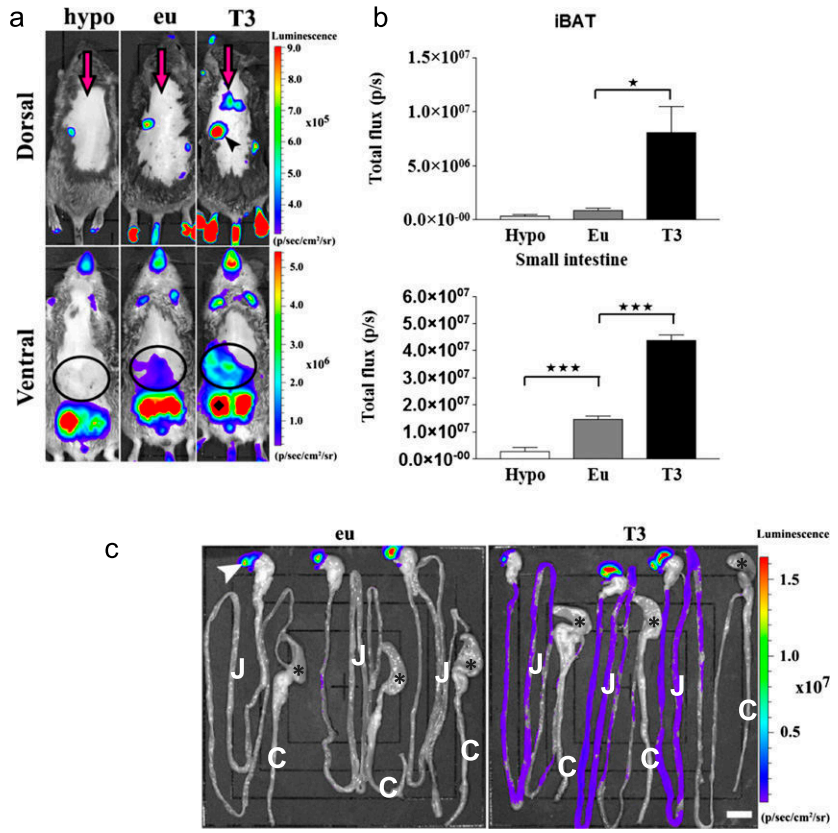

Figure 2. Detection of TH action in live animals. (a) *In vivo* bioluminescence imaging on euthyroid, L-T3-treated (1 μg/g bw injected IP, 24 hours before imaging), and hypothyroid THAI #4 mice, followed by IP luciferin administration. Representative images of hypothyroid (hypo), euthyroid (eu), and L-T3-treated (T3) mice and light intensity diagram of iBAT and small intestine. T3 injection increased light intensity in iBAT. In the small intestine, hypothyroidism decreased, whereas T3 treatment increased light intensity. Dorsal image arrow: iBAT (arrowhead), *saccus cecum* of the stomach; ventral image (circles), small intestine; ♦, testicles. (b) Light intensity diagram of luciferase activity [photons/s (p/s)] in iBAT and small intestine of hypothyroid, euthyroid, and T3-treated THAI #4 mice. Means of p/s ± SEM (n = 3). $*P < 0.05$; $***P < 0.001$ by one-way ANOVA, followed by Newman-Keuls *post hoc* test. (c) Bioluminescence of the gastrointestinal tract is confined to the small intestine. Imaging on an isolated gastrointestinal tract of three euthyroid and three L-T3-treated (1 μg/g bw injected IP, 24 hours before imaging) THAI #4 animals. T3-mediated light-intensity upregulation is mainly restricted to the small intestine, whereas the colon shows an order of magnitude lower luciferase activity. *, cecum; arrowhead, *saccus cecum* of the stomach. Original scale bar, 1 cm. C, colon; J, jejunum.

activity, luciferase activity in the testicles was not inducible by L-T3 injection (Fig. 2a). Live THAI mouse line 23 also responded to L-T3 injection, with elevated reporter activity in the iBAT and small intestine (Supplemental Fig. 2). Thus, THAI mice allow the assessment of TH action both in live animals and in tissue samples. Line 4 permits the study of TH action in a wide variety of tissues, whereas the two other lines hold additional value for specific applications, represented by high reporter response in the pituitary (lines 18 and 23) and higher basal activity in the brain (18), as a result of their different insertion sites.

One of the aspects that provide specificity in TH signaling is differential expression of TRα and TRβ isoforms among tissues; *e.g.*, TRβ predominates in the liver, whereas the TRα isoform predominates in the brain, skeletal muscle, and heart (1, 33). To test if TR subtype specificity could be assessed with the THAI mouse, line 4 animals were treated with GC24, a highly selective TRβ agonist (34). Treatment with GC24 increased luciferase activity by ~2.5-fold in the liver (Fig. 3a) but did not affect TH signaling in the heart (Fig. 3b). As TRE is based on a DR-4 DNA motive, we also tested whether induction of liver X receptor (LXR) signaling, representing another DR-4-dependent pathway, could also be detected in THAI mouse. Administration of the LXR agonist GW3965 to the THAI #4 mouse induced hepatic luciferase expression by ~2.3-fold [control: 1 ± 0.394; GW3965: 2.324 ± 0.362; means ± standard error of the mean (SEM); luciferase/GAPDH (n = 5); $*P < 0.05$ by Student *t* test].

iBAT-specific activation of TH signaling in cold-stimulated THAI mice

Cold exposure is associated with BAT sympathetic activation and several-fold stimulation of the type 2 deiodinase (D2) activity. This saturates local TR without affecting systemic levels of circulating T3 (35). However, it has been challenging to study TH signaling in iBAT under these conditions, given that virtually all downstream targets of T3 in this tissue are equally affected by cyclic adenosine monophosphate. For example, a mouse with disruption of D2-encoding *dio2* only provided limited information, given the compensatory elevation in iBAT sympathetic activity (36). To approach this problem, line 4 mice were exposed to cold (4°C) for 9 and 24 hours. The animals exhibited an ~3.4- and 9.3-fold increase in luciferase activity in iBAT at 9 and 24 hours *vs* control, respectively, whereas the luciferase mRNA was increased 2.8- and 2.7-fold *vs* control in the two time points (Fig. 4a and 4b). TH signaling in iBAT was also detected in live animals imaged for bioluminescence, with a 3.2-fold increase in signal after 24 hours of cold exposure. At all times, TH action in footpad skin remained unchanged. This indicates a highly selective increase in iBAT TH signaling during cold exposure (Fig. 4c and 4d).

That the increase in TH signaling was caused by sympathetic activation was confirmed in THAI mice undergoing cold exposure after unilateral iBAT surgical

Table 3. Responsiveness of Different Tissues and Brain Regions of THAI #4 to Hypothyroidism

	THAI #4 (Hypothyroid)			
Tissue	**Eu (RLU/mg Protein)**	**Hypo (RLU/mg Protein)**	**Fold (Means ± SEM)**	***P* value**
Pit	0.347	0.072	0.21 ± 0.02	0.0005[a]
MBH	0.153	0.076	0.49 ± 0.04	0.0099[a]
HT	0.315	0.136	0.43 ± 0.05	0.0032[a]
CTX	0.163	0.056	0.34 ± 0.06	0.0003[a]
Liver	0.003	0.001	0.44 ± 0.07	0.0446[a]
Heart	0.009	0.001	0.16 ± 0.06	0.0001[a]
BAT	0.037	0.008	0.23 ± 0.1	0.0051[a]
Bone	0.031	0.008	0.26 ± 0.04	0.0034[a]
Muscle	0.008	0.007	–	0.776
Thyroid	0.071	0.078	–	0.439
Intestine	1.683	0.166	0.1 ± 0.01	0.0001[a]
WBC	0.013	0.005	0.42 ± 0.08	0.0412[a]

Animals were rendered hypothyroid by adding 0.1% sodium perchlorate and 0.5% methimazole in drinking water for 3 weeks combined with a low-iodine diet. Luciferase activity was assessed with luciferase assay and expressed as RLU per milligram protein in tissue samples. Luciferase activity of corresponding tissues of hypothyroid *vs* euthyroid animals was compared with Student *t* test (n = 6).

Abbreviations: CTX, cerebral cortex; Eu, euthyroid; HT, hypothalamus; Hypo, hypothyroid; MBH, mediobasal hypothalamus; Pit, pituitary; WBC, white blood cell.

[a] $P < 0.05$.

denervation, which resulted in a strong tendency for a decrease in NE levels in iBAT (Fig. 5a) and prevented the 9-hour, cold exposure-induced, ~twofold increase in NE content that was only observed in the intact iBAT lobe. Furthermore, only the intact iBAT lobe exhibited a ninefold increase in D2 expression and 18-fold acceleration in D2 activity (Fig. 5b and 5c), which then increased local TH signaling. Indeed, only in the intact lobe did luciferase mRNA levels increase by ~2.7-fold (Fig. 5d). It is notable that baseline TH action was not affected by denervation in the animals kept at room temperature.

Discussion

Under most circumstances, TH levels in the circulation are relatively stable, suggesting that TH signaling is homogeneous and steady throughout the body. Although indirect evidence exists that suggests that this is not the case, as a result of the lack of appropriate tools, direct measurement of tissue-specific TH action was not possible. Here, we developed and used a unique transgenic mouse model to show that TH signaling is tissue specific and fluctuates rapidly in a tissue-specific manner. These findings are physiologically relevant given the assessment of TH action using a reporter cassette that operates in the context of endogenously expressed levels of TH transporters, TRs, and transcriptional factors (Fig. 6). That this reporter system reflects physiological levels of TH signaling is illustrated by the fact that the THAI mouse model is sufficiently sensitive to detect a reduction of TH signaling in hypothyroid animals. In addition, the system can detect rapid, tissue-specific changes in TH signaling, such as in the cold-stimulated iBAT. Thus, the THAI model reveals how a studied condition/treatment can

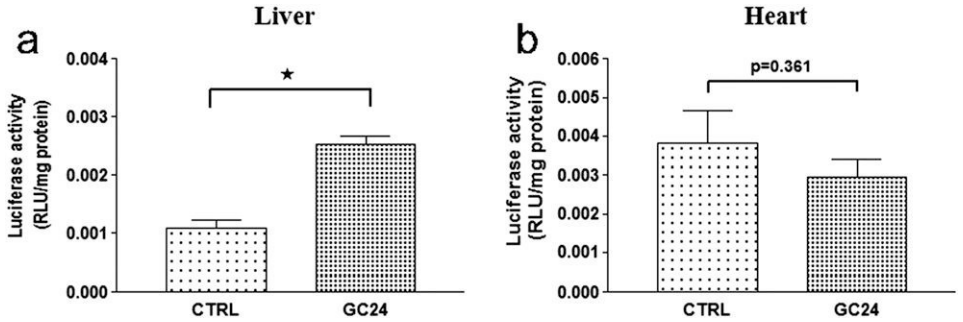

Figure 3. Effect of the TH analog GC24 on tissue-specific TH action. (a) Single injection of the TRβ agonist GC24 (1.53 nM/g bw IP) significantly increased luciferase activity after 24 hours in hypothyroid (0.1% sodium perchlorate and 0.5% methimazole in drinking water for 3 weeks combined with low-iodine diet) THAI #4 mice in the TRβ isoform-dominant liver, whereas (b) luciferase activity did not change in the TRα isoform-dominant heart. Luciferase activity of liver and heart samples was assayed 24 hours after GC24 injection. Means ± SEM (n = 10). *$P < 0.0001$ by Student *t* test. CTRL, control.

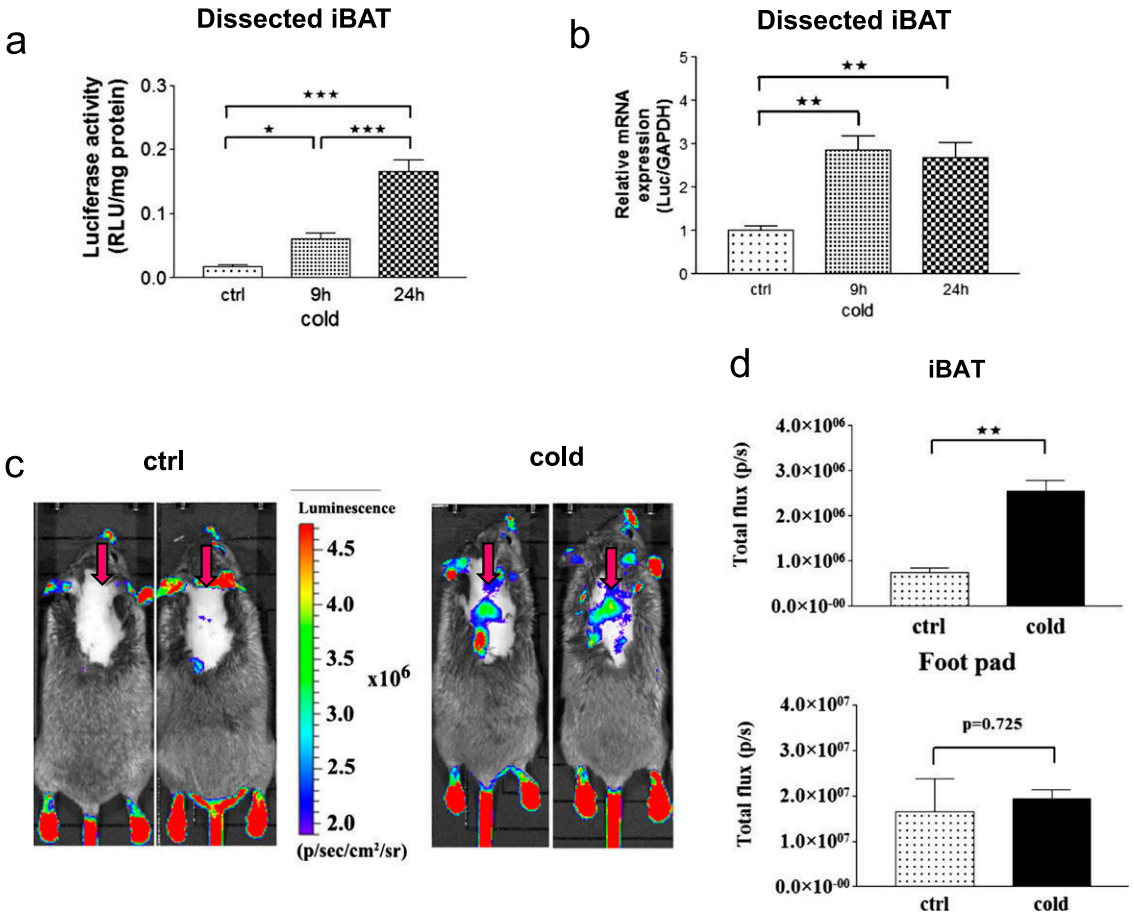

Figure 4. Cold-induced TH action in the iBAT of THAI #4 mice. (a) luciferaseiferase activity is significantly elevated in dissected iBAT samples of the THAI #4 line after 9 hours at 4°C and further increased after 24 hours of cold stress. $*P < 0.05$; $***P < 0.001$ by one-way ANOVA, followed by Newman-Keuls *post hoc* test. Means ± SEM (n = 5). (b) Luciferase mRNA increased after 9 hours in dissected iBAT samples of the THAI #4 line; $**P < 0.01$ by one-way ANOVA, followed by Newman-Keuls *post hoc* test. Means ± SEM (n = 5). (c) *In vivo* bioluminescence imaging on iBAT of THAI #4 subjected to cold stress for 24 hours at 4°C, followed by IP luciferin administration. Representative images of two control and two cold-exposed mice. Arrows indicate iBAT. (d) Light intensity diagram of luciferase activity in iBAT and foot pads of control and cold-induced THAI #4 mice. Luciferase activity of skin above the non–BAT-containing region was deducted from iBAT reporter values. Means of photon/s ± SEM (n = 4). $**P < 0.001$ by Student *t* test.

change TH action in a specific tissue. However, the model is not meant to establish and compare absolute levels of TH signaling in various tissues of the same or different THAI lines.

In vivo, the DR-4 element does not work exclusively as TRE but can also represent a binding site for other nuclear receptors; *e.g.*, it can be also bind to LXR, a cholesterol-mediated nuclear receptor retinoid X receptor (RXR), farnesoid X receptor, pregnane X receptor, and constitute-androstane receptor (37–39). Our finding, that GW3965, an LXR agonist, could induce hepatic luciferase expression approximately twofold in THAI #4 mice, indicates that similar to the endogenous situation, the inserted DR-4 elements can respond to other DR-4-dependent pathways upon pharmacological induction. Thus, TH specificity of the THAI system should be viewed the same way as that of endogenous TREs that do not exclusively respond to TH but might also be affected by other DR-4-dependent, but not/or not directly TH-dependent, pathways. Therefore, under specific conditions, the biological output of a DR-4 response could be the net result of different DR-4-related signals.

Studies of deiodinase-mediated changes in TH signaling have been hindered by the lack of a sufficiently specific and sensitive reporter system, a problem that is now resolved with the development of this mouse model. Up until now, one could only assess tissue-specific TH signaling by measuring mRNA levels of TH-responsive genes (32). However, this approach has limited value, as multiple factors affect the expression of endogenously expressed, TH-responsive genes. Well-known TH-responsive genes, such as spot-14, malic enzyme, and ectonucleotide pyrophosphatase/phosphodiesterase 2, are also regulated by many other factors, including insulin and 17β-estradiol, for example (40, 41). Therefore, expression of these genes could authentically report on TH signaling only in atypical cases, when exclusively, TH levels are altered in the animal. However, typically, it

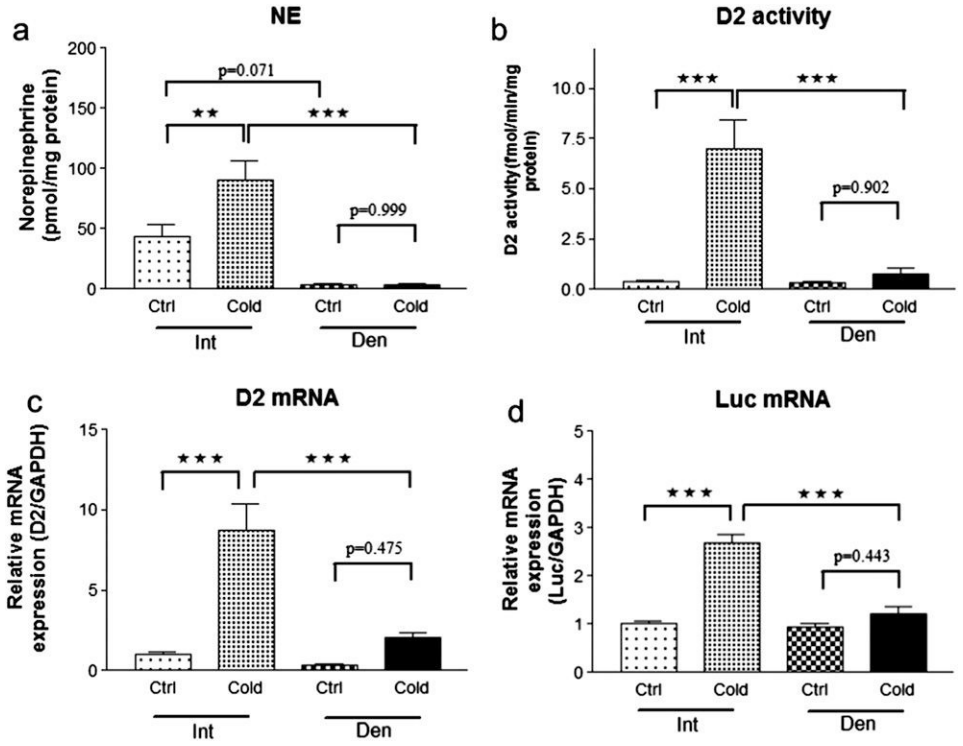

Figure 5. Sympathetic regulation of TH action in iBAT of THAI #4 mice. (a) Nine-hour cold stress increased NE levels by twofold in intact (Int) BAT lobe, whereas the NE level was not influenced in the denervated (Den) lobe. (b) D2 enzymatic activity and (c) mRNA levels were increased by cold stress in dissected, intact iBAT, whereas the denervated side remained unresponsive. (d) Luciferase mRNA level increased 2.7-fold in the intact lobe in response to cold, but TH action was not influenced by cold on the denervated side. Despite sympathetic denervation, luciferase expression did not decrease at room temperature in the denervated lobe compared with the intact lobe. $***P < 0.001$; $**P < 0.01$ by repeated-measures ANOVA, followed by Tukey *post hoc* test. Data are shown as means ± SEM (n = 6).

cannot be determined to what extent these genes were regulated by changes of local TH levels and by other factors. This indicates the need for alternative systems that monitor TH signaling. To avoid problems associated with the responsiveness of endogenous TH-regulated promoters to TH-unrelated signals, we did not perform knockin-powered, targeted insertion of the reporter, 3′ to an endogenous promoter, but rather, applied Sleeping Beauty transposase-mediated delivery of a minimal viral promoter that was made TH responsive with the addition of TREs. As in the 5′−flanking region of many endogenous, TH-responsive genes, two or three TREs are present (18, 42, 43), we inserted three TREs in our transgenic construct. In contrast to our model, the available FINDT3 mouse model uses an artificial chimeric Gal4DNA-binding domain, a TRα ligand-binding domain fusion protein that works independently of endogenous TR and TRE (44). Thus, this system detects T3 availability but cannot assess the changes of physiologically relevant TH action that is a far more complex event and cannot be directly deducted from T3 availability alone. A 2× TRE β-galactosidase mouse model has been reported to assess TH action at embryonic stages, but it is not suitable for studies in the adult brain, and information in adult peripheral organs is missing (45). Furthermore, in contrast to the THAI mouse, neither model allows for quantification of the tissue-specific changes of TH signaling in live animals.

As the THAI model uses the endogenous TRs, it also allows the examination of TH signaling triggered by TH analogs, such as TR-selective agonists; *i.e.*, the TRβ-selective GC24 markedly stimulated activity in the liver but not in the TRα-predominant heart. The observed reporter activity represents the net result of effects shaping the *in vivo* ability of a compound to act in a specific tissue, including tissue and cell penetration, local metabolism of the compound, and interaction with TRs and cofactors.

TRs are distinctive in that even when unoccupied by their ligands, they remain bound to the regulatory regions of TH-dependent genes, slowing down the transcriptional process through the recruitment of corepressors, a process known as gene repression. The binding of T3 increases gene expression through derepression (uncoupling of TR and corepressors) and transactivation (coupling of TR with coactivators). It is remarkable that the THAI mouse exhibits a sufficient signal-to-noise ratio to assess corepression, *i.e.*, a decrease in TH signaling observed during hypothyroidism. Indeed, in the hypothyroid THAI mouse, there is an approximate two- to 10-fold decrease in TH signaling in

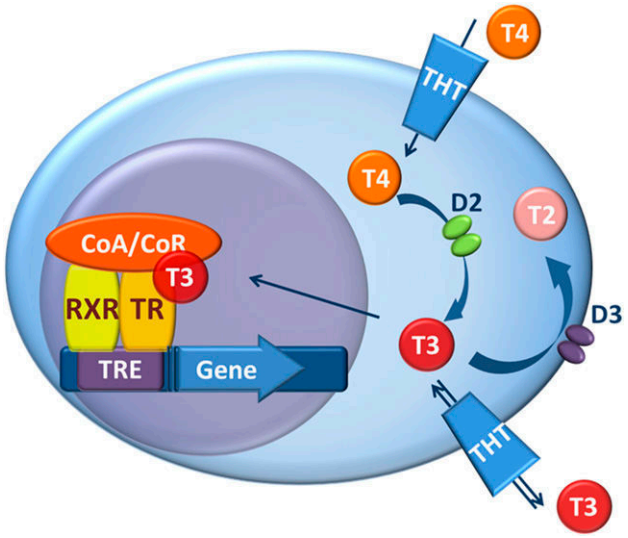

Figure 6. TH action and its regulation by TH transporters and deiodinases. T3 binds the TR/RXR heterodimer attached to a TRE in the regulatory region of TH-responsive genes. The ability of TR/RXR to affect gene transcription is modulated by coactivators/corepressors (CoA/CoR) and factors regulating intracellular TH availability, TH transporters (THT) and TH deiodinases. As the first step in the regulation of TH action, D2 activates T4 by converting it to T3. Type 3 deiodinase (D3) catalyses the inactivating pathway by degrading T3 and converting T4 to the inactive reverse T3. The expression of the two main deiodinases, D2 and D3, varies according to cell type.

different brain regions, the pituitary, and other peripheral organs, including liver, heart, bone, iBAT, white blood cells, and small intestine. The latter is particularly interesting, as it illustrates the high degree of TH responsiveness exhibited by the intestinal epithelium, which is consistent with the observation that patients carrying TRα-inactivating mutations exhibit marked constipation (46). The measurement of TR-mediated gene repression with the THAI mouse in a tissue-specific manner provides an approach to physiological studies of TH signaling and the impact of the deiodinases and transporters.

Although the dosage of L-T4 and L-T3, as used in the present studies, is standard across studies of TH signaling, it is certainly well above the physiological range (32). However, the increase in luciferase activity in cold-stimulated iBAT provides strong evidence that the THAI mouse gauges TH signaling within a physiological context. Protein translation requires time; therefore, an increase of reporter activity can be slower than that of its encoding mRNA. This could explain that whereas an increase of luciferase mRNA reaches its plateau at 9 hours, luciferase activity continues to increase until 24 hours. The model also allowed direct tissue-specific assessment of TH action in iBAT and provided insights into the crosstalk between TH and noradrenergic signaling by revealing that in contrast to the cold-induced changes of TH action, the basal TH action at room temperature is independent of noradrenergic signaling in this tissue (35, 47). These data also demonstrate how robustly THAI mice reveal local tissue-specific up- or downregulation of TH action, independently from circulating TH levels.

The translatability of the present findings is straightforward. Patients with different forms of thyroid disease suffer from momentary or life-long dysregulation of TH signaling. Thus, if we are to correct TH signaling in such patients, we should be able to understand how major elements of TH metabolism and action affect T3-dependent biological effects. For example, >300 million patients with hypothyroidism worldwide are maintained on levothyroxine-replacement therapy (48). The rationale for using only levothyroxine is based on the idea that the deiodinases regulate the amount of T3 required by individual tissues. It has recently been recognized that there are limits to the extent that deiodinases normalize systemic and intracellular T3 during treatment with levothyroxine (15). As a result, patients on levothyroxine are ~10 pounds heavier, 30% to 40% less active, and more likely to be on antidepressives, statins, and beta-blockers, despite normal thyroid-stimulating hormone serum levels (49). We are now in a position to understand why and in which tissues TH signaling is dysregulated during levothyroxine supplementation.

In conclusion, the generated THAI model can assess TH action in live animals and tissue samples. The model is able to capture both increased and decreased levels of endogenous TH signaling. It can be used to study the tissue-specific impact of TH analogs and has the potential to serve as a useful model for testing the impact of endocrine disruptors on the TH economy. Whereas the THAI model overcomes the interfering effect of numerous signals modulating the expression of endogenous, TH-responsive marker genes *via* various promoter-binding sites, its reporter activity can certainly be affected under specific conditions by DR-4-dependent, but not/or not directly TH-related, signals, the same way as endogenous DR-4 works *in vivo*. The THAI mouse reveals that during the preservation of thermal homeostasis, the activation of the sympathetic nervous system induced elevation of TH action in the iBAT of mice in a cold environment, but the sympathetic nervous system has no effect on TH action in the iBAT of mice at room temperature, indicating highly different regulation of TH action under these two conditions.

Acknowledgments

The technical help of A. Juhász is gratefully acknowledged. We thank Dr. Zs. Izsvák (Berlin, Germany) and L. Mátes (Szeged, Hungary) for the SB100X construct, Perry Hackett of Addgene for the pt2-BH transposon cloning vector (plasmid no. 26554), and Dr. T. Scanlan (Portland, OR) for GC24.

Financial Support: This work was supported by the Hungarian National Brain Research Program [Grants KTIA_13_NAP_A_I/3 (to C.F.) and KTIA_13_NAP_A_I/4 (to B.G.)] and Hungarian Scientific Research Fund [Grants OTKA K109415 (to B.G.) and K109710 (to C.F.)].

Author Contributions: P.M. conducted experiments, analyzed results, and wrote the manuscript. M.B., B.B., M.T., I.H., Z.H., B.S., Z.T., and R.S. conducted experiments. F.E. and G.S. performed founder generation. R.M.L. and A.C.B. analyzed results and wrote the manuscript. C.F. and B.G. conceived of the project, designed and performed experiments, analyzed results, wrote the manuscript, and acquired the funding.

Correspondence: Csaba Fekete, MD, PhD, or Balázs Gereben, DVM, PhD, Department of Endocrine Neurobiology, Institute of Experimental Medicine, Hungarian Academy of Sciences, 43 Szigony Street, Budapest, Hungary H-1083. E-mail: fekete.csaba@koki.mta.hu; or gereben.balazs@koki.mta.hu.

Disclosure Summary: The authors have nothing to disclose.

References

1. Zhang J, Lazar MA. The mechanism of action of thyroid hormones. *Annu Rev Physiol*. 2000;**62**(1):439–466.
2. Ortiga-Carvalho TM, Sidhaye AR, Wondisford FE. Thyroid hormone receptors and resistance to thyroid hormone disorders. *Nat Rev Endocrinol*. 2014;**10**(10):582–591.
3. Brent GA, Larsen PR, Harney JW, Koenig RJ, Moore DD. Functional characterization of the rat growth hormone promoter elements required for induction by thyroid hormone with and without a co-transfected beta type thyroid hormone receptor. *J Biol Chem*. 1989;**264**(1):178–182.
4. Glass CK, Franco R, Weinberger C, Albert VR, Evans RM, Rosenfeld MG. A c-erb-A binding site in rat growth hormone gene mediates trans-activation by thyroid hormone. *Nature*. 1987; **329**(6141):738–741.
5. Chatonnet F, Guyot R, Benoît G, Flamant F. Genome-wide analysis of thyroid hormone receptors shared and specific functions in neural cells. *Proc Natl Acad Sci USA*. 2013;**110**(8):E766–E775.
6. Gereben B, Zavacki AM, Ribich S, Kim BW, Huang SA, Simonides WS, Zeöld A, Bianco AC. Cellular and molecular basis of deiodinase-regulated thyroid hormone signaling. *Endocr Rev*. 2008;**29**(7):898–938.
7. Fekete C, Lechan RM. Central regulation of hypothalamic-pituitary-thyroid axis under physiological and pathophysiological conditions. *Endocr Rev*. 2014;**35**(2):159–194.
8. Visser WE, Friesema EC, Jansen J, Visser TJ. Thyroid hormone transport in and out of cells. *Trends Endocrinol Metab*. 2008;**19**(2): 50–56.
9. Refetoff S, DeWind LT, DeGroot LJ. Familial syndrome combining deaf-mutism, stuppled epiphyses, goiter and abnormally high PBI: possible target organ refractoriness to thyroid hormone. *J Clin Endocrinol Metab*. 1967;**27**(2):279–294.
10. Friesema EC, Grueters A, Biebermann H, Krude H, von Moers A, Reeser M, Barrett TG, Mancilla EE, Svensson J, Kester MH, Kuiper GG, Balkassmi S, Uitterlinden AG, Koehrle J, Rodien P, Halestrap AP, Visser TJ. Association between mutations in a thyroid hormone transporter and severe X-linked psychomotor retardation. *Lancet*. 2004;**364**(9443):1435–1437.
11. Dumitrescu AM, Liao XH, Best TB, Brockmann K, Refetoff S. A novel syndrome combining thyroid and neurological abnormalities is associated with mutations in a monocarboxylate transporter gene. *Am J Hum Genet*. 2004;**74**(1):168–175.
12. Boelen A, Kwakkel J, Fliers E. Beyond low plasma T3: local thyroid hormone metabolism during inflammation and infection. *Endocr Rev*. 2011;**32**(5):670–693.
13. Pihlajamäki J, Boes T, Kim EY, Dearie F, Kim BW, Schroeder J, Mun E, Nasser I, Park PJ, Bianco AC, Goldfine AB, Patti ME. Thyroid hormone-related regulation of gene expression in human fatty liver. *J Clin Endocrinol Metab*. 2009;**94**(9):3521–3529.
14. Werneck de Castro JP, Fonseca TL, Ueta CB, McAninch EA, Abdalla S, Wittmann G, Lechan RM, Gereben B, Bianco AC. Differences in hypothalamic type 2 deiodinase ubiquitination explain localized sensitivity to thyroxine. *J Clin Invest*. 2015;**125**(2): 769–781.
15. Gereben B, McAninch EA, Ribeiro MO, Bianco AC. Scope and limitations of iodothyronine deiodinases in hypothyroidism. *Nat Rev Endocrinol*. 2015;**11**(11):642–652.
16. Tancevski I, Rudling M, Eller P. Thyromimetics: a journey from bench to bed-side. *Pharmacol Ther*. 2011;**131**(1):33–39.
17. Verge CF, Konrad D, Cohen M, Di Cosmo C, Dumitrescu AM, Marcinkowski T, Hameed S, Hamilton J, Weiss RE, Refetoff S. Diiodothyropropionic acid (DITPA) in the treatment of MCT8 deficiency. *J Clin Endocrinol Metab*. 2012;**97**(12):4515–4523.
18. Toyoda N, Zavacki AM, Maia AL, Harney JW, Larsen PR. A novel retinoid X receptor-independent thyroid hormone response element is present in the human type 1 deiodinase gene. *Mol Cell Biol*. 1995; **15**(9):5100–5112.
19. Kollár A, Kvárta-Papp Z, Egri P, Gereben B. Different types of luciferase reporters show distinct susceptibility to T3-evoked downregulation. *Thyroid* 2016;**26**(1):179–182.
20. Mátés L, Chuah MK, Belay E, Jerchow B, Manoj N, Acosta-Sanchez A, Grzela DP, Schmitt A, Becker K, Matrai J, Ma L, Samara-Kuko E, Gysemans C, Pryputniewicz D, Miskey C, Fletcher B, VandenDriessche T, Ivics Z, Izsvák Z. Molecular evolution of a novel hyperactive Sleeping Beauty transposase enables robust stable gene transfer in vertebrates. *Nat Genet*. 2009;**41**(6):753–761.
21. Egri P, Gereben B. Minimal requirements for ubiquitination-mediated regulation of thyroid hormone activation. *J Mol Endocrinol*. 2014;**53**(2):217–226.
22. Ivics Z, Mátés L, Yau TY, Landa V, Zidek V, Bashir S, Hoffmann OI, Hiripi L, Garrels W, Kues WA, Bösze Z, Geurts A, Pravenec M, Rülicke T, Izsvák Z. Germline transgenesis in rodents by pronuclear microinjection of Sleeping Beauty transposons. *Nat Protoc*. 2014; **9**(4):773–793.
23. Errijgers V, Van Dam D, Gantois I, Van Ginneken CJ, Grossman AW, D'Hooge R, De Deyn PP, Kooy RF. FVB.129P2-Pde6b(+) Tyr(c-ch)/Ant, a sighted variant of the FVB/N mouse strain suitable for behavioral analysis. *Genes Brain Behav*. 2007;**6**(6): 552–557.
24. Mátés L. Rodent transgenesis mediated by a novel hyperactive Sleeping Beauty transposon system. *Methods Mol Biol*. 2011;**738**: 87–99.
25. Coligan JE, Bierer B, Margulies, DH, Shevach EM, Strober W, eds. *Current Protocols in Immunology*. New York, NY: Wiley Online; 2017.
26. Koprowski H, Mocarelli P, Wiktor TJ. Antibody response in vitro to an animal virus: production of rabies virus neutralizing antibodies by mouse cells in culture. *Proc Natl Acad Sci USA*. 1972; **69**(9):2433–2436.
27. Kanda R, Shang Y, Tsuji S, Eguchi-Kasai K, Hayata I. An improved culture system of mouse peripheral blood lymphocytes for analysis of radiation-induced chromosome aberrations. *Biosci Rep*. 2004; **24**(6):641–650.
28. Potter CJ, Luo L. Splinkerette PCR for mapping transposable elements in Drosophila. *PLoS One*. 2010;**5**(4):e10168.
29. Morales JR, Ballesteros I, Deniz JM, Hurtado O, Vivancos J, Nombela F, Lizasoain I, Castrillo A, Moro MA. Activation of liver X receptors promotes neuroprotection and reduces brain inflammation in experimental stroke. *Circulation*. 2008;**118**(14): 1450–1459.

30. Pulinilkunnil T, He H, Kong D, Asakura K, Peroni OD, Lee A, Kahn BB. Adrenergic regulation of AMP-activated protein kinase in brown adipose tissue in vivo. *J Biol Chem*. 2011;**286**(11): 8798–8809.
31. Horváth G, Gölöncsér F, Csölle C, Király K, Andó RD, Baranyi M, Koványi B, Máté Z, Hoffmann K, Algaier I, Baqi Y, Müller CE, Von Kügelgen I, Sperlágh B. Central P2Y12 receptor blockade alleviates inflammatory and neuropathic pain and cytokine production in rodents. *Neurobiol Dis*. 2014;**70**:162–178.
32. Bianco AC, Anderson G, Forrest D, Galton VA, Gereben B, Kim BW, Kopp PA, Liao XH, Obregon MJ, Peeters RP, Refetoff S, Sharlin DS, Simonides WS, Weiss RE, Williams GR. American thyroid association guide to investigating thyroid hormone economy and action in rodent and cell models. *Thyroid*. 2014;**24**(1):88–168.
33. Moran C, Chatterjee K. Resistance to thyroid hormone due to defective thyroid receptor alpha. *Best Pract Res Clin Endocrinol Metab*. 2015;**29**(4):647–657.
34. Borngraeber S, Budny MJ, Chiellini G, Cunha-Lima ST, Togashi M, Webb P, Baxter JD, Scanlan TS, Fletterick RJ. Ligand selectivity by seeking hydrophobicity in thyroid hormone receptor. *Proc Natl Acad Sci USA*. 2003;**100**(26):15358–15363.
35. Bianco AC, Silva JE. Intracellular conversion of thyroxine to triiodothyronine is required for the optimal thermogenic function of brown adipose tissue. *J Clin Invest*. 1987;**79**(1):295–300.
36. Christoffolete MA, Linardi CC, de Jesus L, Ebina KN, Carvalho SD, Ribeiro MO, Rabelo R, Curcio C, Martins L, Kimura ET, Bianco AC. Mice with targeted disruption of the Dio2 gene have cold-induced overexpression of the uncoupling protein 1 gene but fail to increase brown adipose tissue lipogenesis and adaptive thermogenesis. *Diabetes*. 2004;**53**(3):577–584.
37. Echchgadda I, Song CS, Oh T, Ahmed M, De La Cruz IJ, Chatterjee B. The xenobiotic-sensing nuclear receptors pregnane X receptor, constitutive androstane receptor, and orphan nuclear receptor hepatocyte nuclear factor 4alpha in the regulation of human steroid-/bile acid-sulfotransferase. *Mol Endocrinol*. 2007;**21**(9): 2099–2111.
38. Quack M, Frank C, Carlberg C. Differential nuclear receptor signalling from DR4-type response elements. *J Cell Biochem*. 2002; **86**(3):601–612.
39. Kalaany NY, Mangelsdorf DJ. LXRS and FXR: the yin and yang of cholesterol and fat metabolism. *Annu Rev Physiol*. 2006;**68**(1): 159–191.
40. Ishihara A, Matsumoto E, Horikawa K, Kudo T, Sakao E, Nemoto A, Iwase K, Sugiyama H, Tamura Y, Shibata S, Takiguchi M. Multifactorial regulation of daily rhythms in expression of the metabolically responsive gene spot14 in the mouse liver. *J Biol Rhythms*. 2007;**22**(4):324–334.
41. Sárvári M, Kalló I, Hrabovszky E, Solymosi N, Rodolosse A, Vastagh C, Auer H, Liposits Z. Hippocampal gene expression is highly responsive to estradiol replacement in middle-aged female rats. *Endocrinology*. 2015;**156**(7):2632–2645.
42. Xiong S, Chirala SS, Hsu MH, Wakil SJ. Identification of thyroid hormone response elements in the human fatty acid synthase promoter. *Proc Natl Acad Sci USA*. 1998;**95**(21):12260–12265.
43. Hartong R, Wang N, Kurokawa R, Lazar MA, Glass CK, Apriletti JW, Dillmann WH. Delineation of three different thyroid hormone-response elements in promoter of rat sarcoplasmic reticulum Ca2+ATPase gene. Demonstration that retinoid X receptor binds 5′ to thyroid hormone receptor in response element 1. *J Biol Chem*. 1994;**269**(17):13021–13029.
44. Quignodon L, Legrand C, Allioli N, Guadaño-Ferraz A, Bernal J, Samarut J, Flamant F. Thyroid hormone signaling is highly heterogeneous during pre- and postnatal brain development. *J Mol Endocrinol*. 2004;**33**(2):467–476.
45. Nucera C, Muzzi P, Tiveron C, Farsetti A, La Regina F, Foglio B, Shih SC, Moretti F, Della Pietra L, Mancini F, Sacchi A, Trimarchi F, Vercelli A, Pontecorvi A. Maternal thyroid hormones are transcriptionally active during embryo-foetal development: results from a novel transgenic mouse model. *J Cell Mol Med*. 2010; **14**(10):2417–2435.
46. Bochukova E, Schoenmakers N, Agostini M, Schoenmakers E, Rajanayagam O, Keogh JM, Henning E, Reinemund J, Gevers E, Sarri M, Downes K, Offiah A, Albanese A, Halsall D, Schwabe JW, Bain M, Lindley K, Muntoni F, Vargha-Khadem F, Dattani M, Farooqi IS, Gurnell M, Chatterjee K. A mutation in the thyroid hormone receptor alpha gene [published correction appears in N Engl J Med. 2012;367(15):1474]. *N Engl J Med*. 2012;**366**(3): 243–249.
47. Silva JE, Larsen PR. Adrenergic activation of triiodothyronine production in brown adipose tissue. *Nature*. 1983;**305**(5936): 712–713.
48. Jonklaas J, Bianco AC, Bauer AJ, Burman KD, Cappola AR, Celi FS, Cooper DS, Kim BW, Peeters RP, Rosenthal MS, Sawka AM, American Thyroid Association Task Force on Thyroid Hormone Replacement. Guidelines for the treatment of hypothyroidism: prepared by the american thyroid association task force on thyroid hormone replacement. *Thyroid*. 2014;**24**(12):1670–1751.
49. Peterson SJ, McAninch EA, Bianco AC. Is a normal TSH synonymous with "euthyroidism" in levothyroxine monotherapy? *J Clin Endocrinol Metab*. 2016;**101**(12):4964–4973.

Table S1.

Taqman probes used for real-time PCR

Gene	Name	Accession Nr.
Luciferase	Firefly luciferase enzyme	AIY9ZTZ
dio2	Type 2 deiodinase	Mm00515664_m1
GAPDH	glyceraldehyde-3-phosphate dehydrogenase	Mm99999915_g1

Table S2.

Serum free thyroid hormone levels and body weight of THAI mice

	WT	**THAI #4**	P value	**THAI #23**	P value	**THAI #18**	P value
fT4 (pmol/L)	13.44 ± 1.81	10.57 ± 1.96	0.325	12.86±1.44	0.811	12.89±2.03	0.846
fT3 (pmol/L)	5.33 ± 0.74	4.26 ± 0.41	0.249	4.27±0.36	0.247	4.40±0.39	0.309
body weight (g)	29.83 ± 1.27	32.93 ± 1.31	0.14	28.33±0.42	0.223	27.5±1.51	0.344

Results are expressed as means ± SEM (n=4). No significant difference was found (wt *vs.* THAI) by Student's t-test.

Table S3.

Metabolic phenotyping and body composition of THAI mice

	WT	THAI #4	P value
lean body mass %	80.51 ± 2.03	81.92 ± 1.53	0.6
fat mass %	13.07 ± 2.27	12.79 ± 1.77	0.92
daily average RER VCO2/VO2	0.86 ± 0.03	0.86 ± 0.01	0.91
daily average VO2 (ml/kg lean body/h)	3746.49 ± 328	4072.59 ± 184	0.42

Results are expressed as means ± SEM (n=4). No significant difference was found (wt *vs.* THAI) by Student's t-test.

Fig. S1.

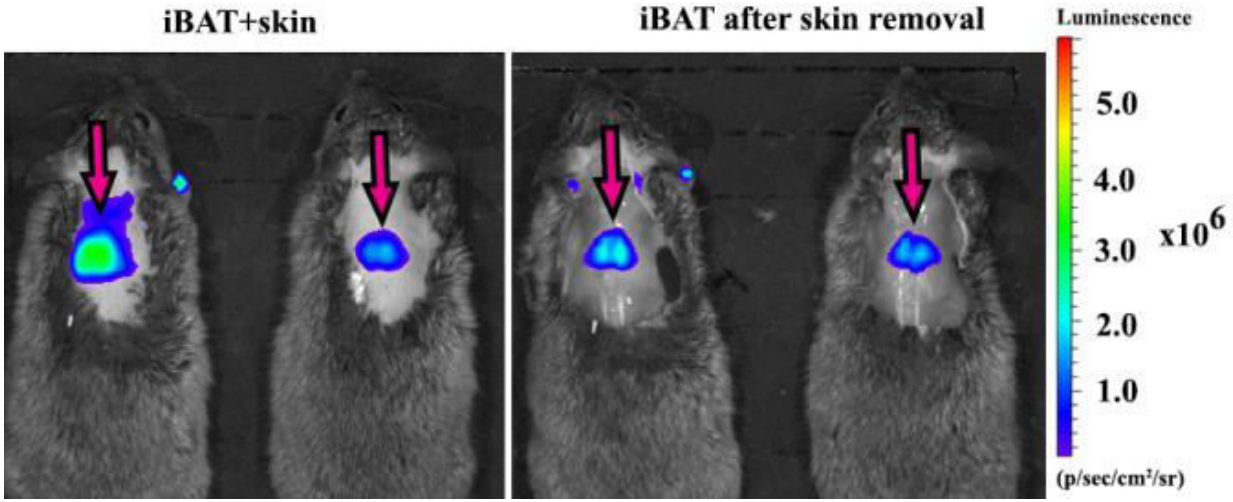

Bioluminescence in #4 THAI mice. Bioluminescence of the interscapular region of live THAI #4 mice originates from the iBAT. Animals were injected with L-T3 (1 µg/g bw *i.p.* 24h before imaging). The animals were anesthetised before imaging. Intact animal (left) and direct imaging of iBAT after removal of skin of the interscapular region (right).

Fig. S2.

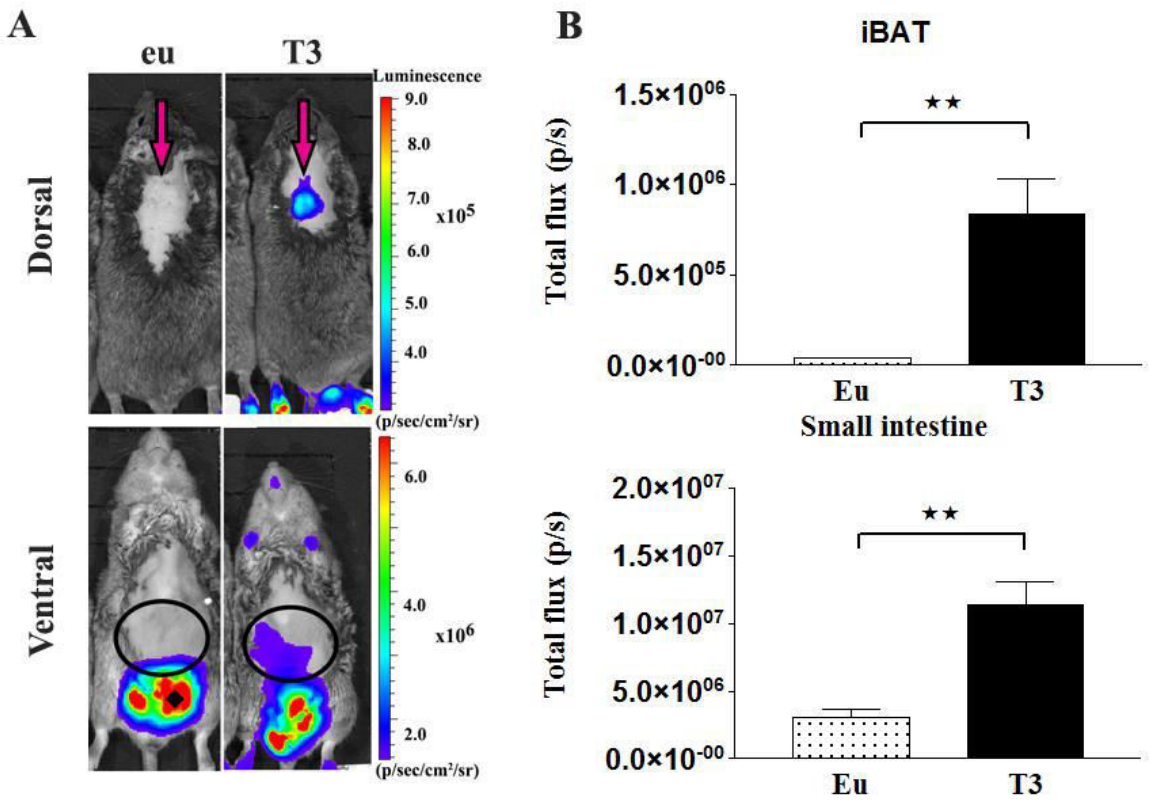

Detection of TH action in live #23 animals. (a) In vivo bioluminescence imaging on euthyroid and L-T3-treated (1 µg/g bw injected i.p. 24h before imaging) THAI #23 mice followed by i.p. luciferin administration. Representative images of euthyroid (eu) and L-T3 treated (T3) mice and light intensity diagram of iBAT and small intestine. L-T3 injection increased light intensity in iBAT and small intestine. Dorsal image arrow: iBAT; Ventral image circle: intestine; ♦: testicles (b) Light intensity diagram (photon/sec) of luciferase activity in iBAT and small intestine of euthyroid and L-T3-treated THAI #23 mice. Mean of photon/sec ± SEM (n=5) ** $P<0.01$ by Student's t-test.